SUPPLEMENTARY INFORMATION

Unraveling the the Correlation between Biological Effects and Halogen Substituents in Cobalt bis(dicarbollide)

Katarzyna Zakret-Drozdowska[1], Bożena Szermer-Olearnik[1], Waldemar Goldeman[2], Michalina Gos[1], Dawid Drozdowski[3], Anna Gągor[3], Tomasz M. Goszczyński[1*]

[1] Laboratory of Biomedical Chemistry, Hirszfeld Institute of Immunology and Experimental Therapy, Polish Academy of Sciences, 53-114 Wrocław, Poland
[2] Department of Organic and Medicinal Chemistry, Faculty of Chemistry, Wrocław University of Science and Technology, 50-370 Wrocław, Poland
[3] Institute of Low Temperature and Structure Research, Polish Academy of Sciences, 50-422 Wrocław, Poland
[*]Corresponding author: Tomasz M. Goszczyński , goszczynski@hirszfeld.pl

Table of contents

1. Analytical data

1.1. Characterization of **[CoSAN-F$_2$]$^-$**

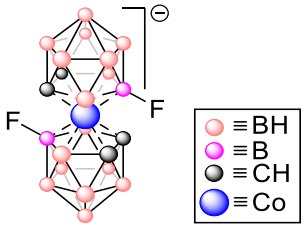

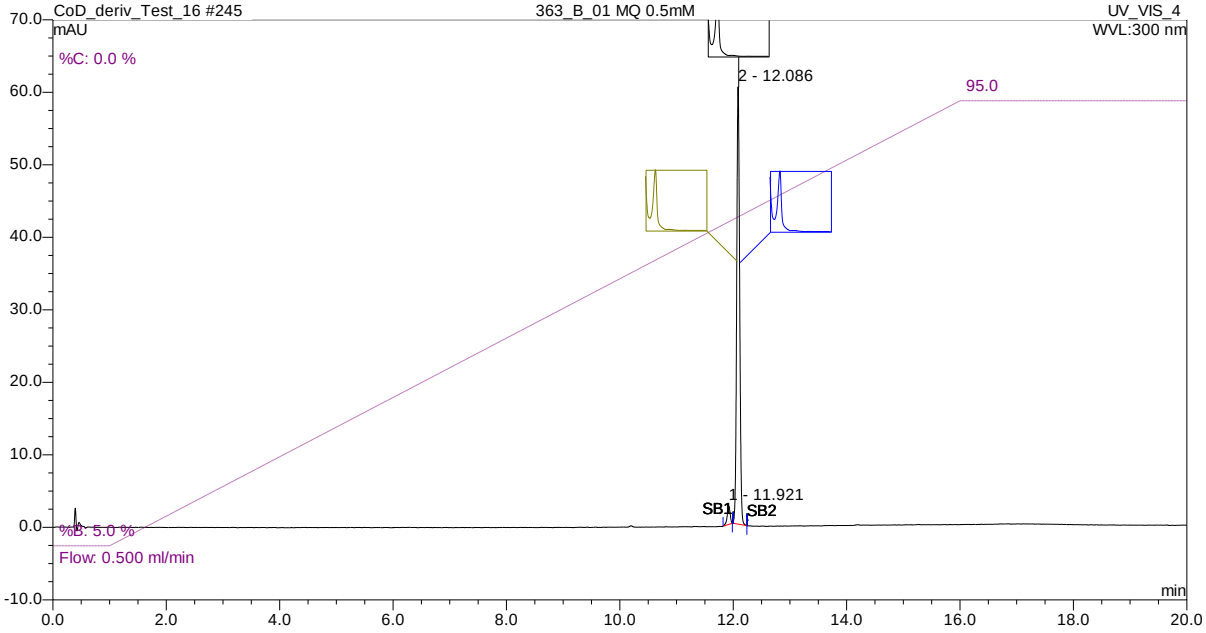

Fig. S1. HPLC chromatogram of [CoSAN-F$_2$]$^-$. Purity – 96.03%

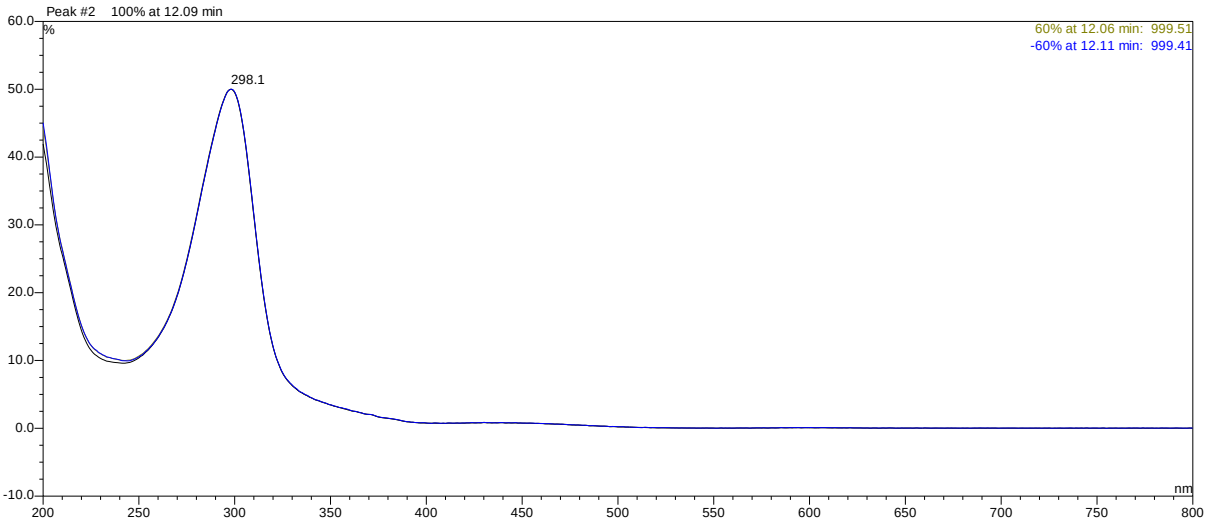

Fig. S2. UV-VIS spectrum of [CoSAN-F$_2$]$^-$ (peak purity analysis).

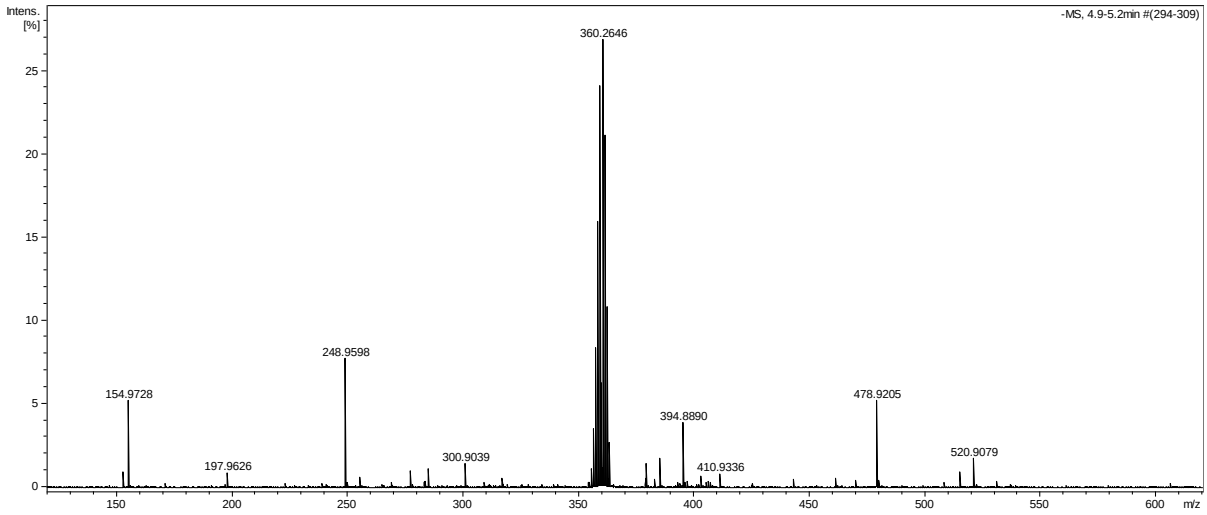

Fig. S3. ESI-MS spectrum of [CoSAN-F_2]$^-$.

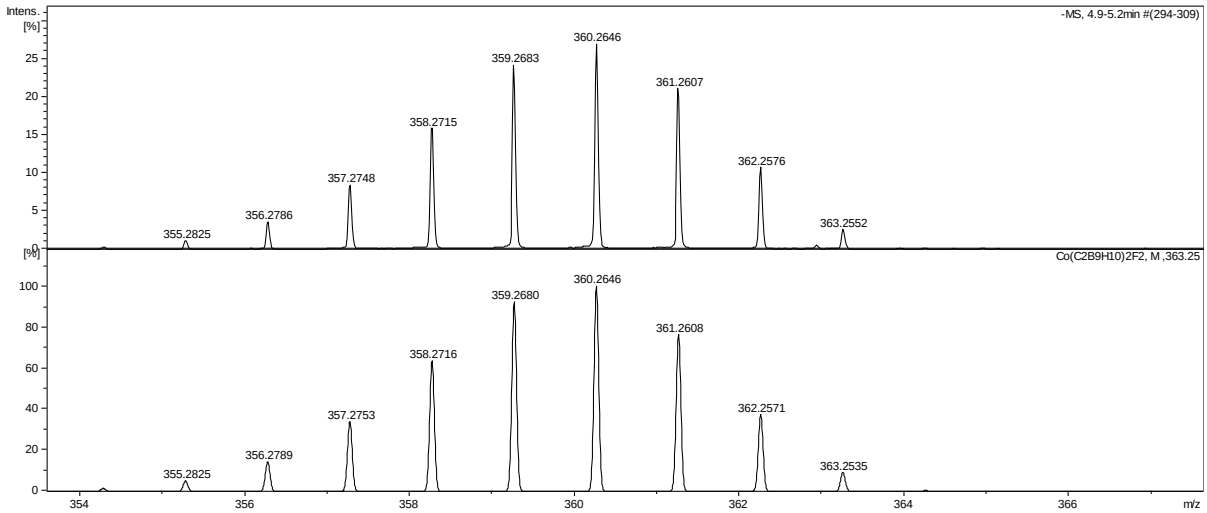

Fig. S4. Measured (top) and simulated (bottom) ESI-MS spectrum of [CoSAN-F_2]$^-$ – isotope pattern.

1.1.1.NMR spectra of **[CoSAN-F_2] × 1-Chloromethyl-1,4-diazoniabicyclo[2.2.2]octane] salt**

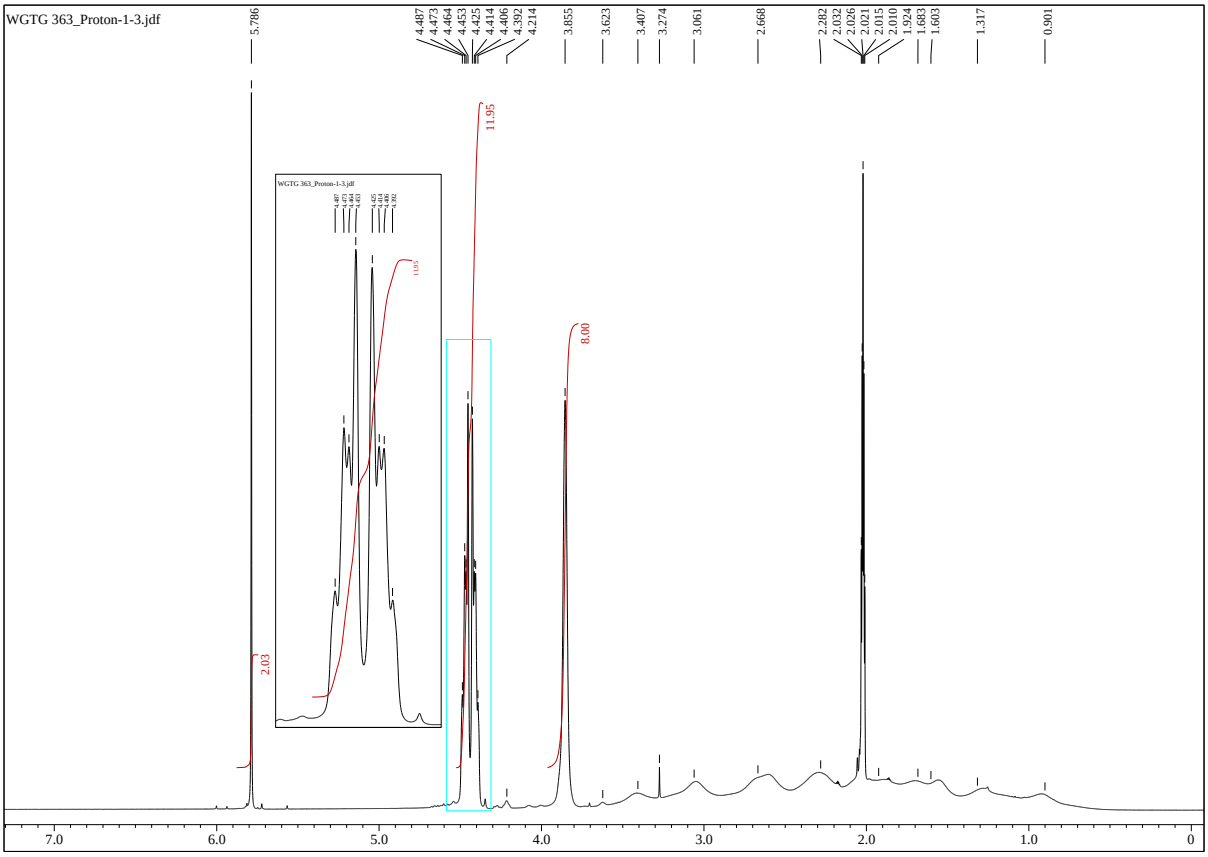

Fig. S5. ^{1}H NMR spectrum of [CoSAN-F_2] × 1-Chloromethyl-1,4-diazoniabicyclo[2.2.2]octane] salt in acetone-d_6 (400 MHz).

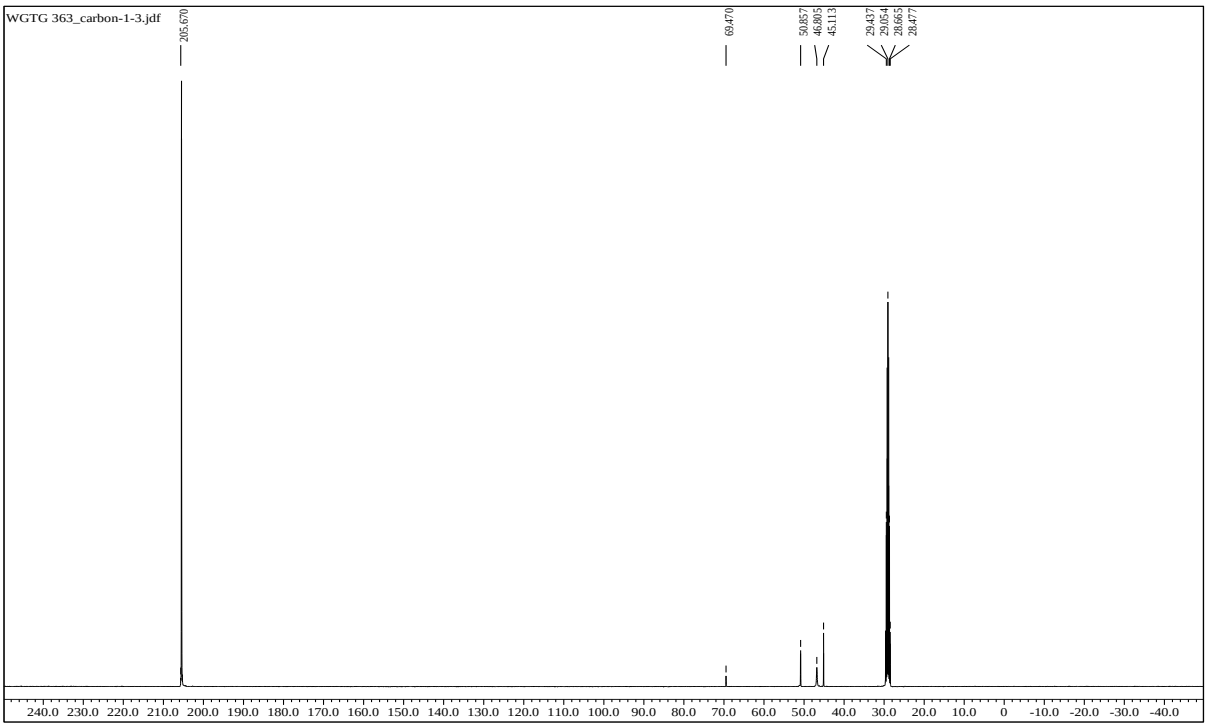

Fig. S6. $^{13}C\{^{1}H\}$ NMR spectrum of [[CoSAN-F_2] × 1-Chloromethyl-1,4-diazoniabicyclo[2.2.2]octane salt in acetone-d_6 (100 MHz).

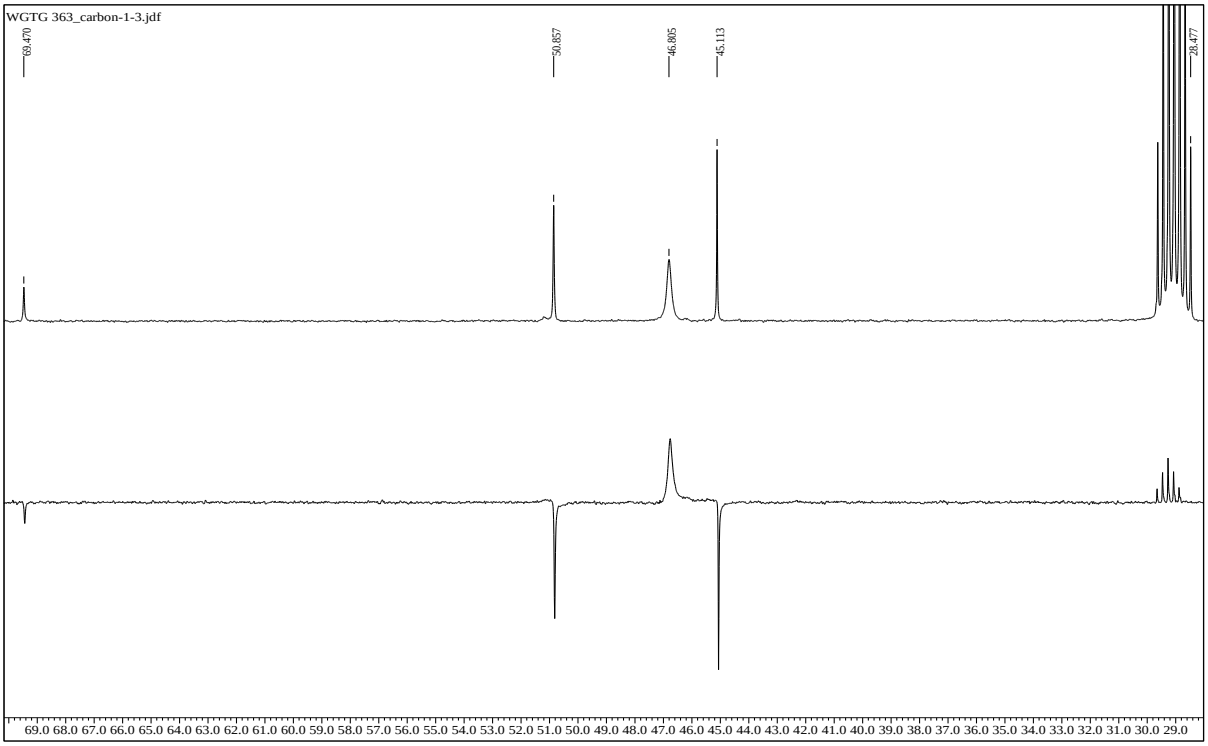

Fig. S7. Expanded $^{13}C\{^{1}H\}$ NMR (top) and DEPT 135 (bottom) spectra of [[CoSAN-F_2] × 1-Chloromethyl-1,4-diazoniabicyclo[2.2.2]octane] salt in acetone-d_6 (100 MHz).

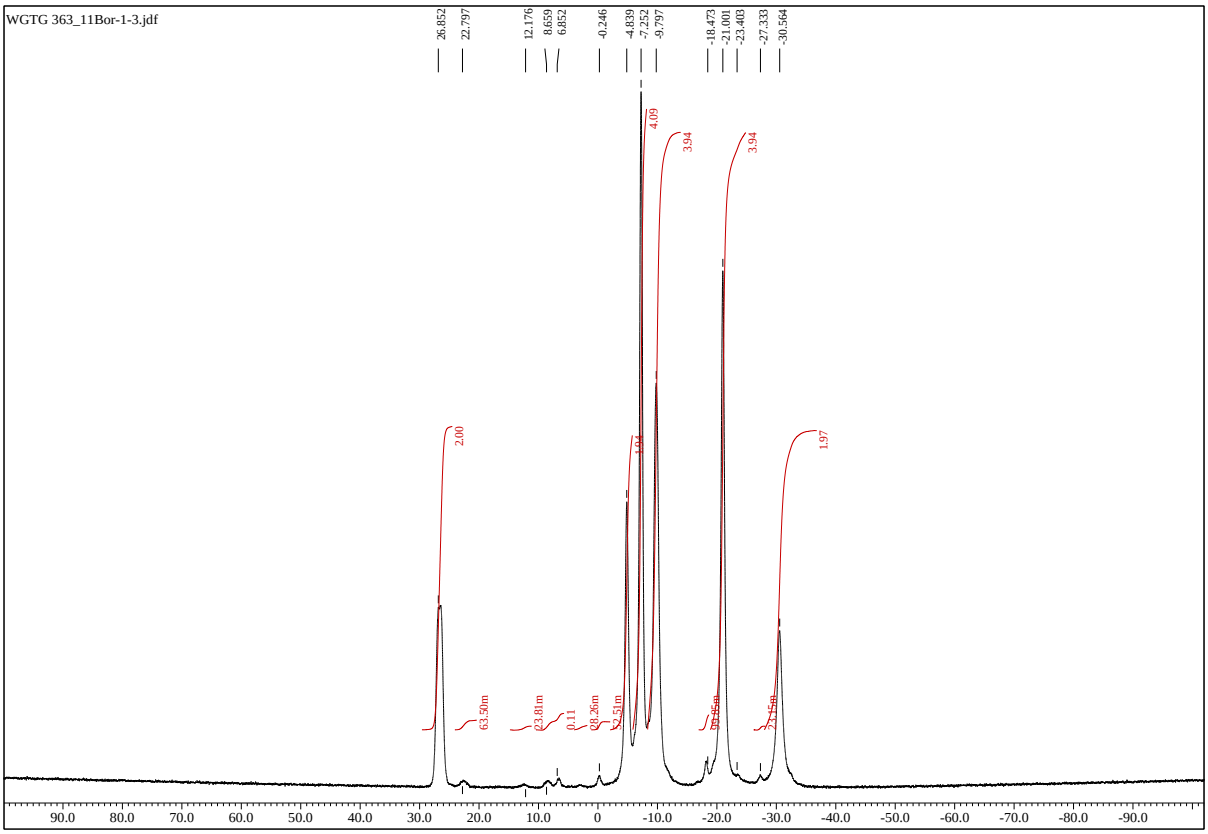

Fig. S8. $^{11}B\{^{1}H\}$ NMR spectrum of [[CoSAN-F_2] × 1-Chloromethyl-1,4-diazoniabicyclo[2.2.2]octane] salt in acetone-d_6 (128 MHz).

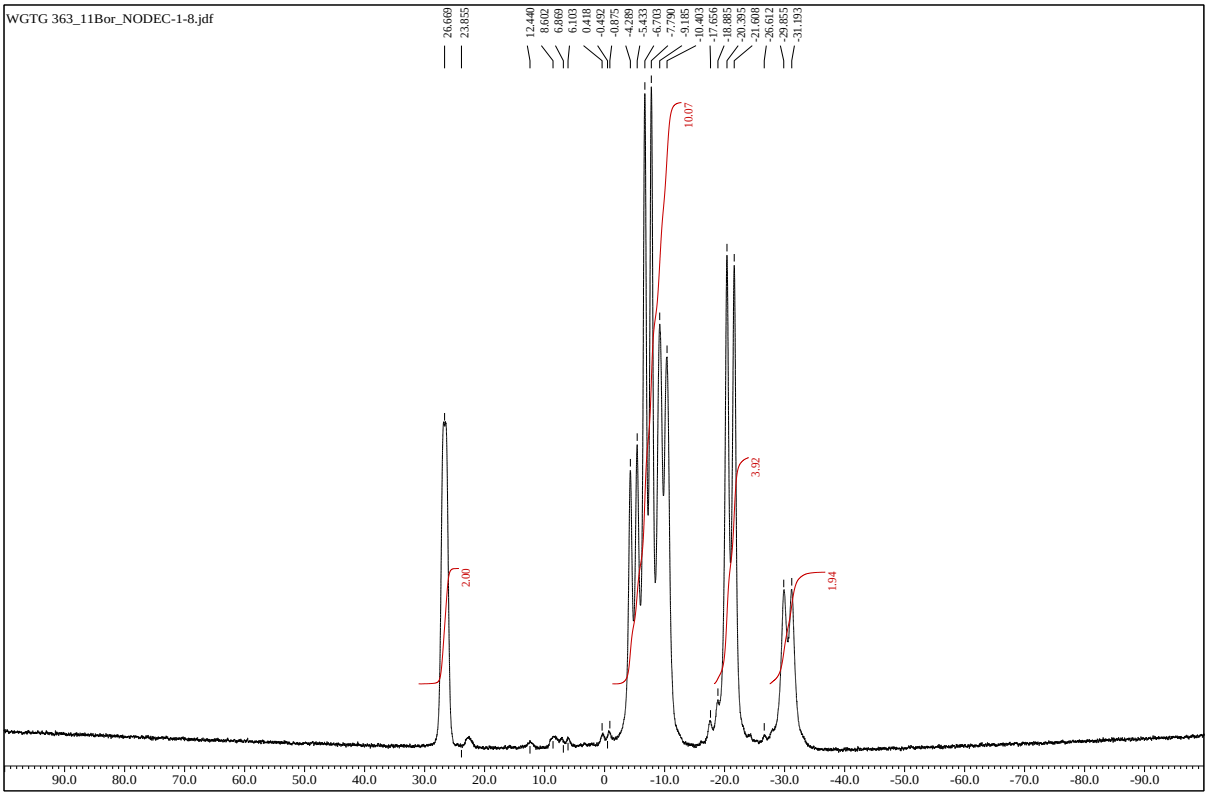

Fig. S9. ^{11}B NMR spectrum of [[CoSAN-F_2] × 1-Chloromethyl-1,4-diazoniabicyclo[2.2.2]octane] salt in acetone-d_6 (128 MHz).

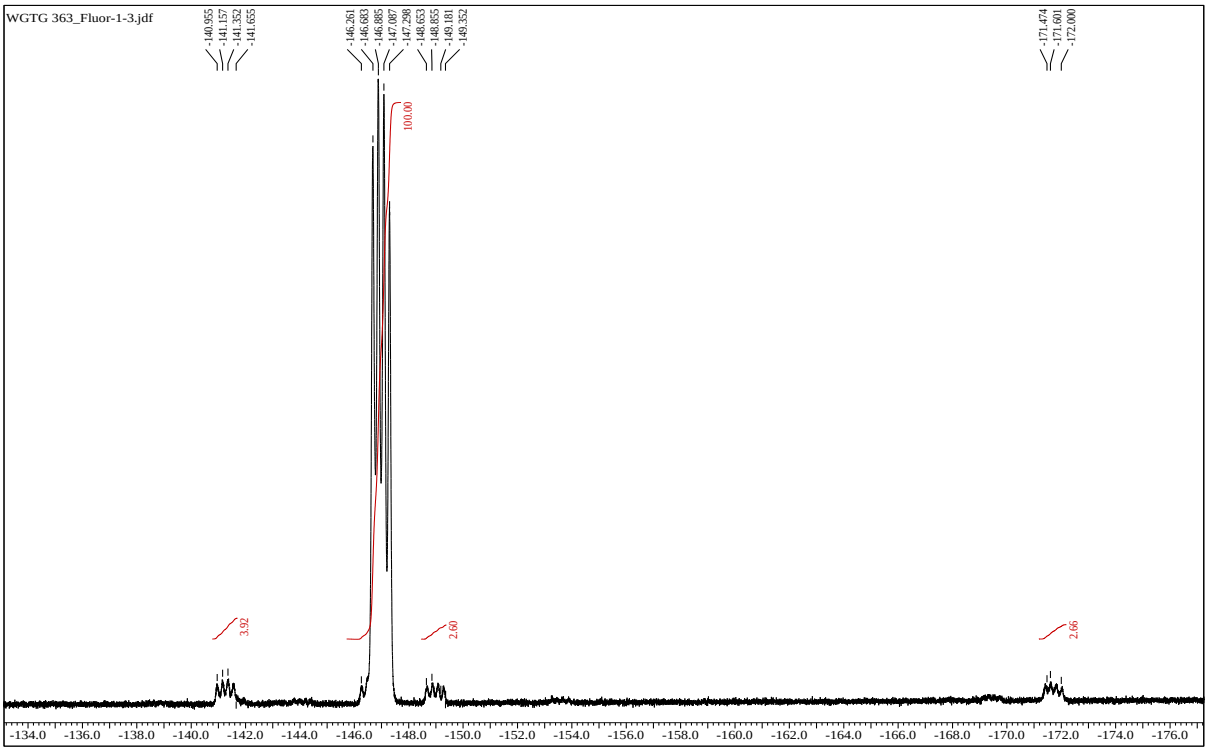

Fig. S10. ^{19}F NMR spectrum of [CoSAN-F_2] × 1-Chloromethyl-1,4-diazoniabicyclo[2.2.2]octane salt in acetone-d_6 (376 MHz).

1.1.2. NMR spectra of **H[CoSAN-F_2]**

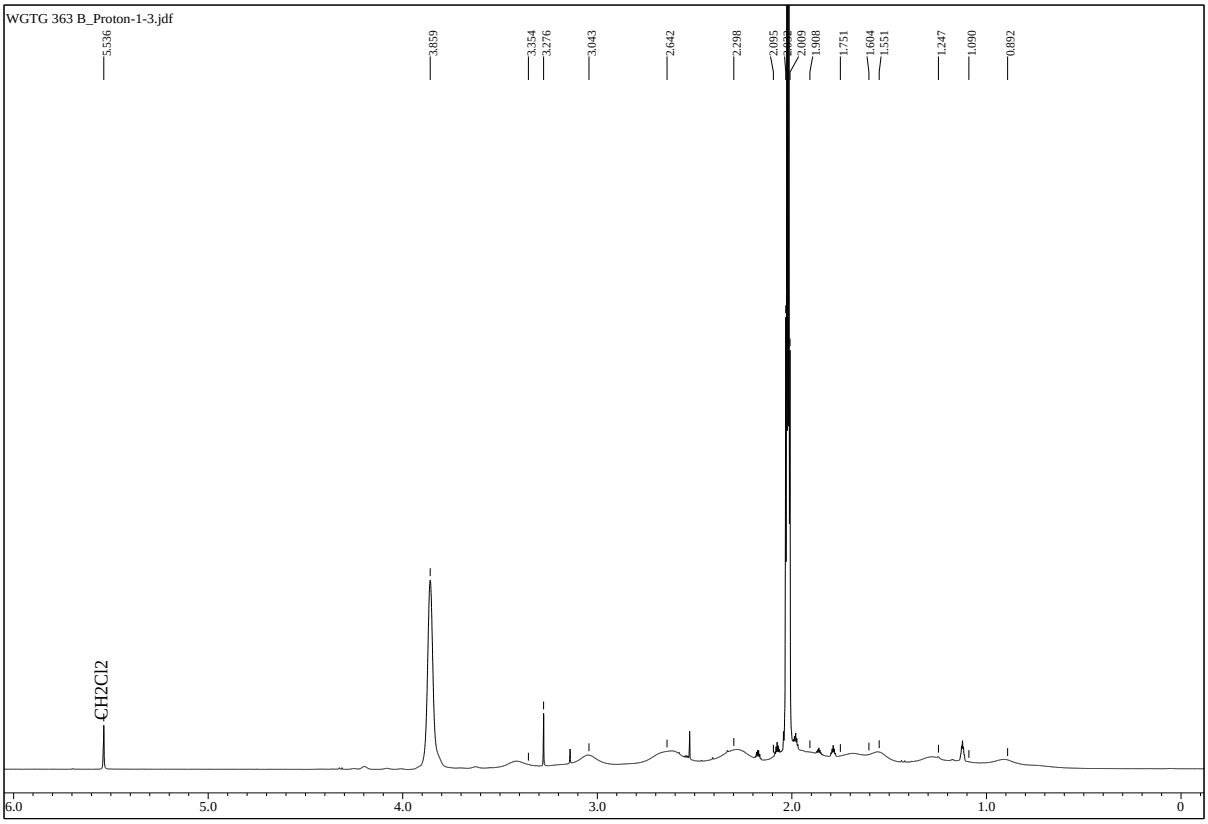

Fig. S11. ^{1}H NMR spectrum of H[CoSAN-F_2] in acetone-d_6 (400 MHz).

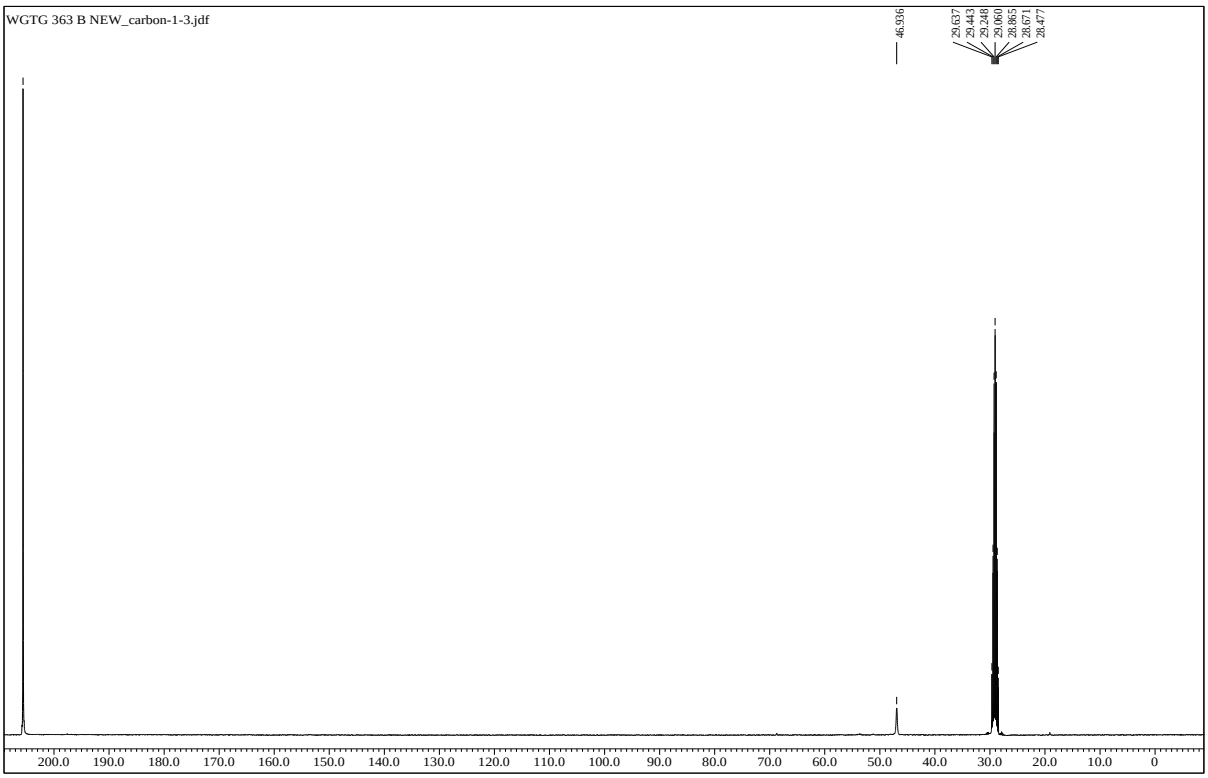

Fig. S12. $^{13}C\{^{1}H\}$ NMR spectrum of H[CoSAN-F_2] in acetone-d_6 (100 MHz).

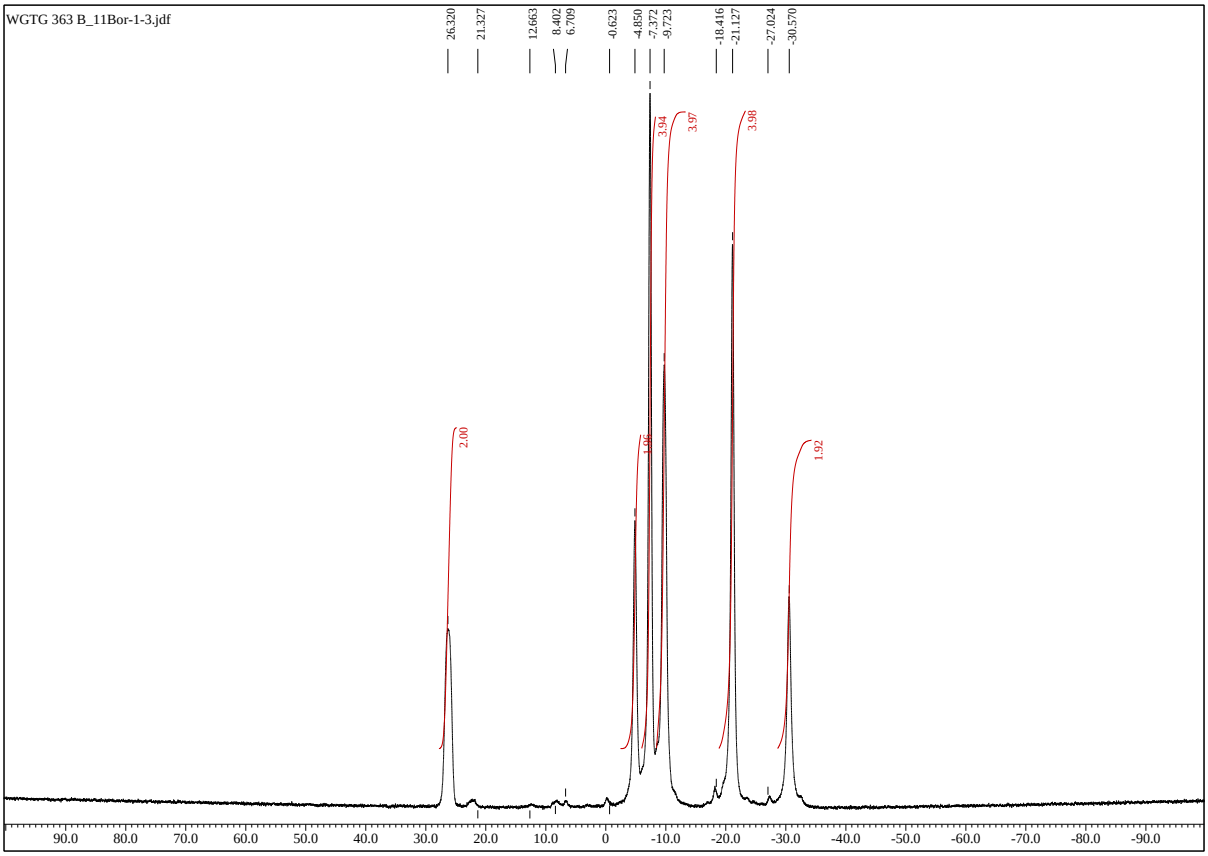

Fig. S13. $^{11}B\{^{1}H\}$ NMR spectrum of H[CoSAN-F_2] in acetone-d_6 (128 MHz).

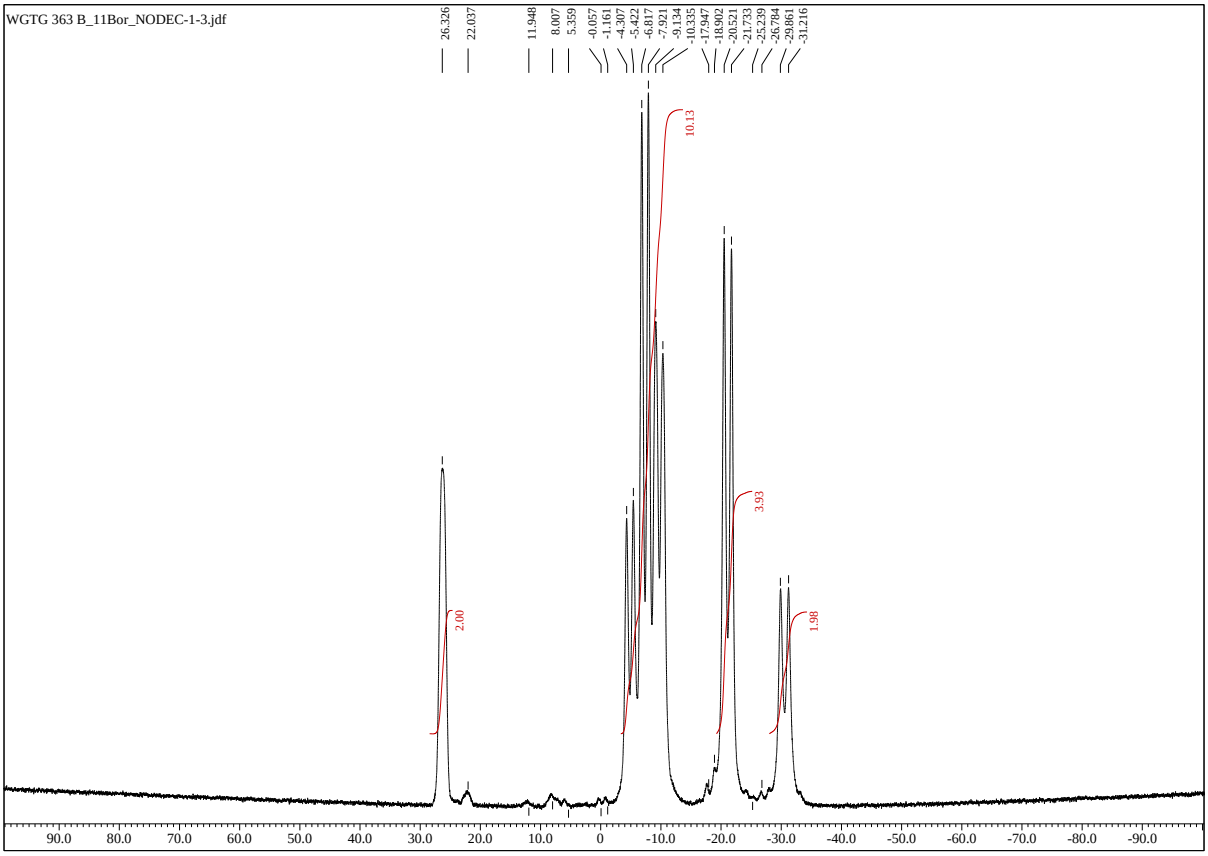

Fig. S14. ^{11}B NMR spectrum of H[CoSAN-F_2] in acetone-d_6 (128 MHz).

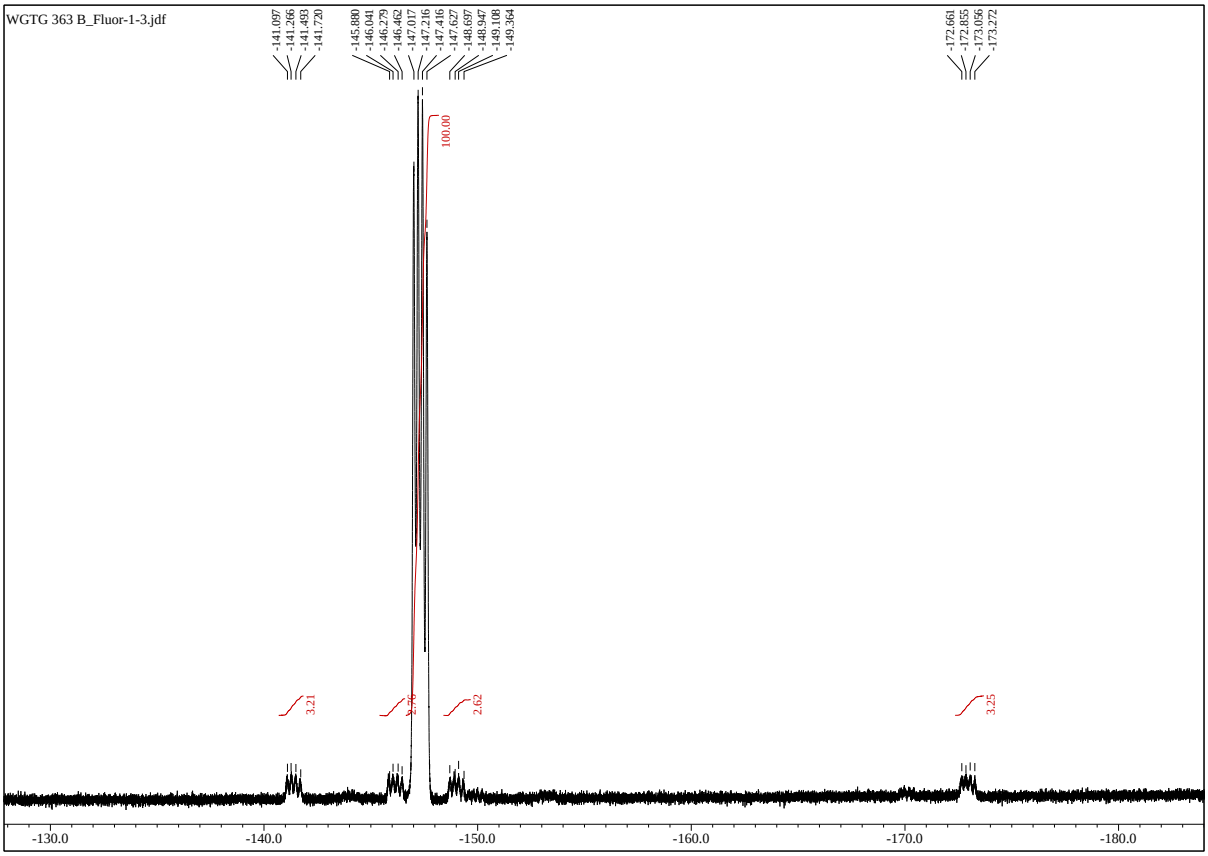

Fig. S15. ^{19}F NMR spectrum of H[CoSAN-F_2] in acetone-d_6 (376 MHz).

1.1.3.Characterization of **H[CoSAN-F]** – the major side product of **H[CoSAN-F$_2$]** synthesis

Mass spectra of the major side product - H[CoSAN-F]). Retention time of 11.91 min. (3.97%) on the full gradient chromatogram (Fig. S1)

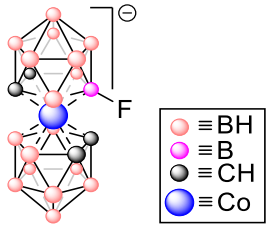

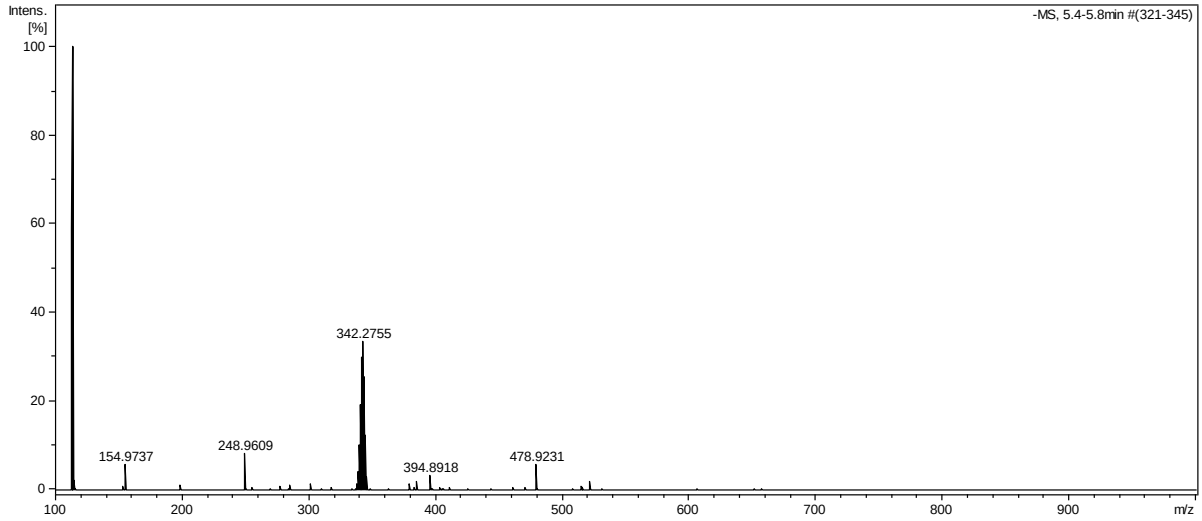

Fig. S16. ESI-MS spectrum of H[CoSAN-F].

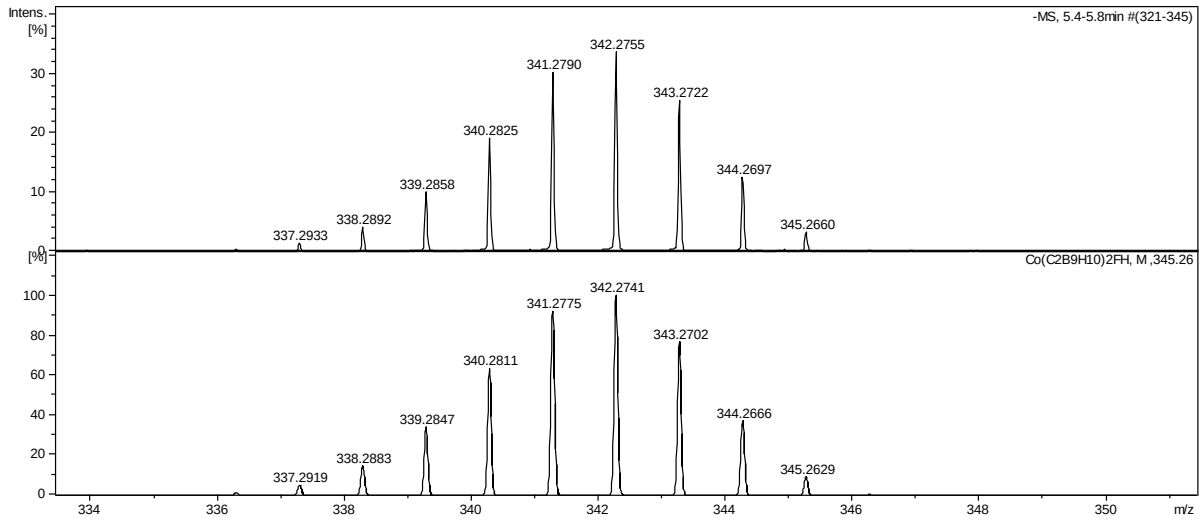

Fig. S17. Measured (top) and simulated (bottom) ESI-MS spectrum of H[CoSAN-F] – isotope pattern.

1.2. Characterization of **[CoSAN-Cl$_2$]$^-$**

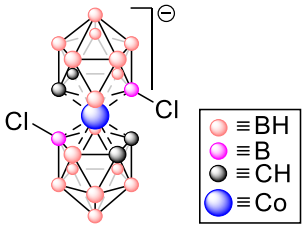

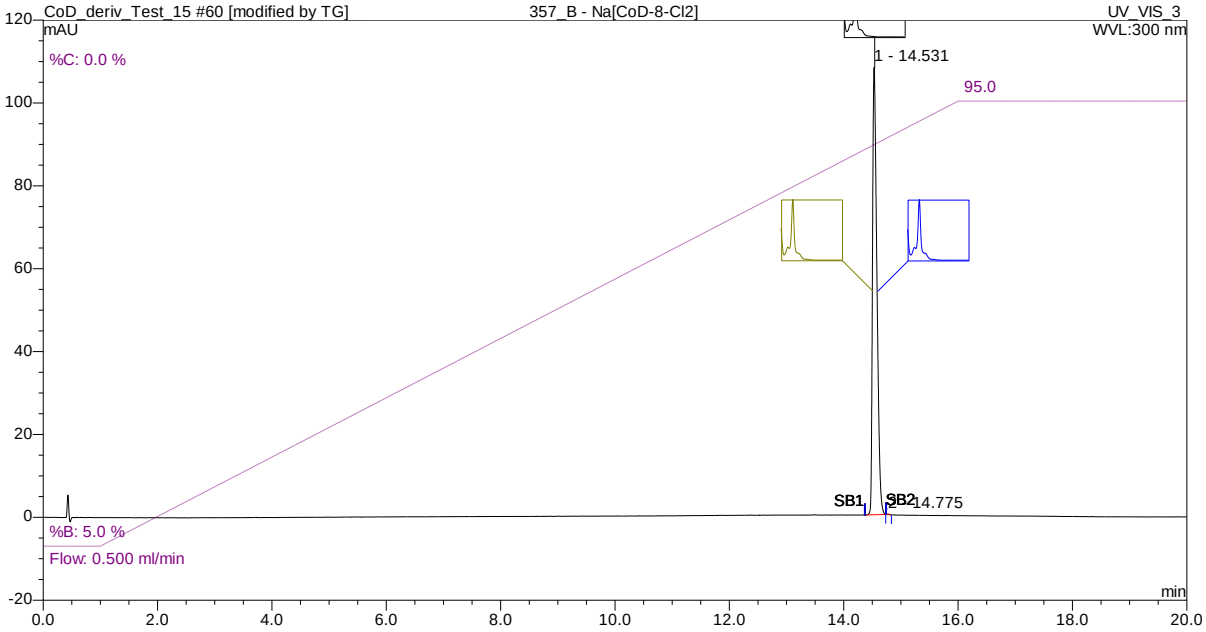

Fig. S18. HPLC chromatogram of [CoSAN-Cl$_2$]$^-$. Purity – 99.93%

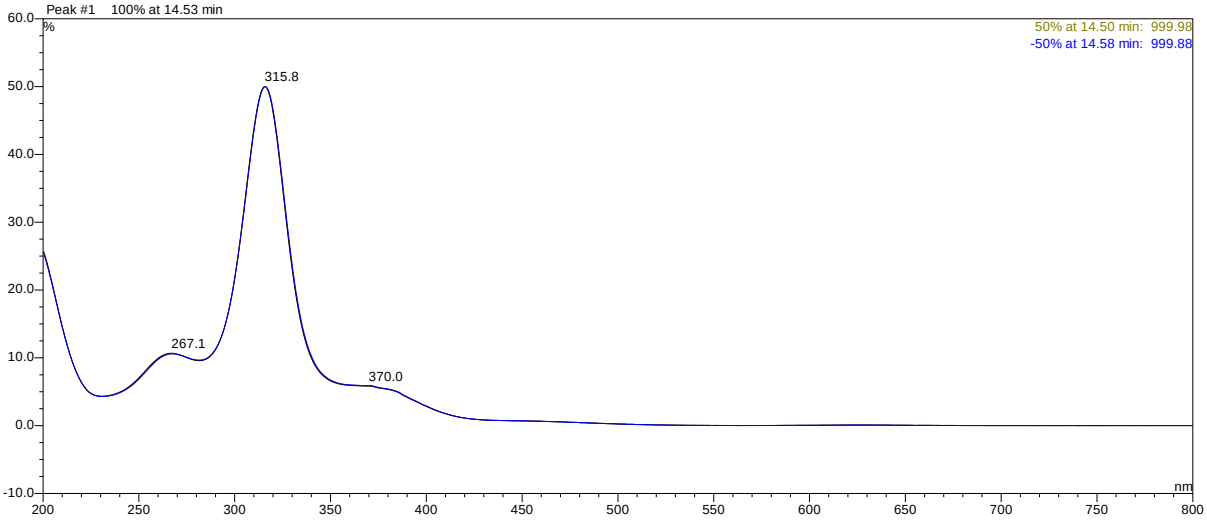

Fig. S19. UV-VIS spectrum of [CoSAN-Cl$_2$]$^-$ (peak purity analysis).

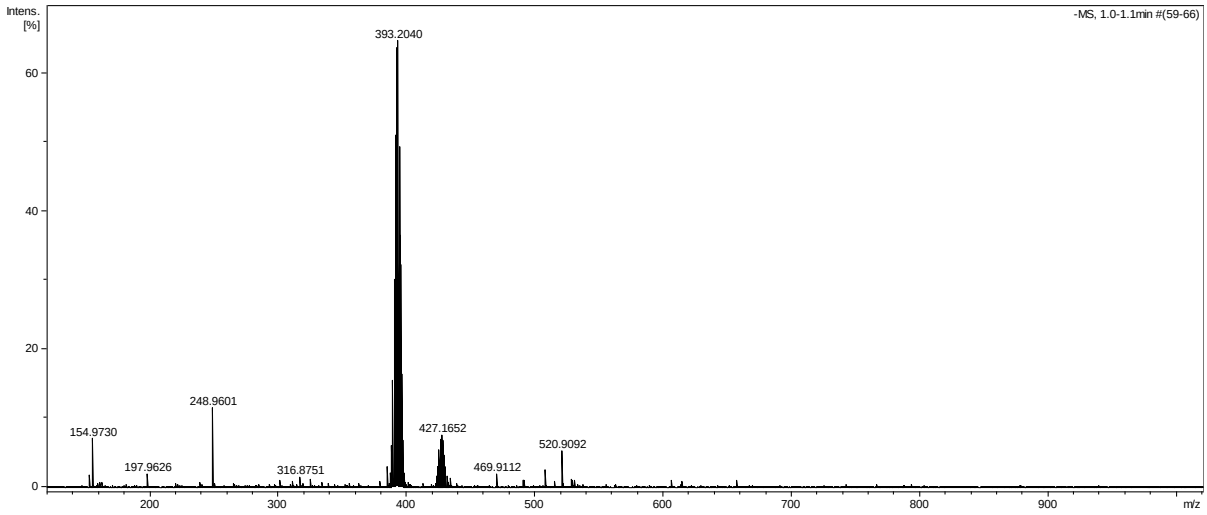

Fig. S20. ESI-MS spectrum of [CoSAN-Cl$_2$]$^-$.

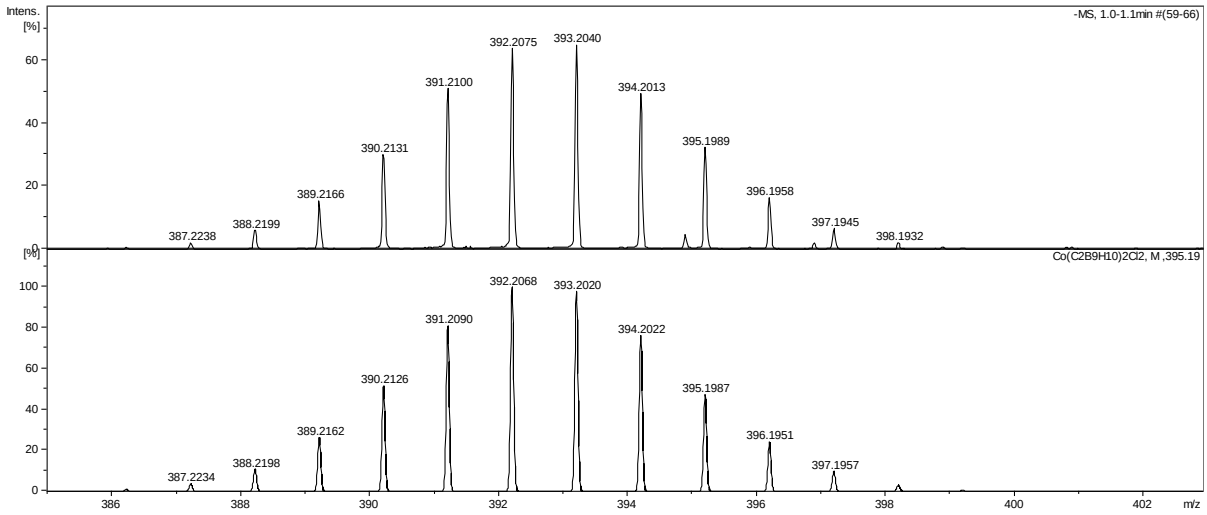

Fig. S21. Measured (top) and simulated (bottom) ESI-MS spectrum of [CoSAN-Cl$_2$]$^-$ – isotope pattern.

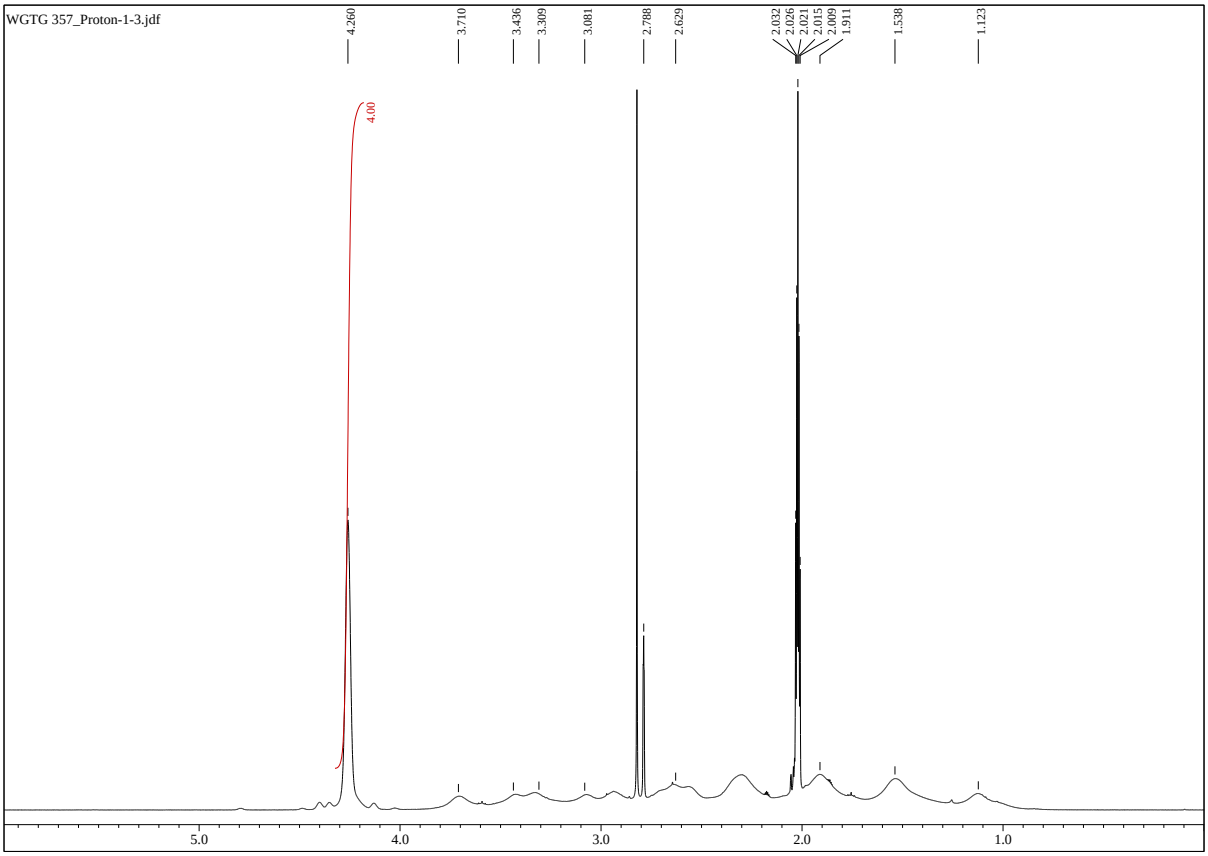

Fig. S22. ^{1}H NMR spectrum of Cs[CoSAN-Cl_2] in acetone-d_6 (400 MHz).

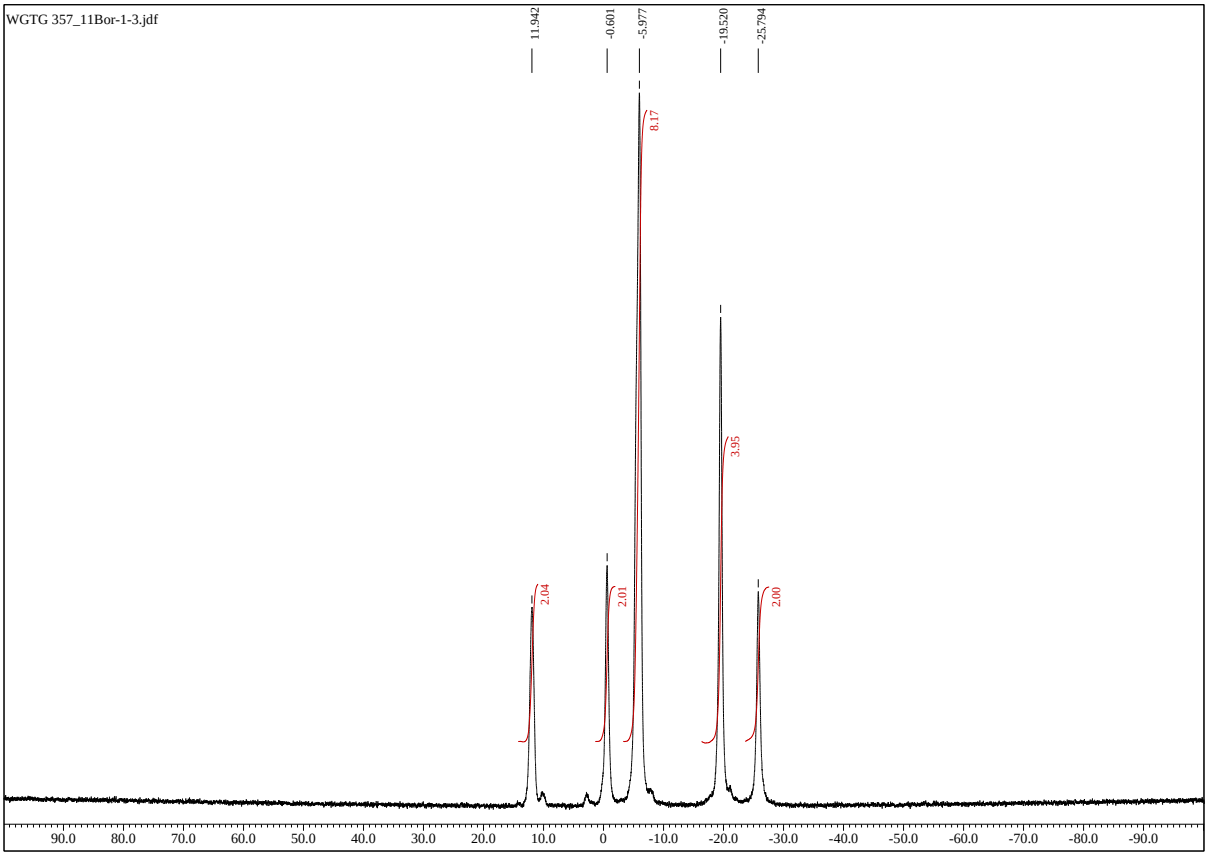

Fig. S23. $^{11}B\{^{1}H\}$ NMR spectrum of Cs[CoSAN-Cl_2] in acetone-d_6 (128 MHz).

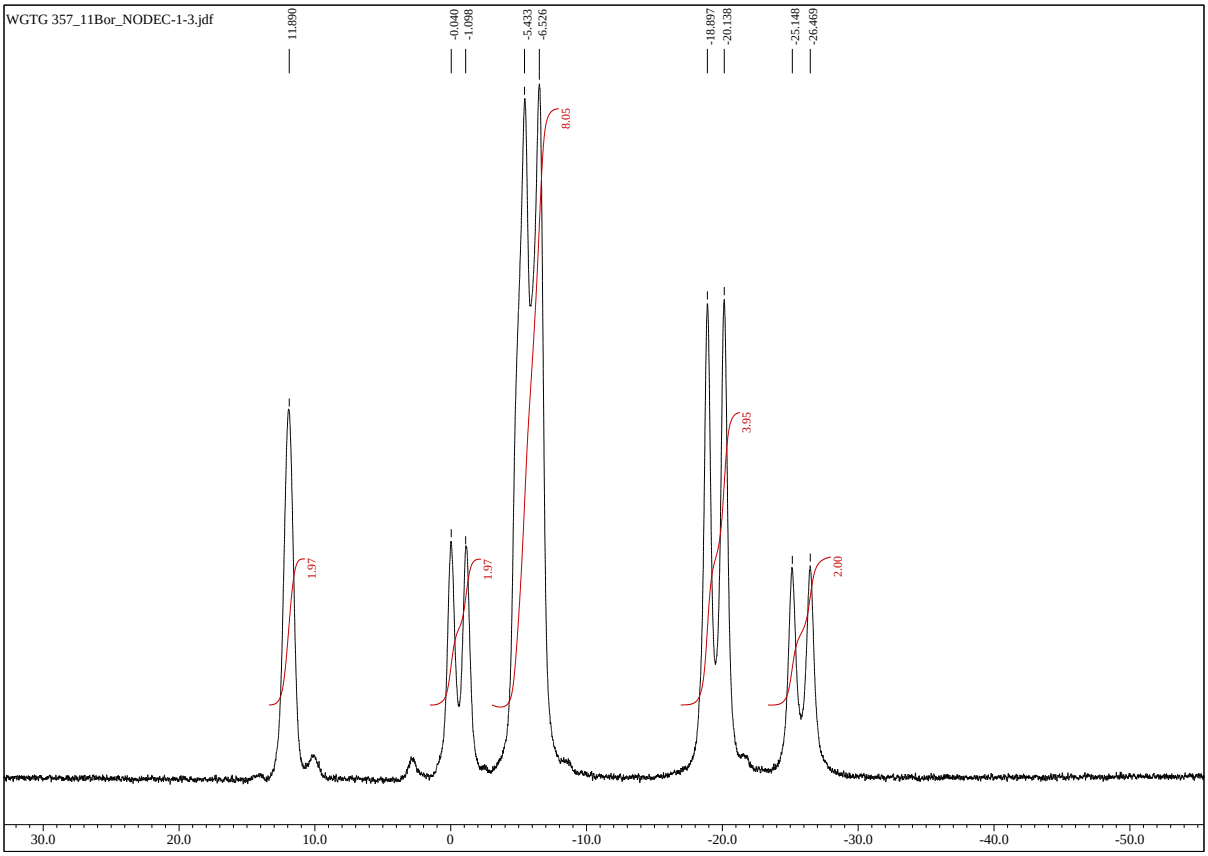

Fig. S24. ^{11}B NMR spectrum of Cs[CoSAN-Cl_2] in acetone-d_6 (128 MHz).

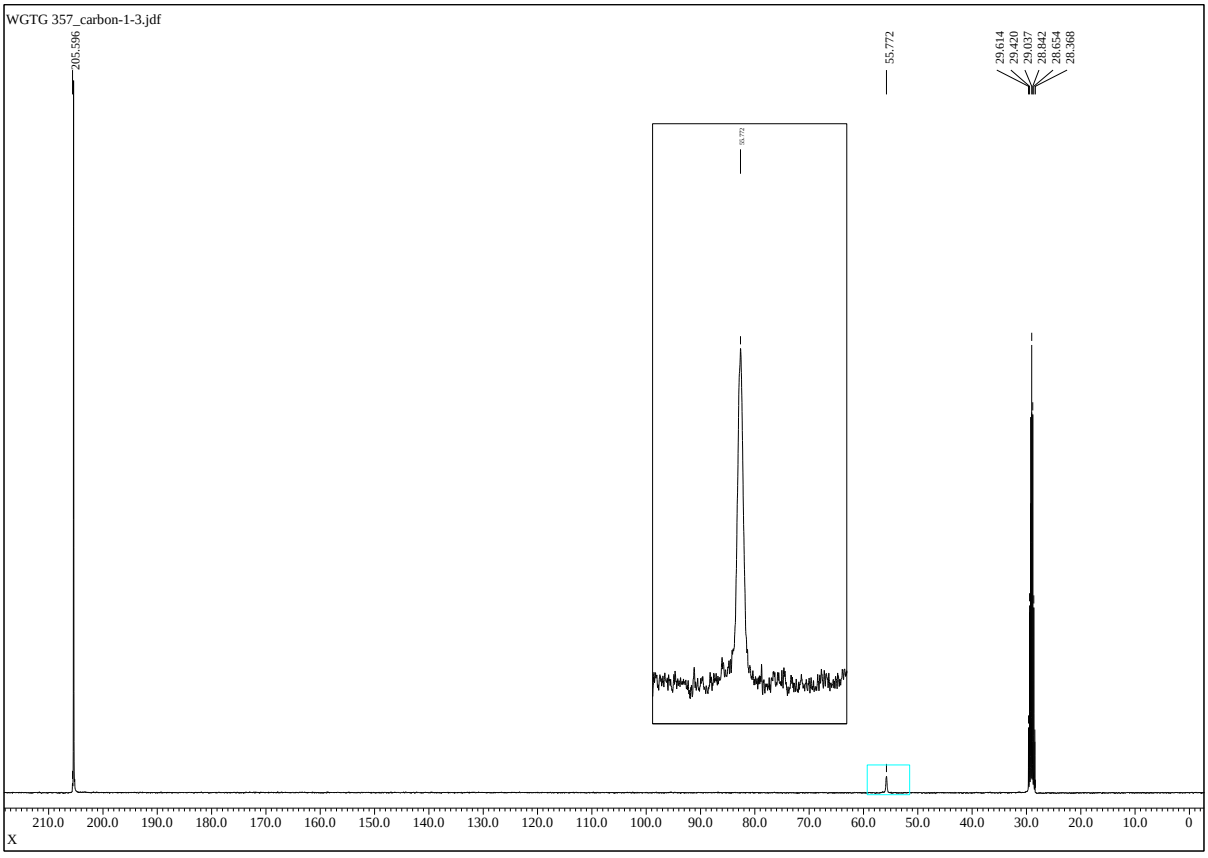

Fig. S25. $^{13}C\{^1H\}$ NMR spectrum of Cs[CoSAN-Cl_2] in acetone-d_6 (100 MHz).

1.3. Characterization of **[CoSAN-Br$_2$]$^-$**

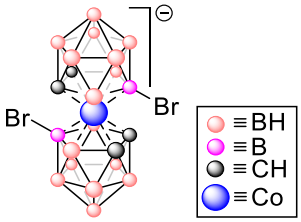

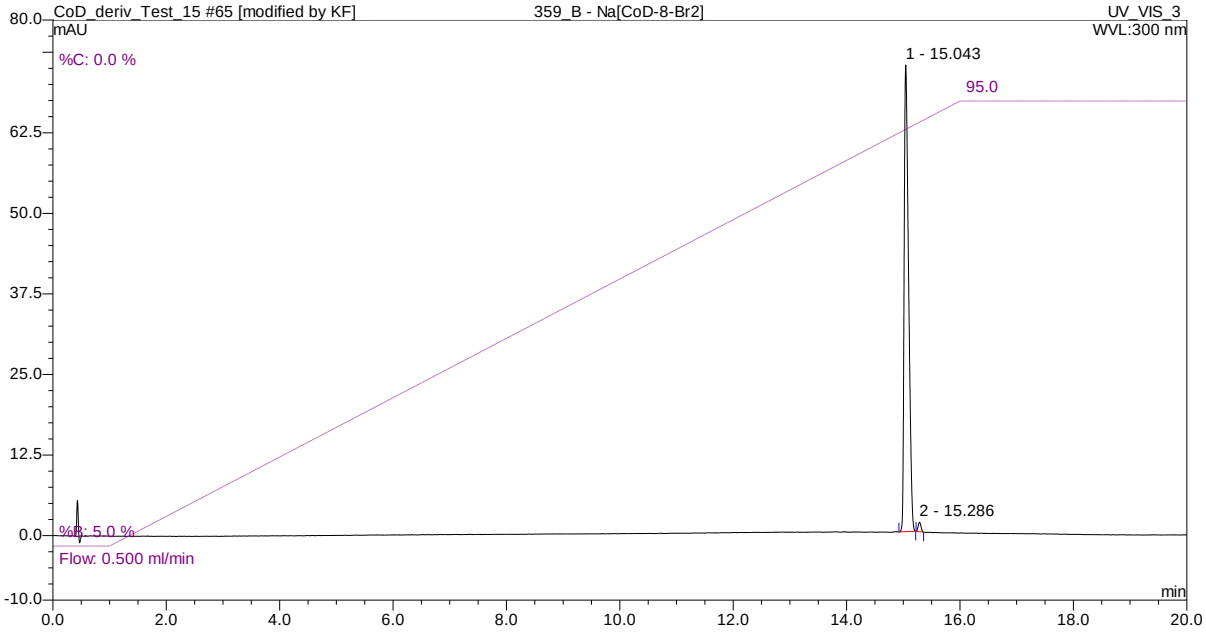

Fig. S26. HPLC chromatogram of [CoSAN-Br$_2$]$^-$. Purity – 98.73%

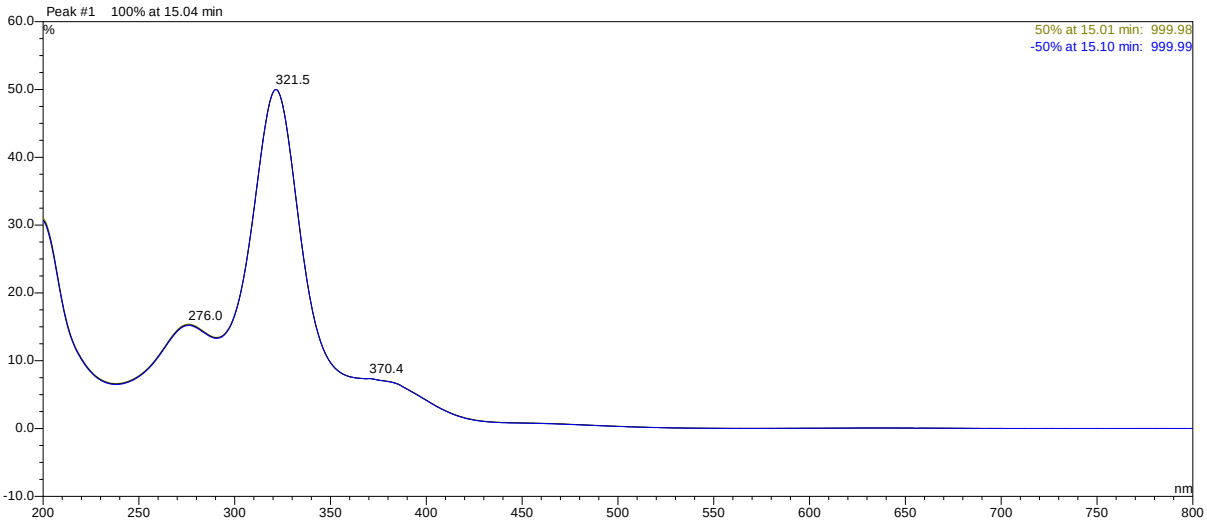

Fig. S27. UV-VIS spectrum of [CoSAN-Br$_2$]$^-$ (peak purity analysis).

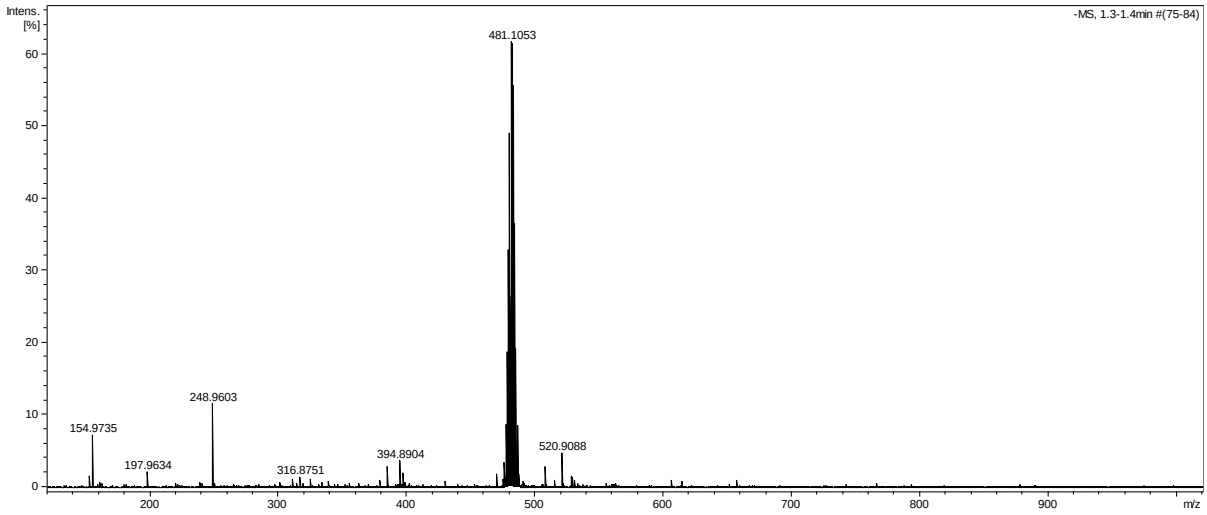

Fig. S28. ESI-MS spectrum of $[CoSAN\text{-}Br_2]^-$

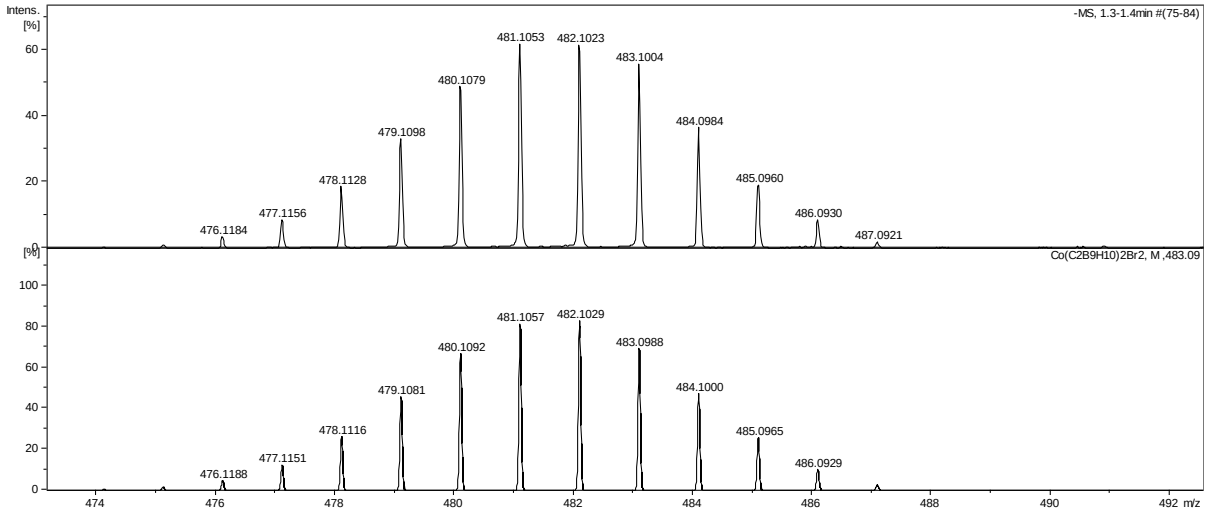

Fig. S29. Measured (top) and simulated (bottom) ESI-MS spectrum of $[CoSAN\text{-}Br_2]^-$ – isotope pattern.

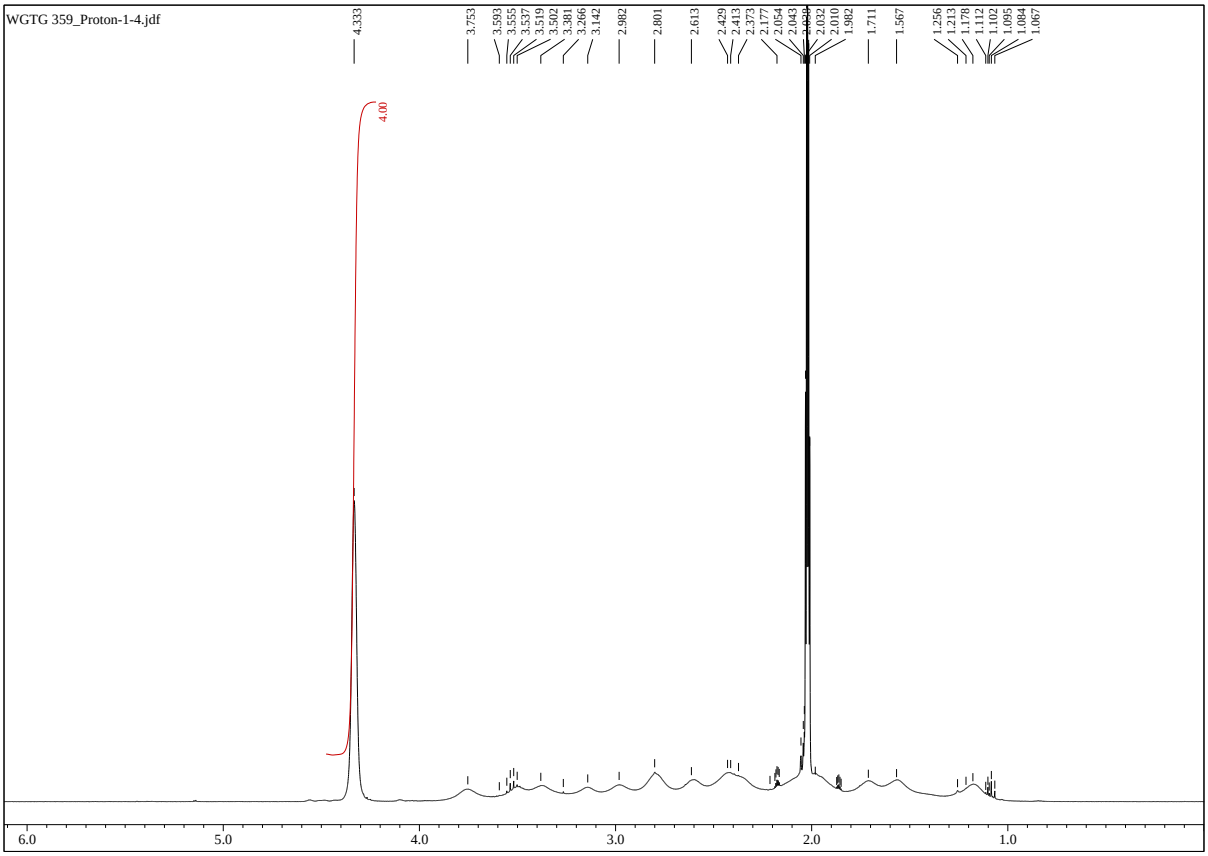

Fig. S30. ^{1}H NMR spectrum of Cs[CoSAN-Br$_2$] in acetone-d$_6$ (400 MHz).

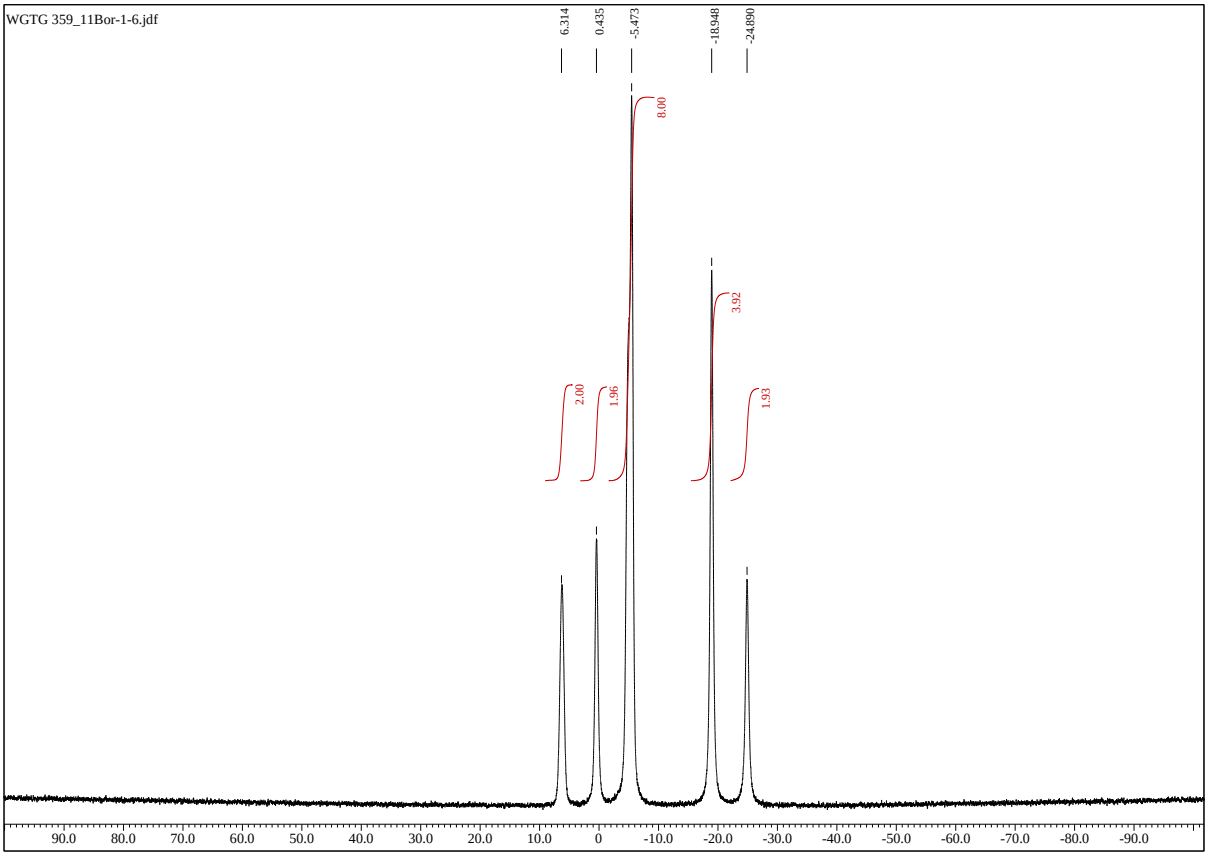

Fig. S31. Fig. S28. $^{11}B\{^{1}H\}$ NMR spectrum of Cs[CoSAN-Br$_2$] in acetone-d$_6$ (128 MHz).

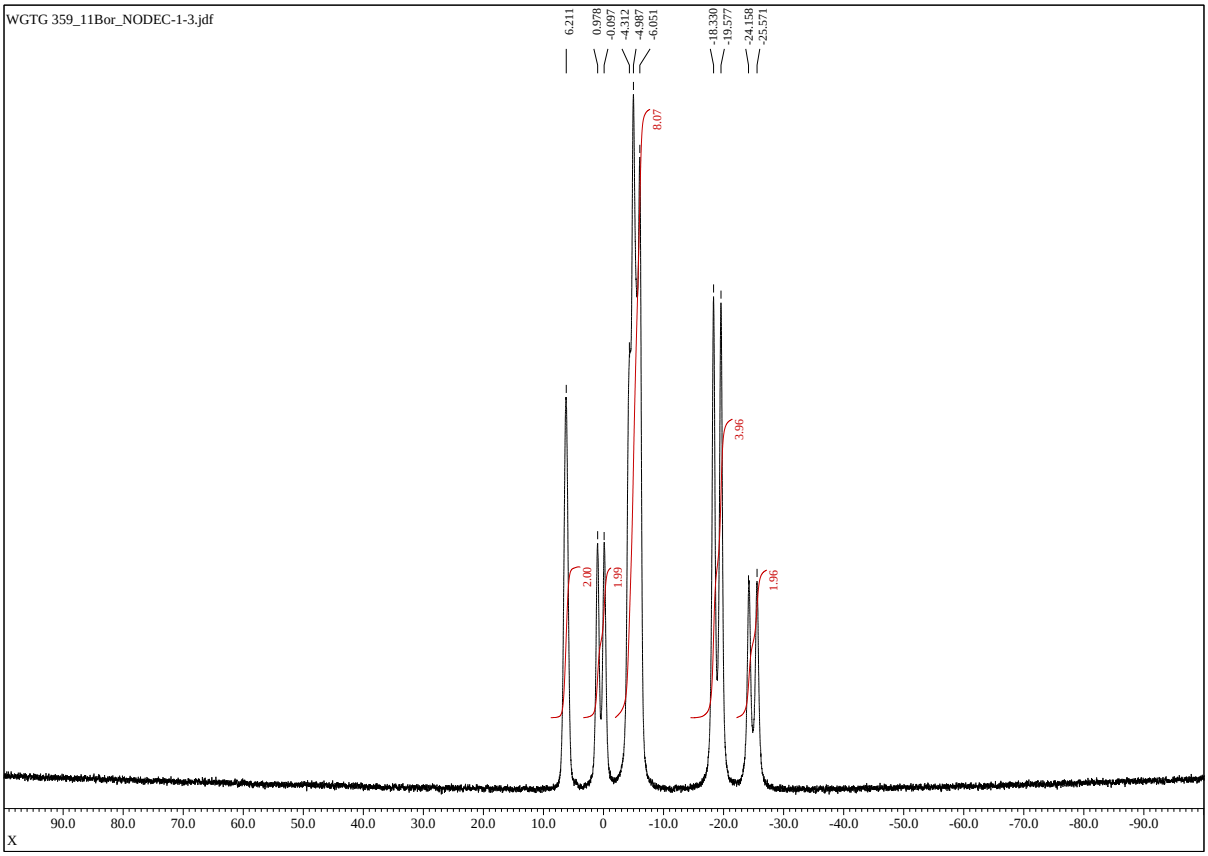

Fig. S32. ^{11}B NMR spectrum of Cs[CoSAN-Br_2] in acetone-d_6 (128 MHz).

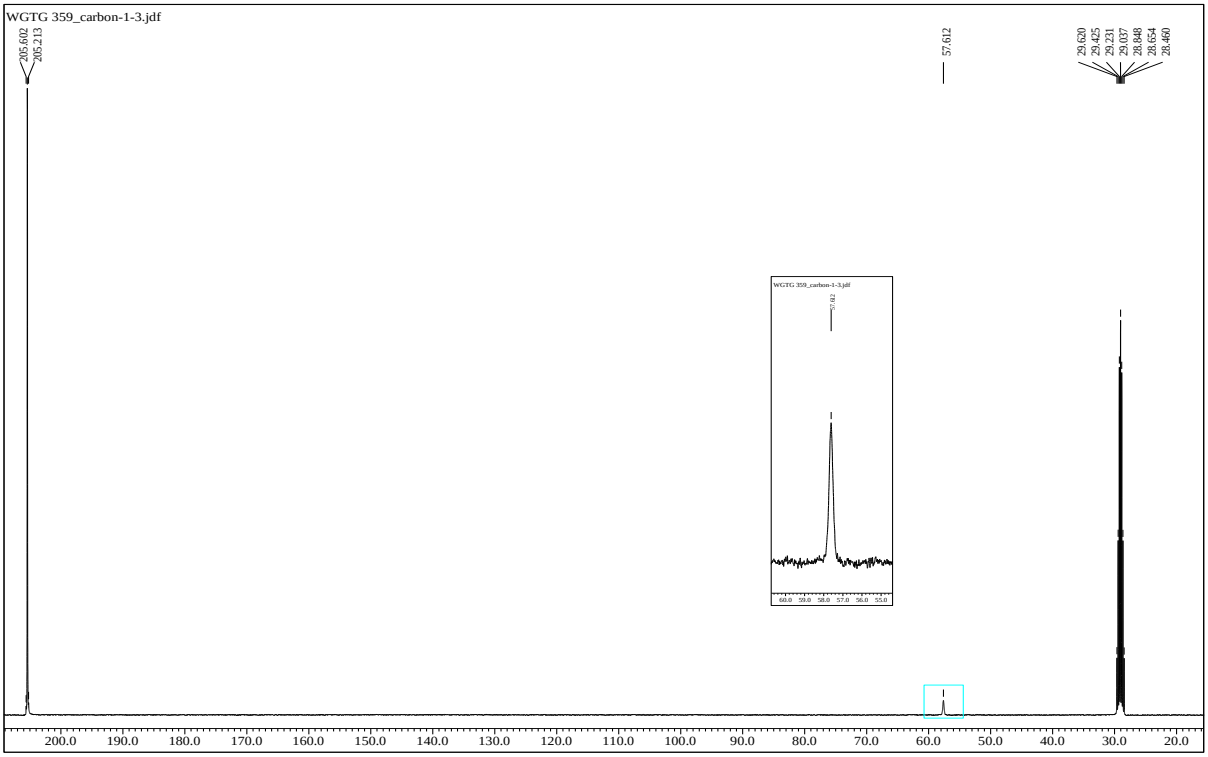

Fig. S33. $^{13}C\{^1H\}$ NMR spectrum of Cs[CoSAN-Br_2] in acetone-d_6 (100 MHz).

1.4. Characterization of **[CoSAN-I$_2$]$^-$**

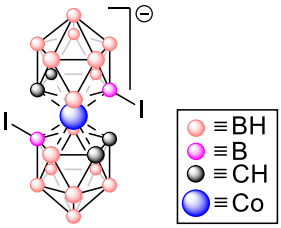

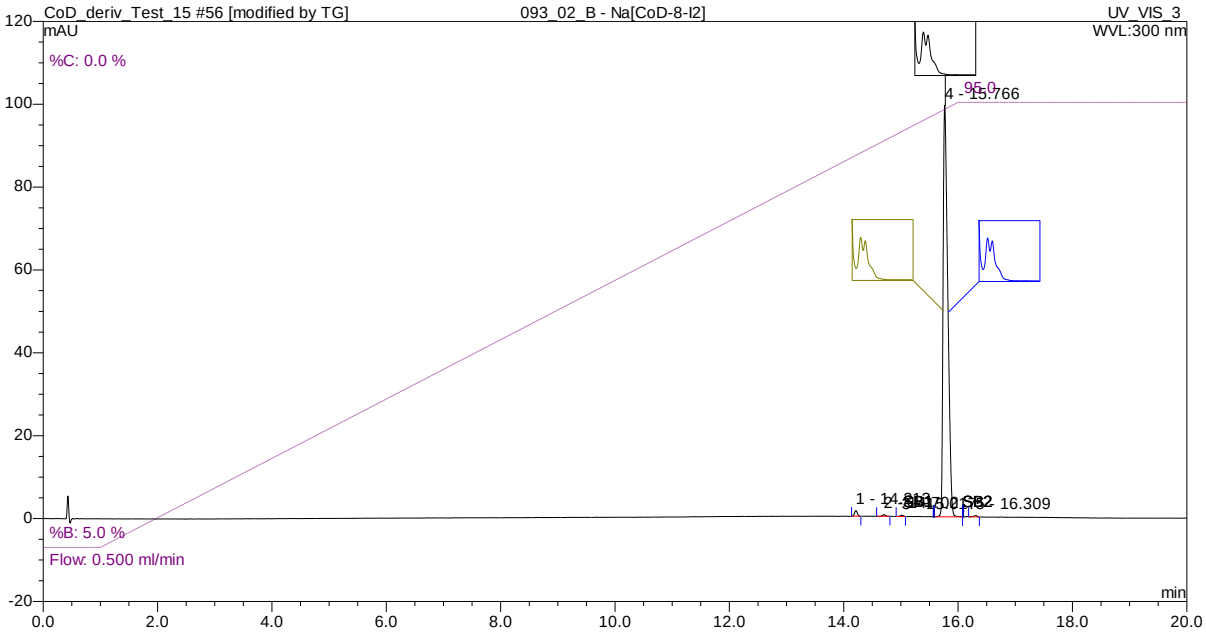

Fig. S34. HPLC chromatogram of [CoSAN-I$_2$]$^-$. Purity – 98.54%

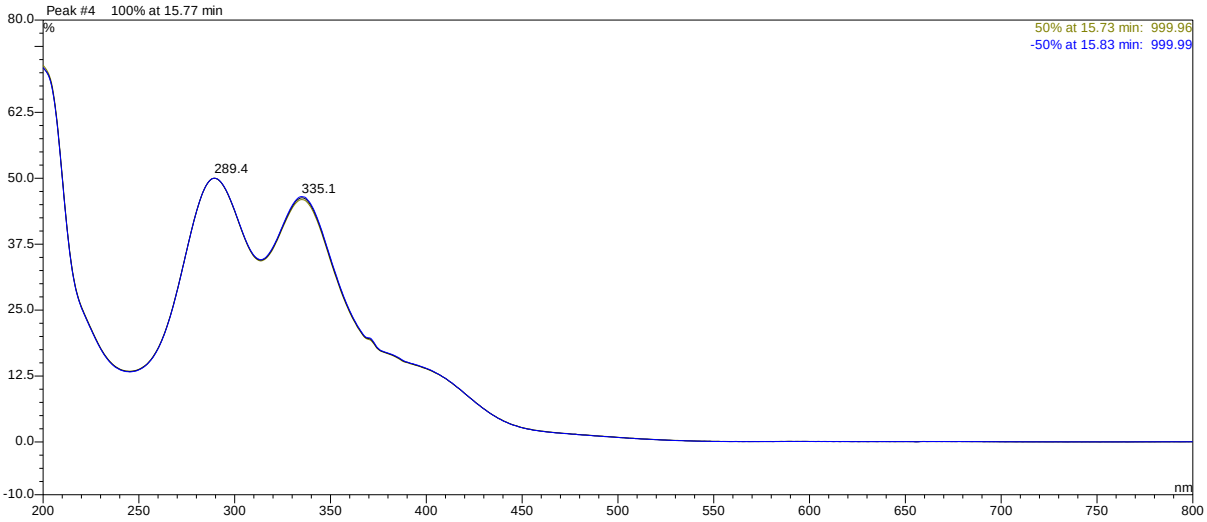

Fig. S35. UV-VIS spectrum of [CoSAN-I$_2$]$^-$ (peak purity analysis).

1.5. Characterization of **[CoSAN-Cl]$^-$**

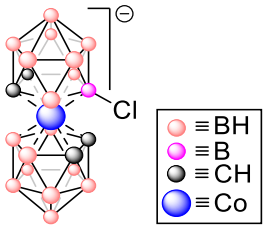

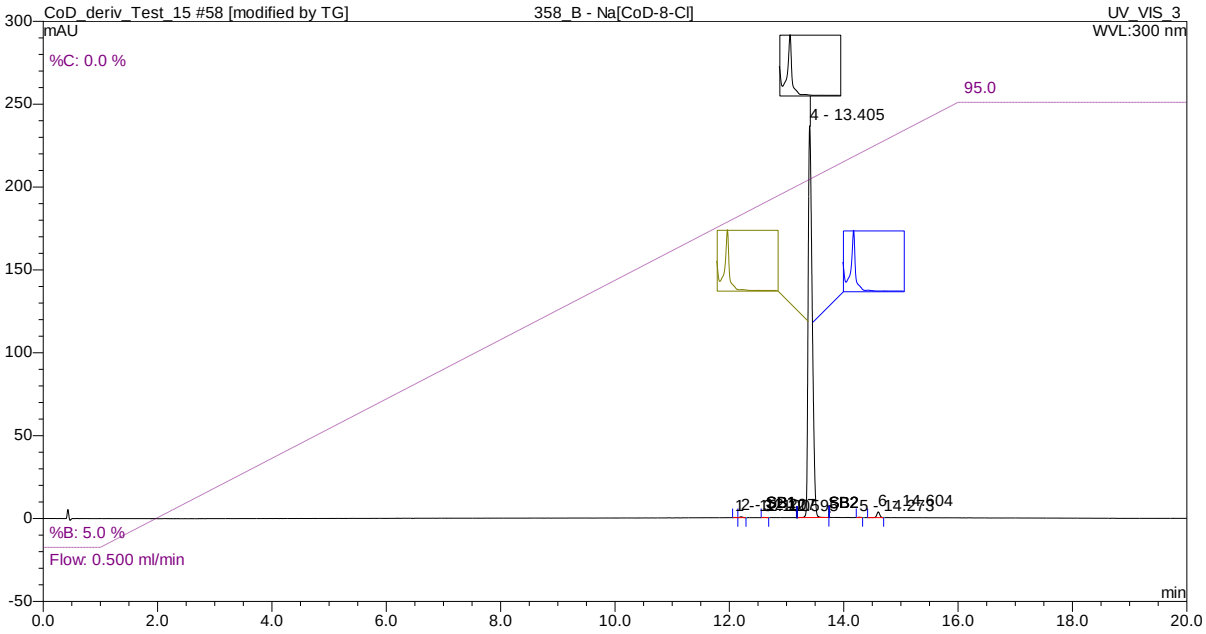

Fig. S36. HPLC chromatogram of [CoSAN-Cl]$^-$. Purity – 98.73%

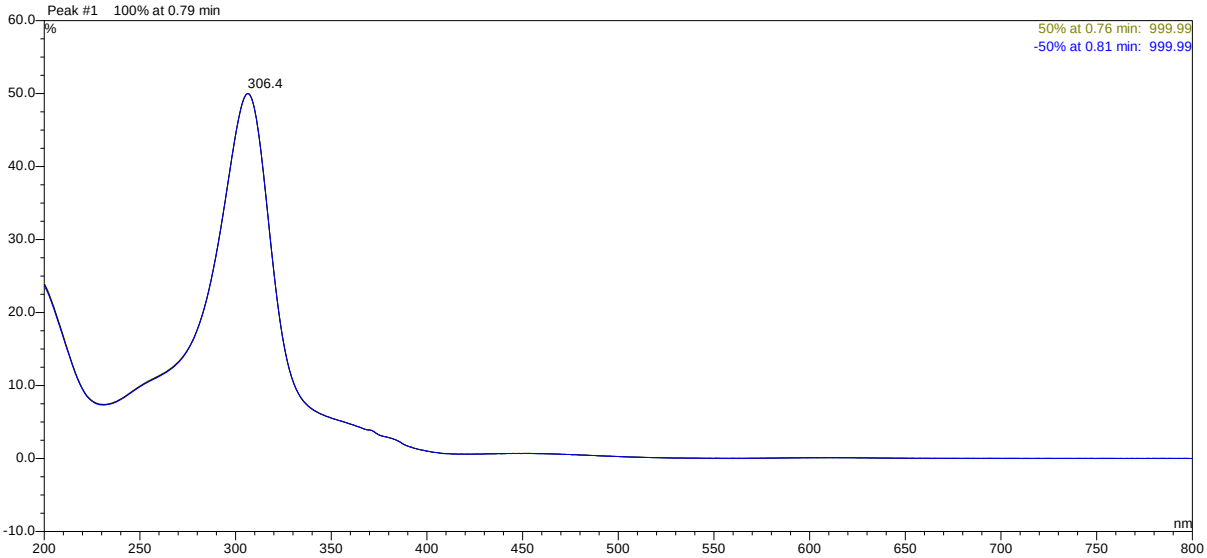

Fig. S37. UV-VIS spectrum of [CoSAN-Cl]$^-$ (peak purity analysis).

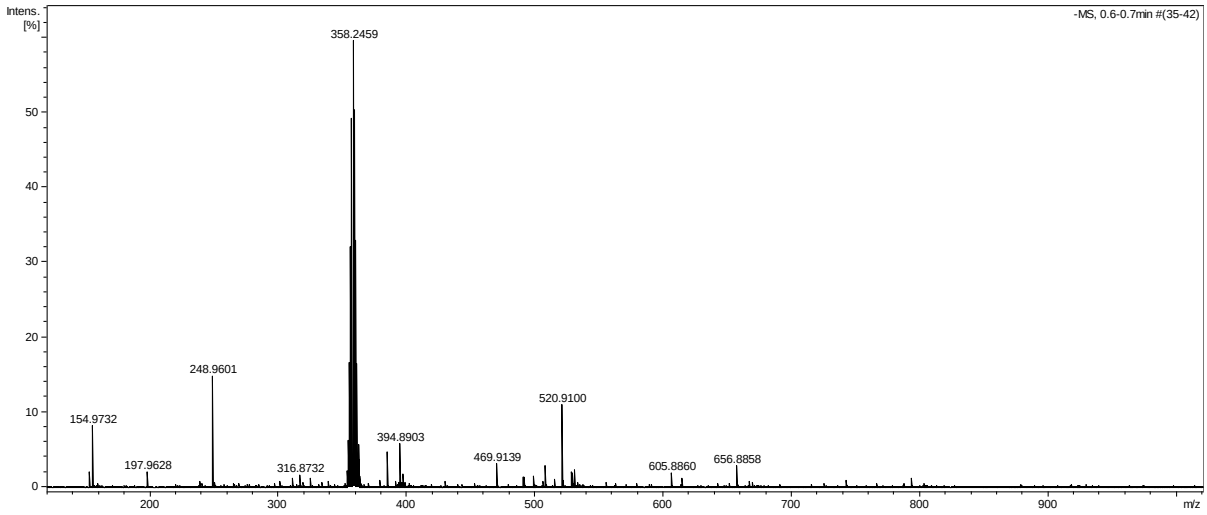

Fig. S38. ESI-MS spectrum of $[CoSAN\text{-}Cl]^-$.

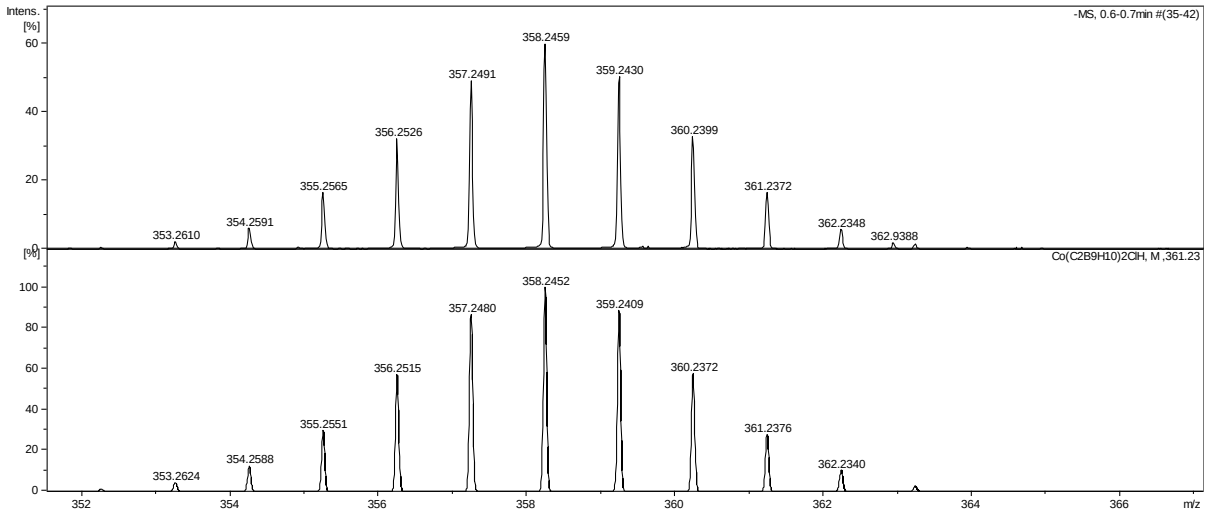

Fig. S39. Measured (top) and simulated (bottom) ESI-MS spectrum of $[CoSAN\text{-}Cl]^-$ – isotope pattern.

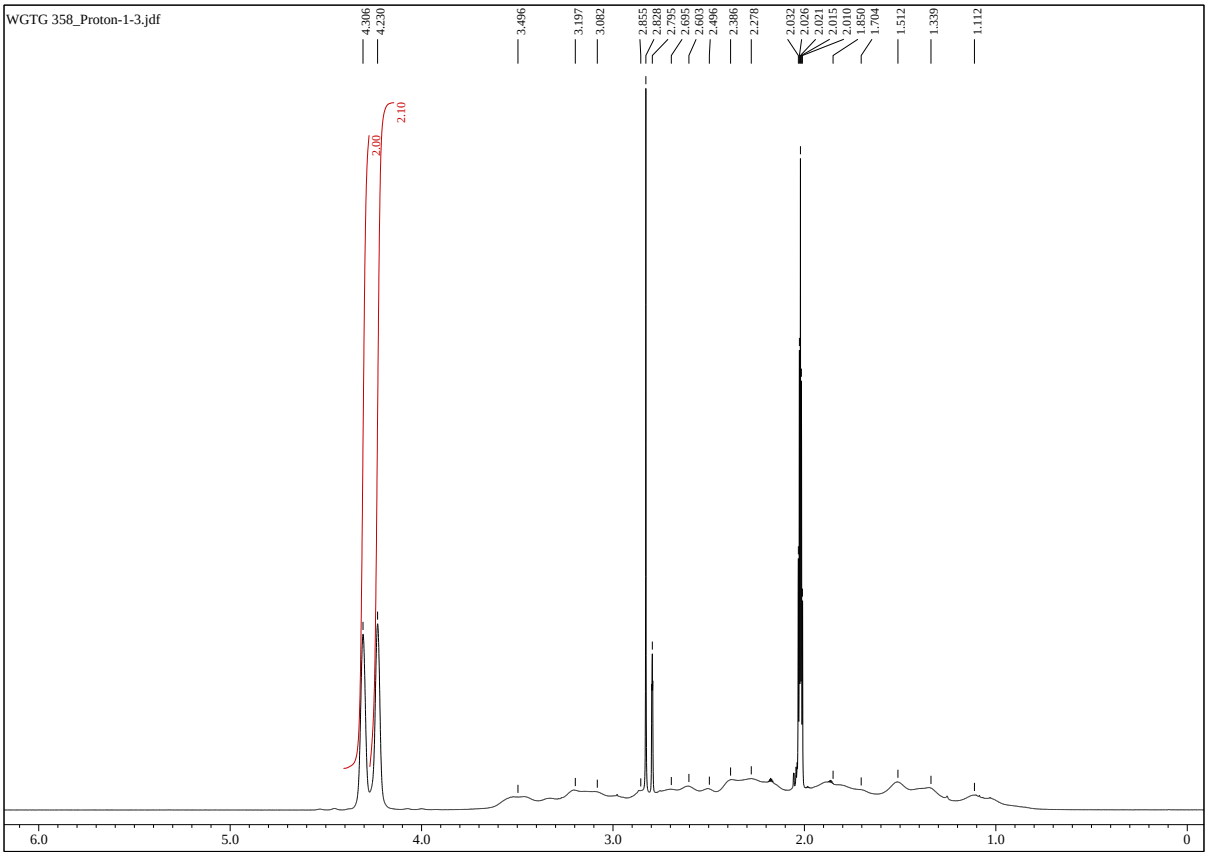

Fig. S40. ^{1}H NMR spectrum of Cs[CoSAN-Cl] in acetone-d_6 (400 MHz).

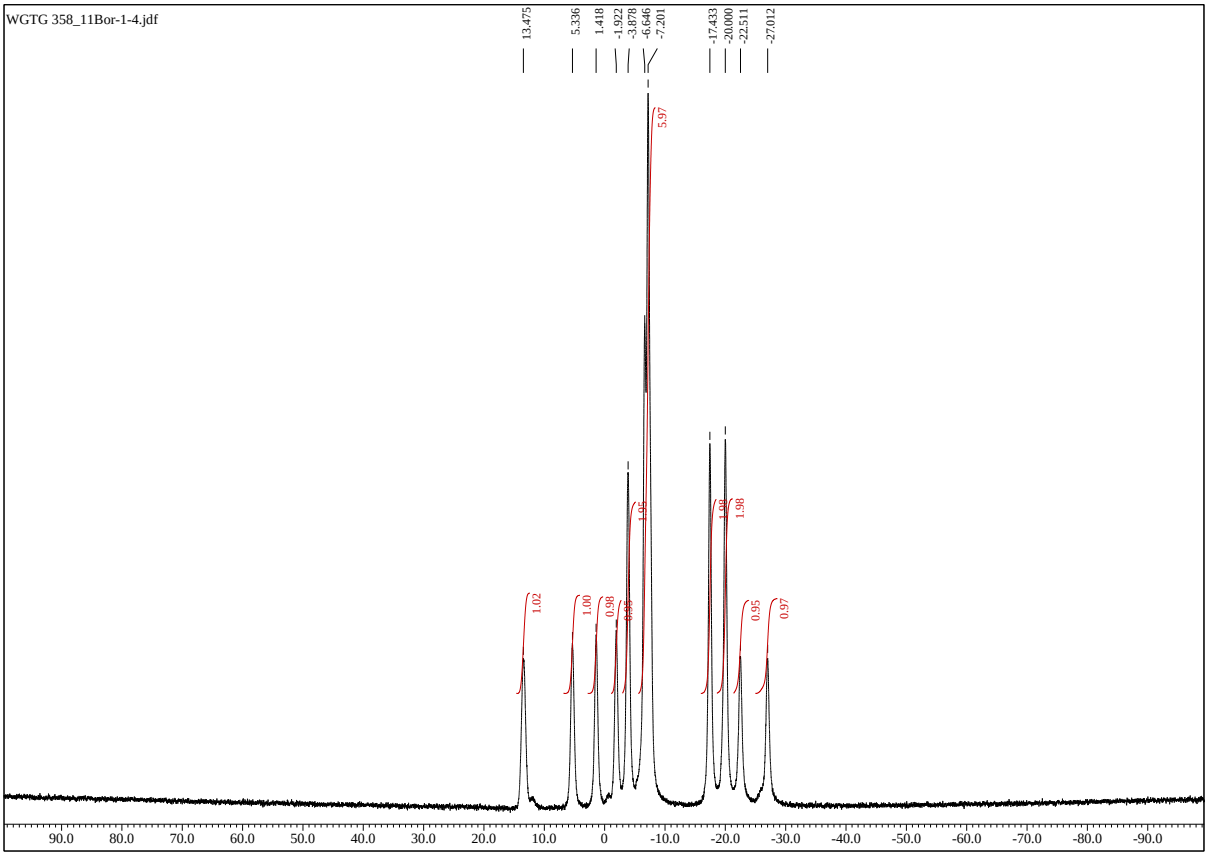

Fig. S41. $^{11}B\{^{1}H\}$ NMR spectrum of Cs[CoSAN-Cl] in acetone-d_6 (128 MHz).

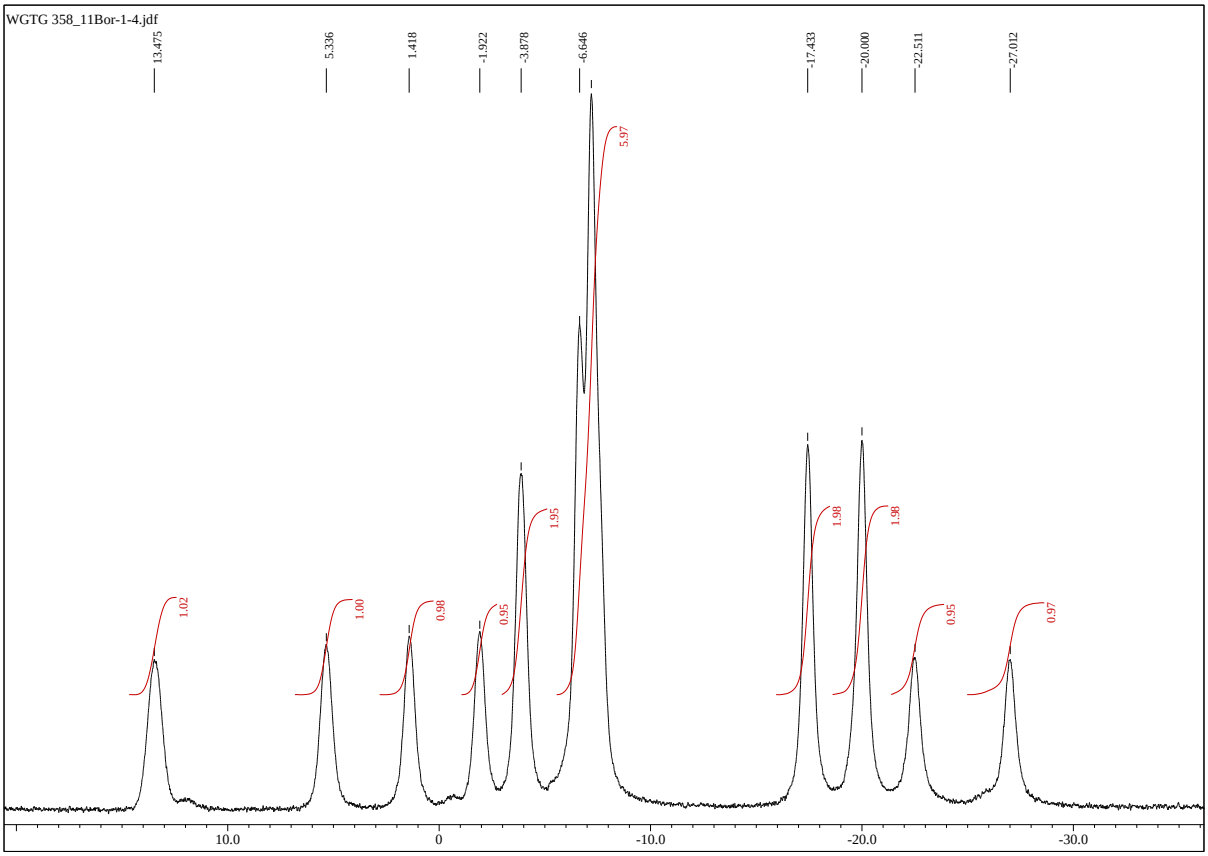

Fig. S42. Expanded $^{11}B\{^{1}H\}$ NMR spectrum of Cs[CoSAN-Cl] in acetone-d_6 (128 MHz).

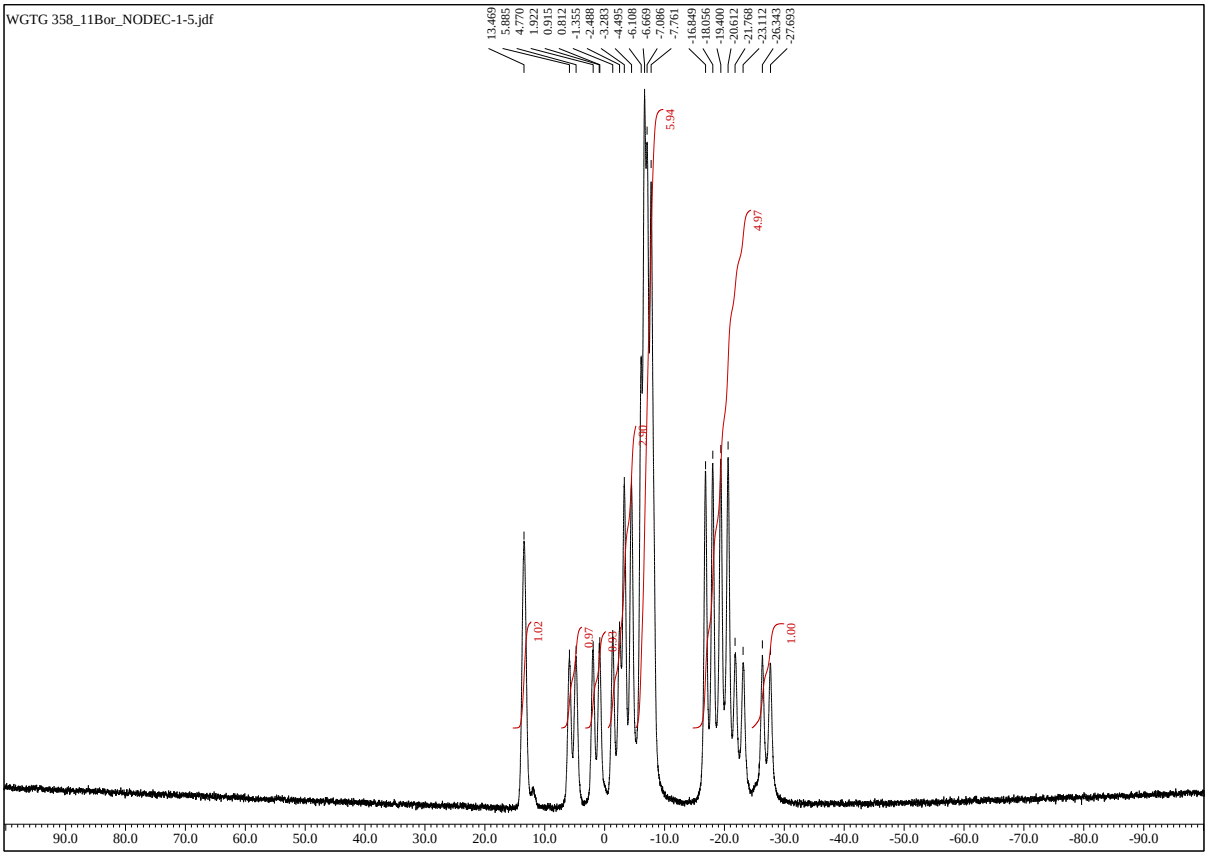

Fig. S43. ^{11}B NMR spectrum of Cs[CoSAN-Cl]in acetone-d_6 (128 MHz).

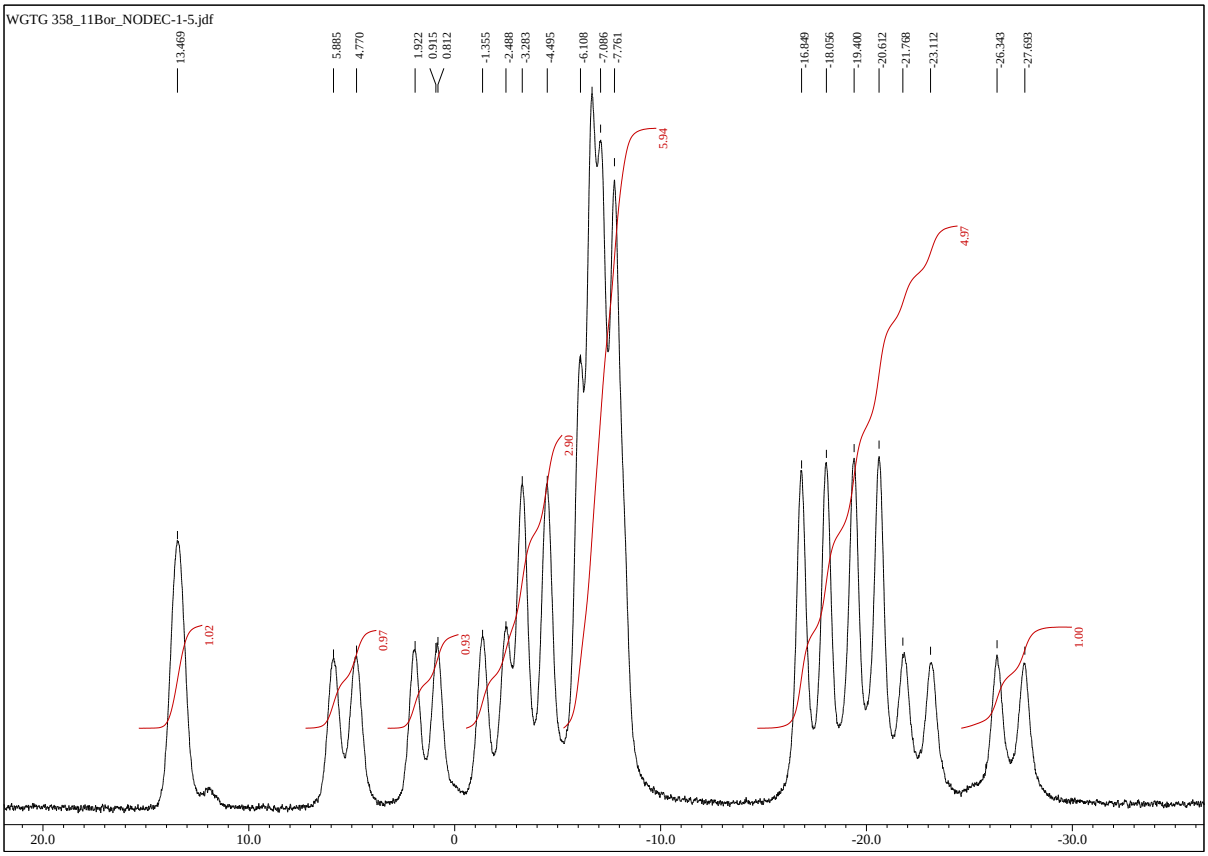

Fig. S44. Expanded ^{11}B NMR spectrum of Cs[CoSAN-Cl]in acetone-d_6 (128 MHz).

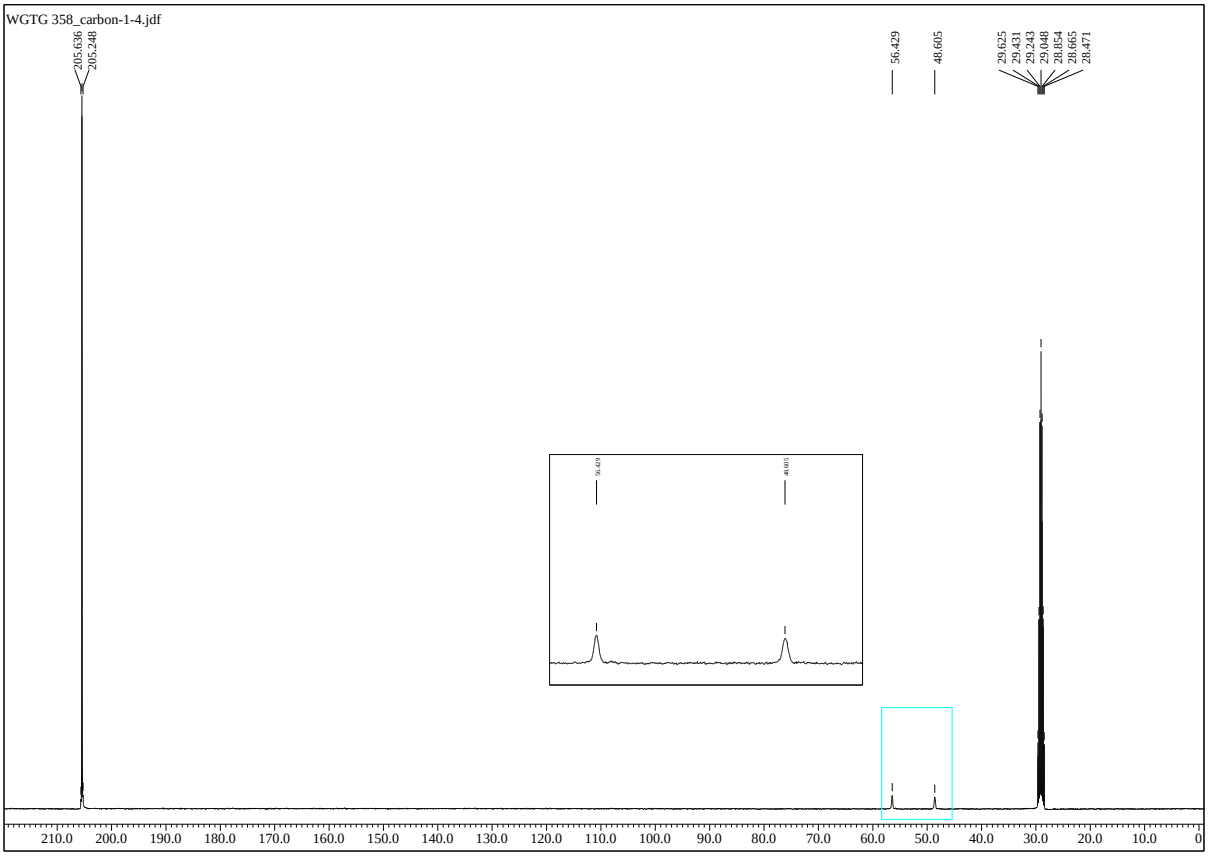

Fig. S45. $^{13}C\{^1H\}$ NMR spectrum of Cs[CoSAN-Cl] in acetone-d_6 (100 MHz).

1.6. Characterization of **[CoSAN-Br]**$^-$

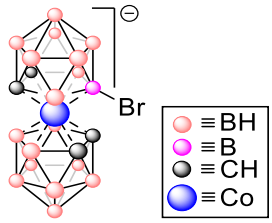

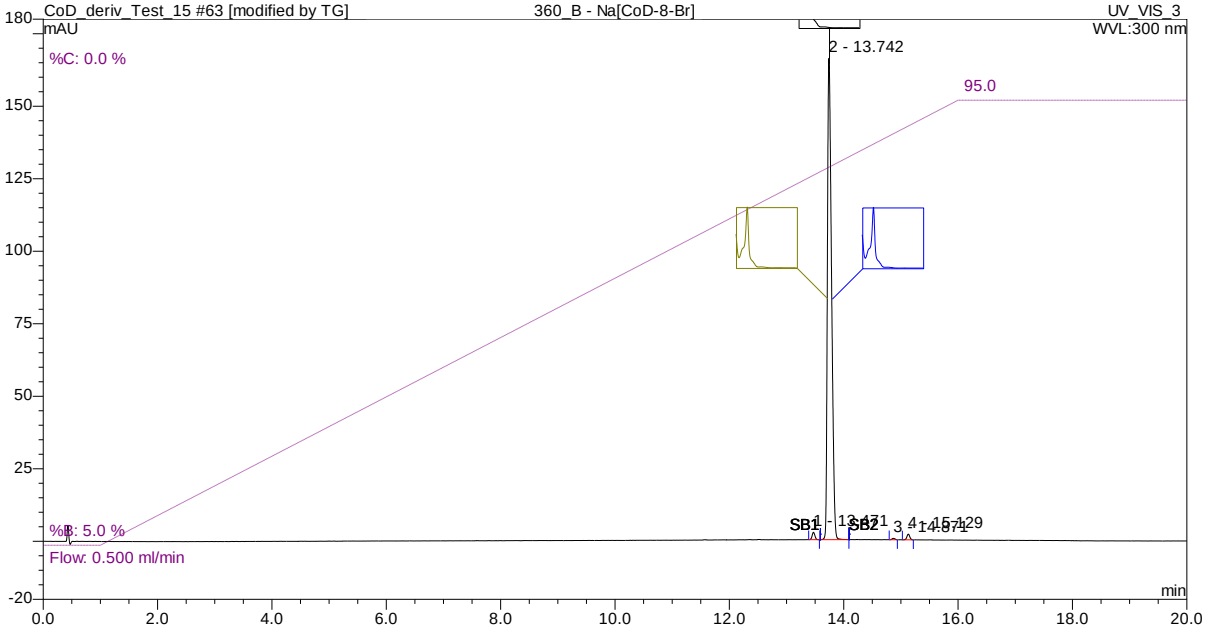

Fig. S46. HPLC chromatogram of [CoSAN-Br]$^-$. Purity – 98.01%

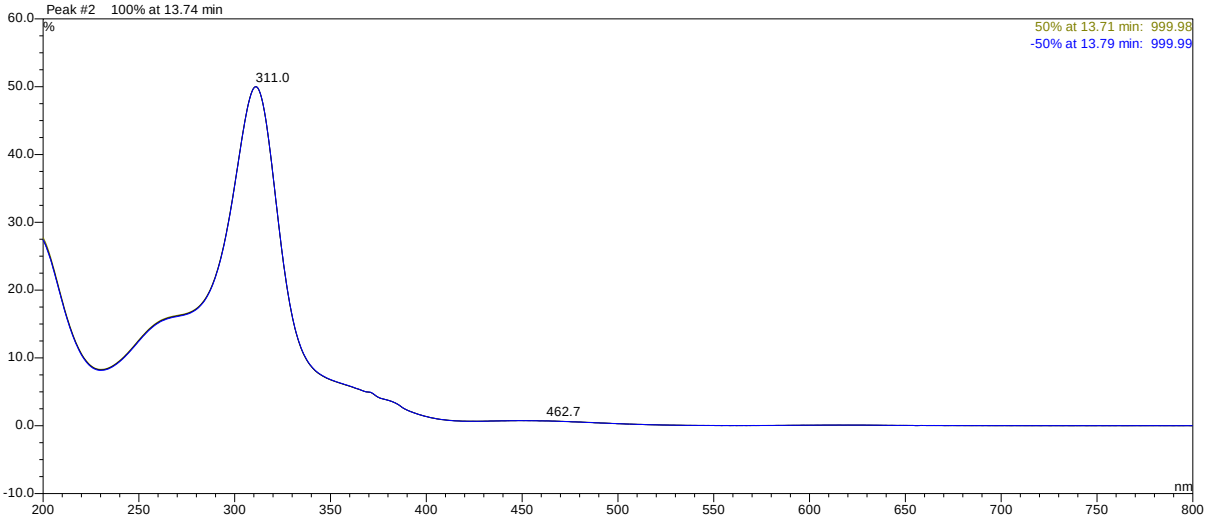

Fig. S47. UV-VIS spectrum of [CoSAN-Br]$^-$ (peak purity analysis).

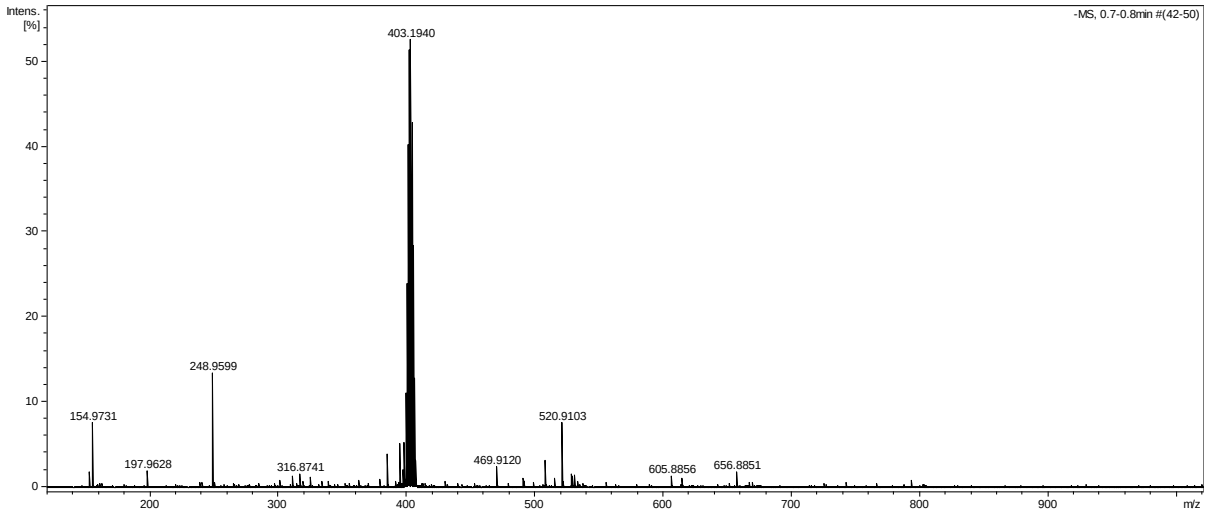

Fig. S48. ESI-MS spectrum of [CoSAN-Br]$^-$.

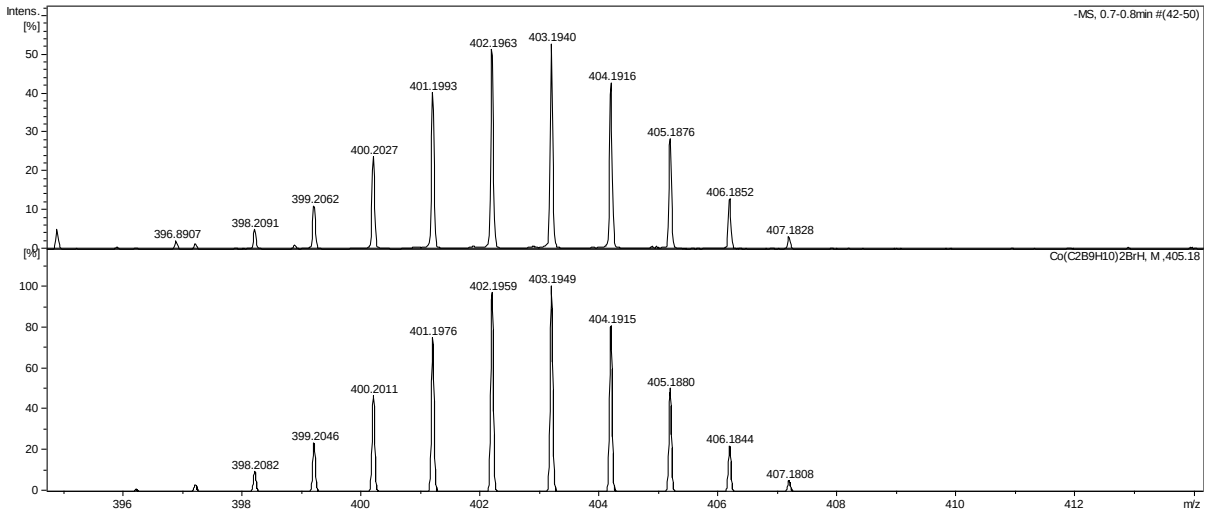

Fig. S49. Measured (top) and simulated (bottom) ESI-MS spectrum of [CoSAN-Br]$^-$ – isotope pattern.

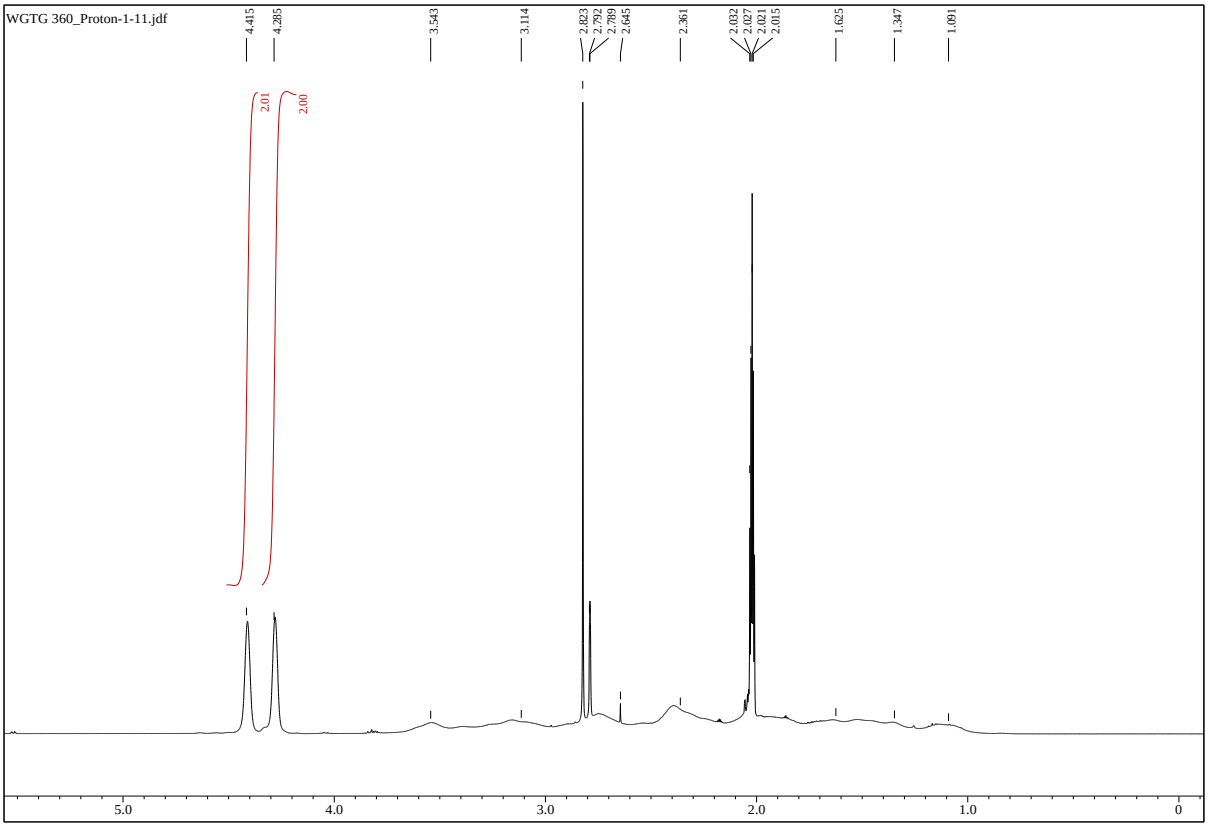

Fig. S50. ^{1}H NMR spectrum of Cs[CoSAN-Br] in acetone-d_6 (400 MHz).

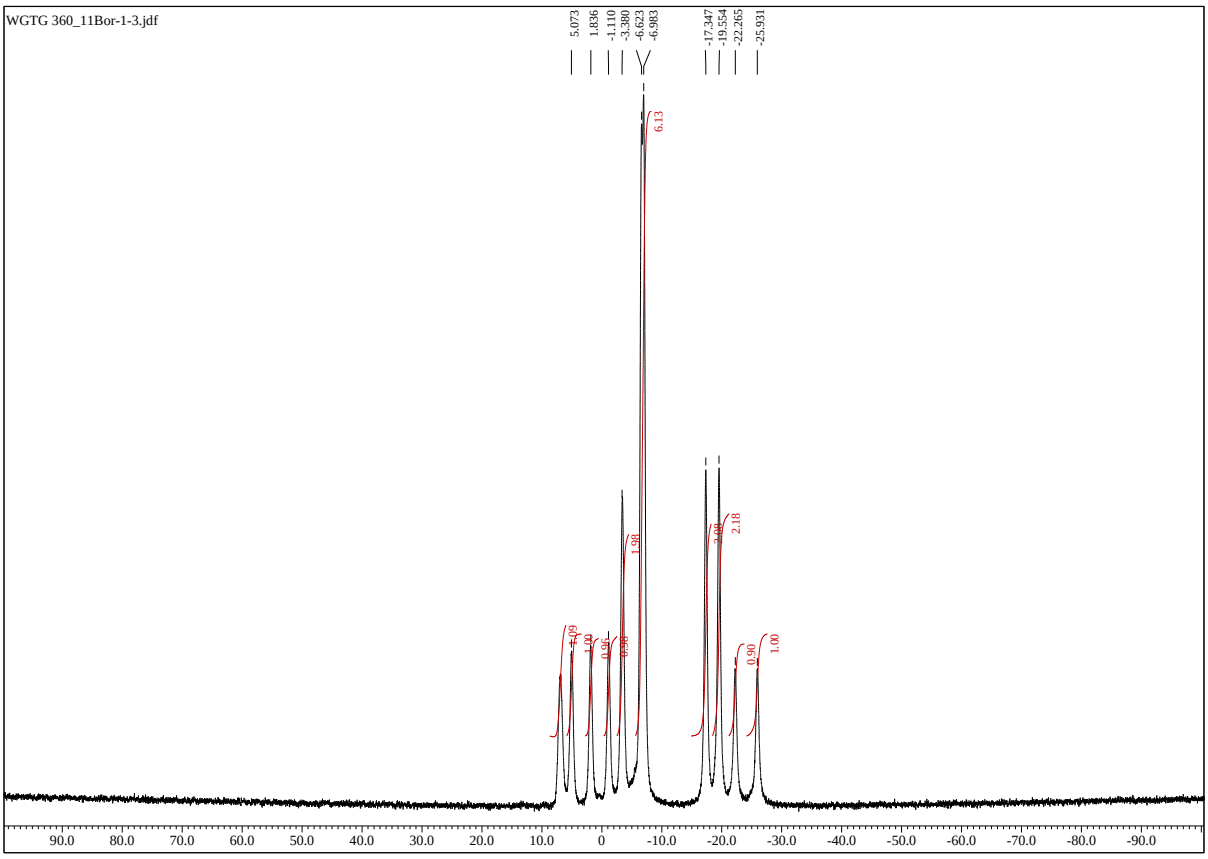

Fig. S51. $^{11}B\{^{1}H\}$ NMR spectrum of Cs[CoSAN-Br] in acetone-d_6 (128 MHz).

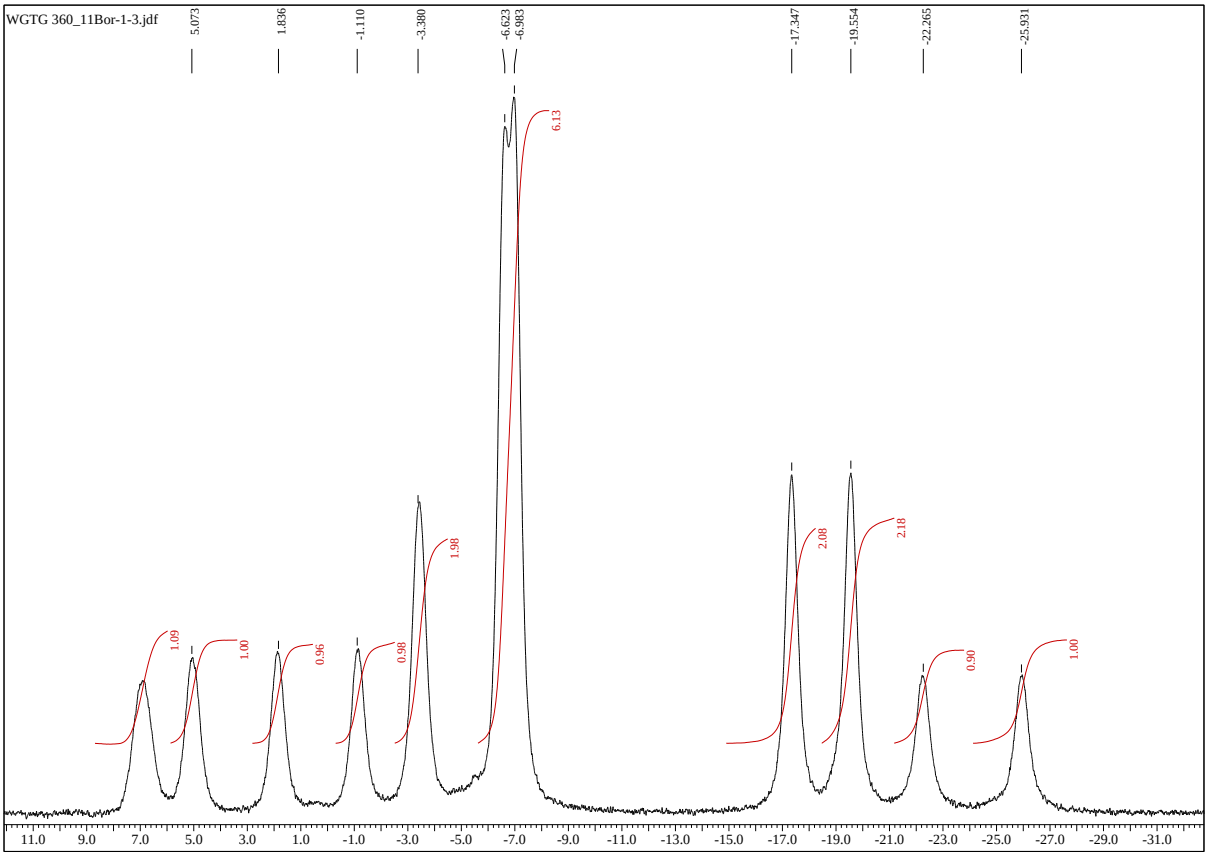

Fig. S52. Expanded $^{11}B\{^{1}H\}$ NMR spectrum of Cs[CoSAN-Br] in acetone-d_6 (128 MHz).

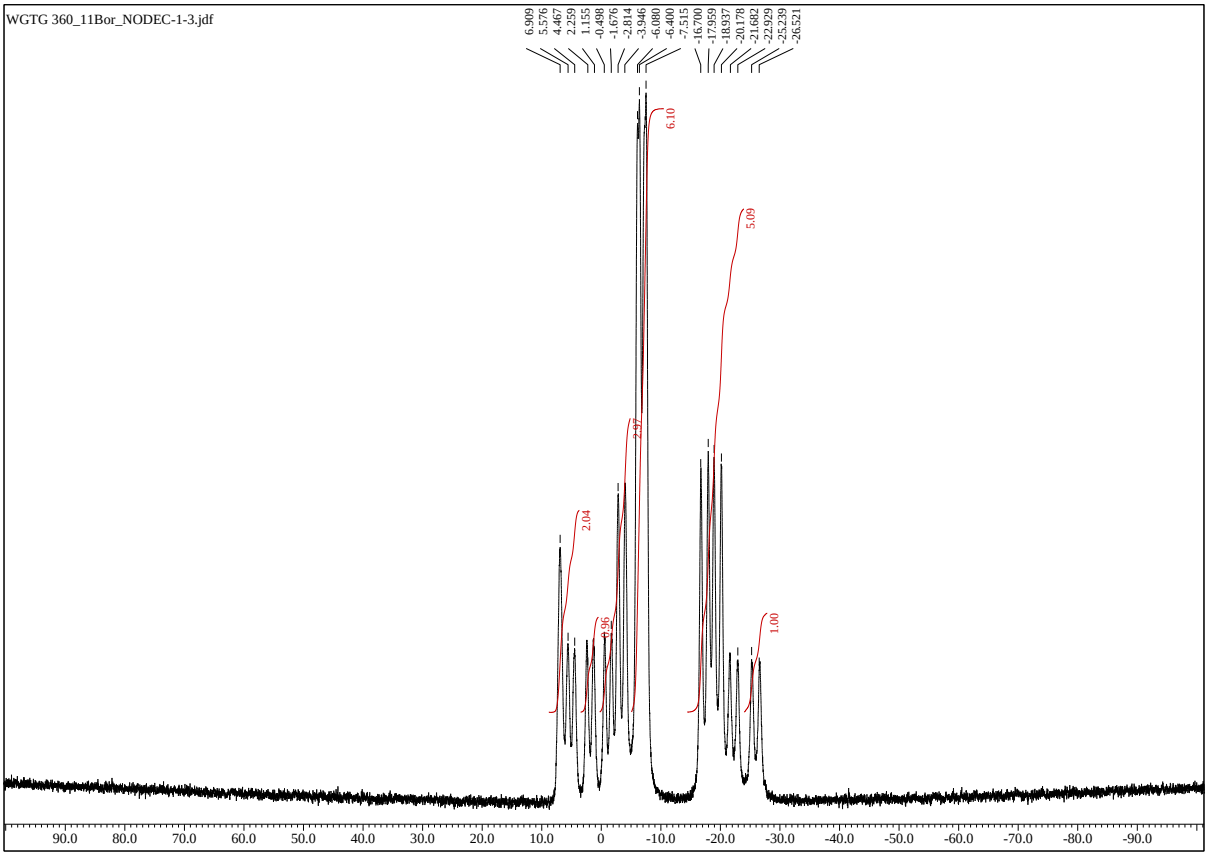

Fig. S53. ^{11}B NMR spectrum of Cs[CoSAN-Br] in acetone-d_6 (128 MHz).

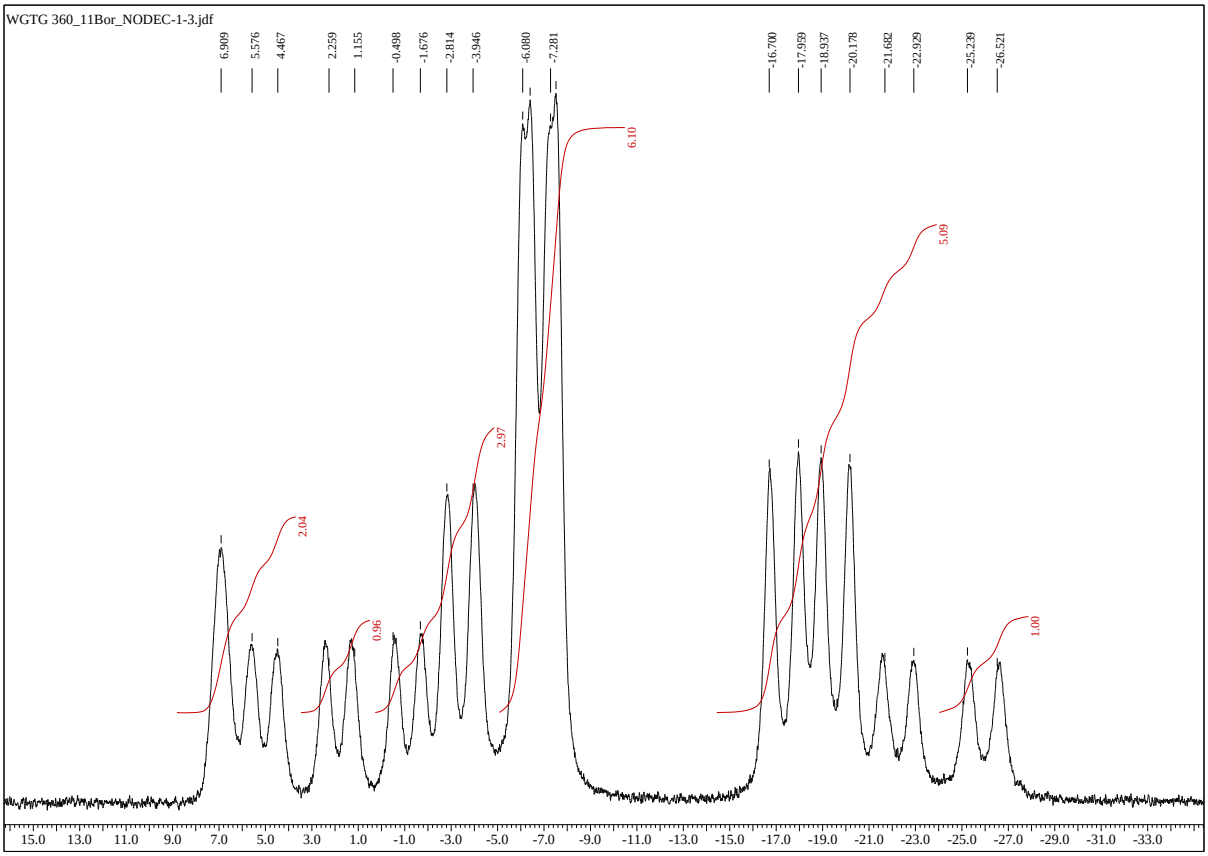

Fig. S54. Expanded ^{11}B NMR spectrum of Cs[CoSAN-Br] in acetone-d_6 (128 MHz).

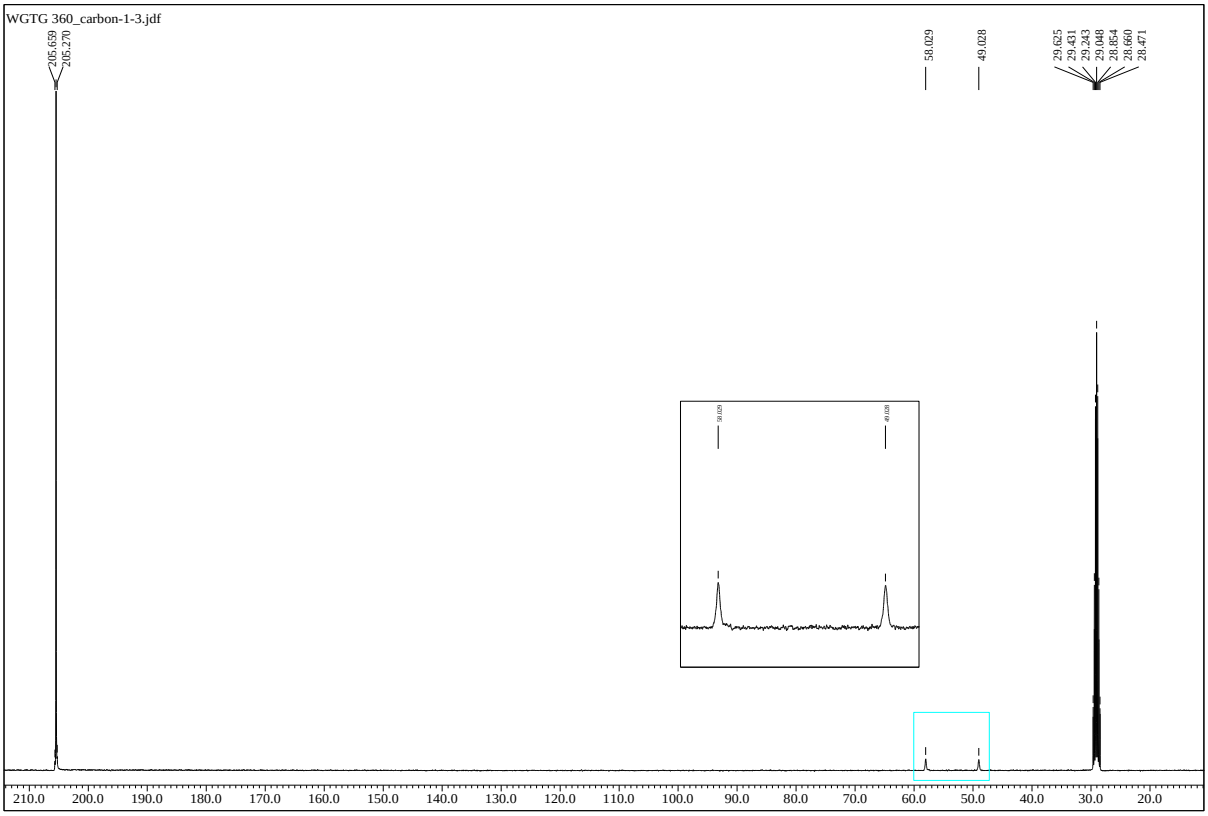

Fig. S55. $^{13}C\{^1H\}$ NMR spectrum of Cs[CoSAN-Br] in acetone-d_6 (100 MHz).

1.7. Characterization of **[CoSAN-I]**$^{-}$

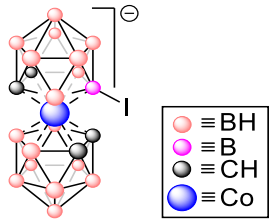

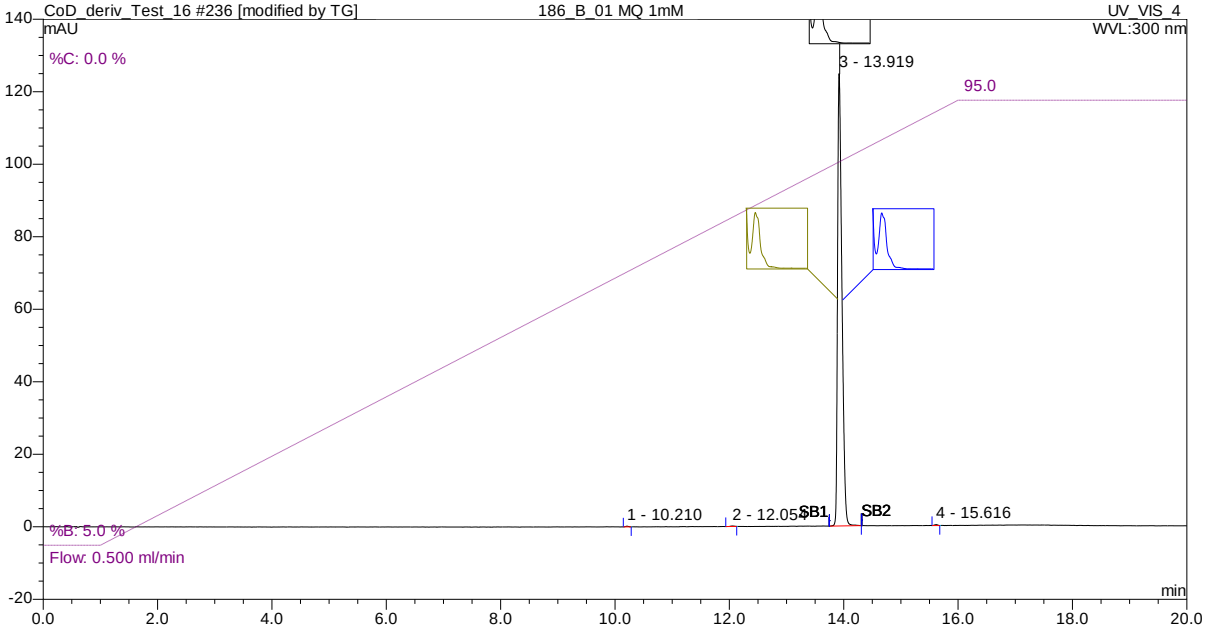

Fig. S56. HPLC chromatogram of [CoSAN-I]$^{-}$. Purity – 99.68%

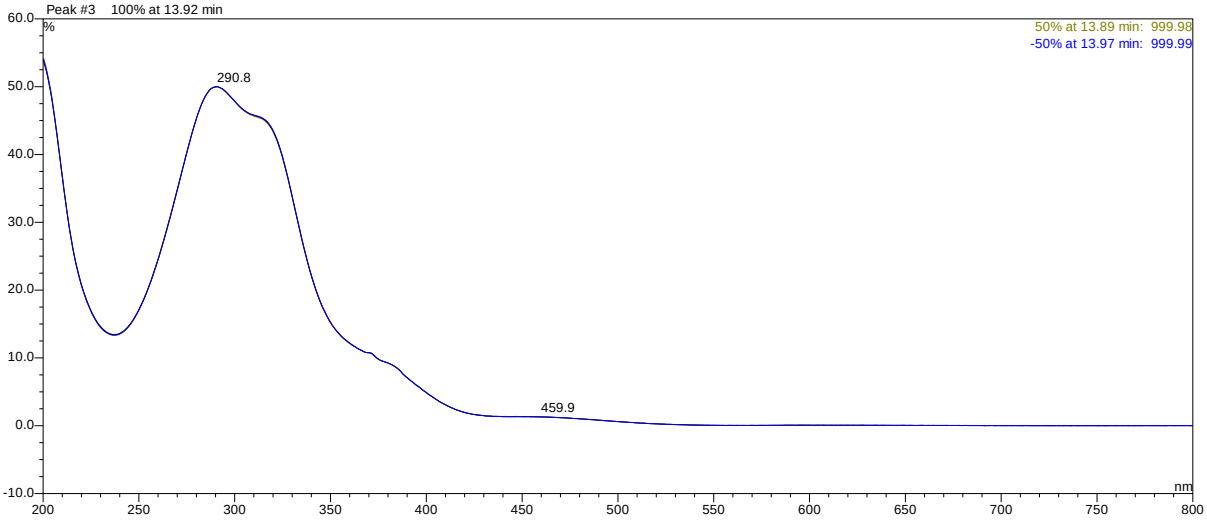

Fig. S57. UV-VIS spectrum of [CoSAN-I]$^{-}$ (peak purity analysis).

1.8. Characterization of **[CoSAN-Cl,Br]**$^-$

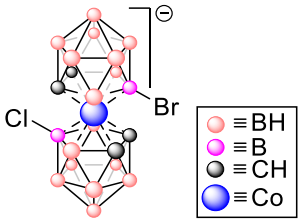

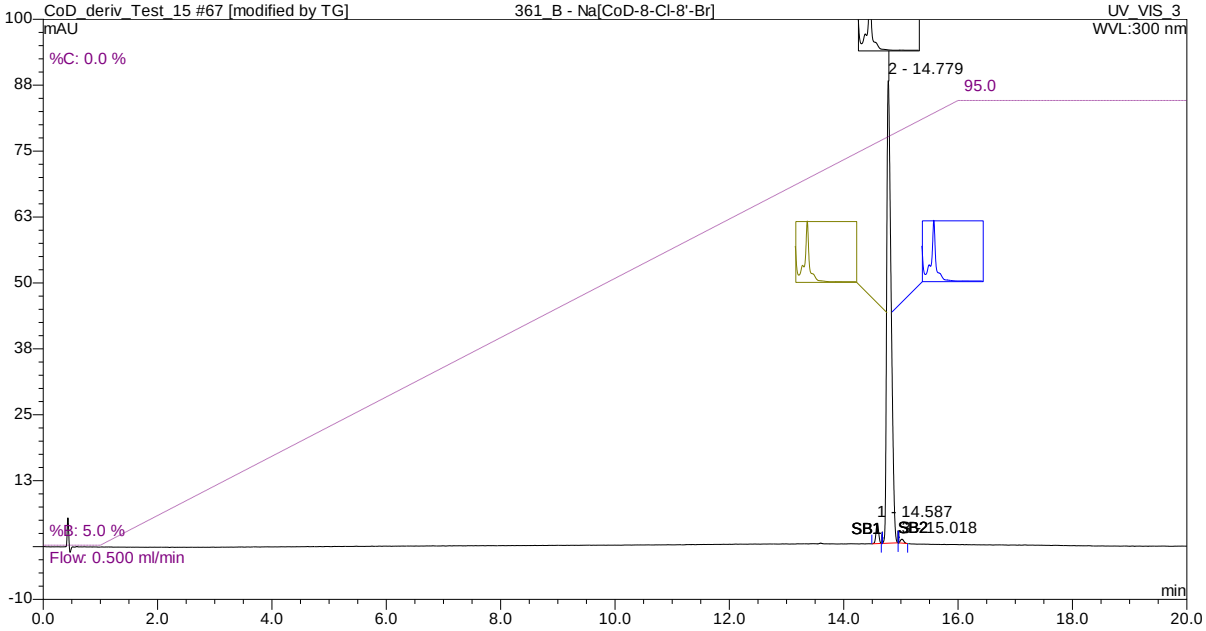

Fig. S58. HPLC chromatogram of [CoSAN-Cl,Br]$^-$. Purity – 96.82%

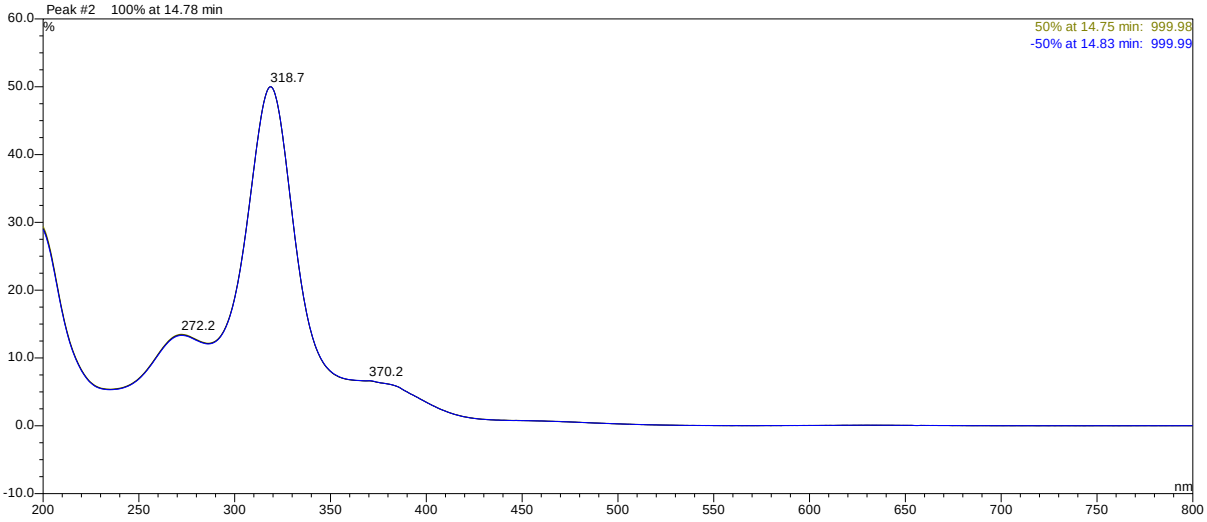

Fig. S59. UV-VIS spectrum of [CoSAN-Cl,Br]$^-$ (peak purity analysis).

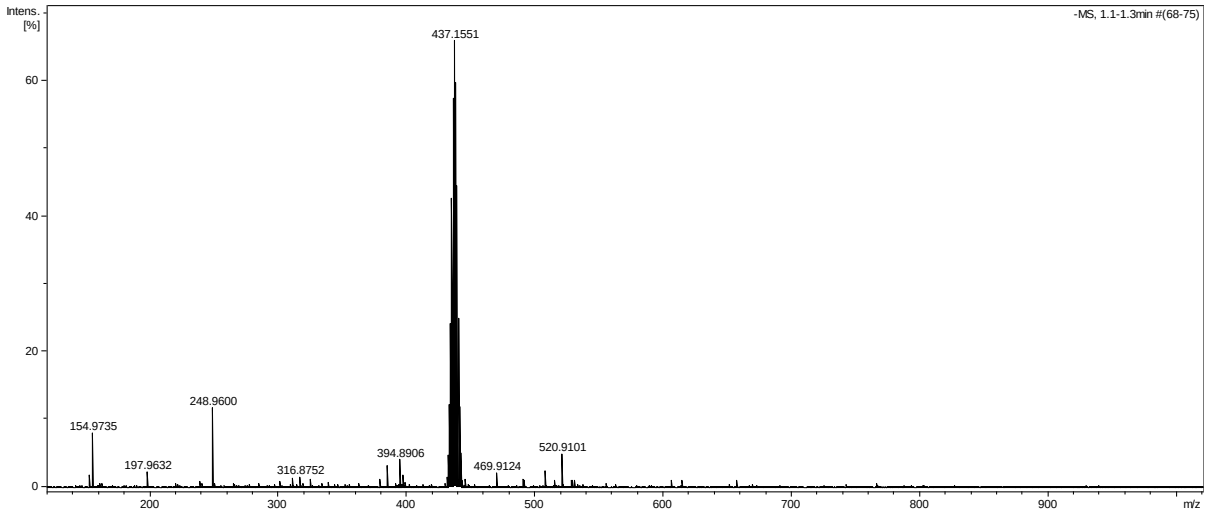

Fig. S60. ESI-MS spectrum of $[CoSAN\text{-}Cl,Br]^-$.

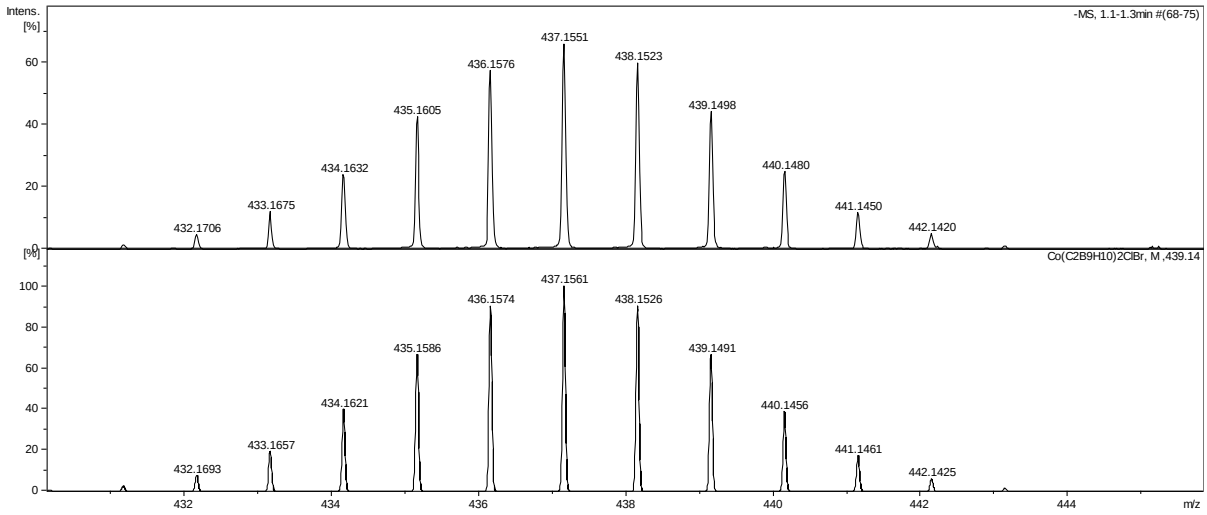

Fig. S61. Measured (top) and simulated (bottom) ESI-MS spectrum of $[CoSAN\text{-}Cl,Br]^-$ – isotope pattern.

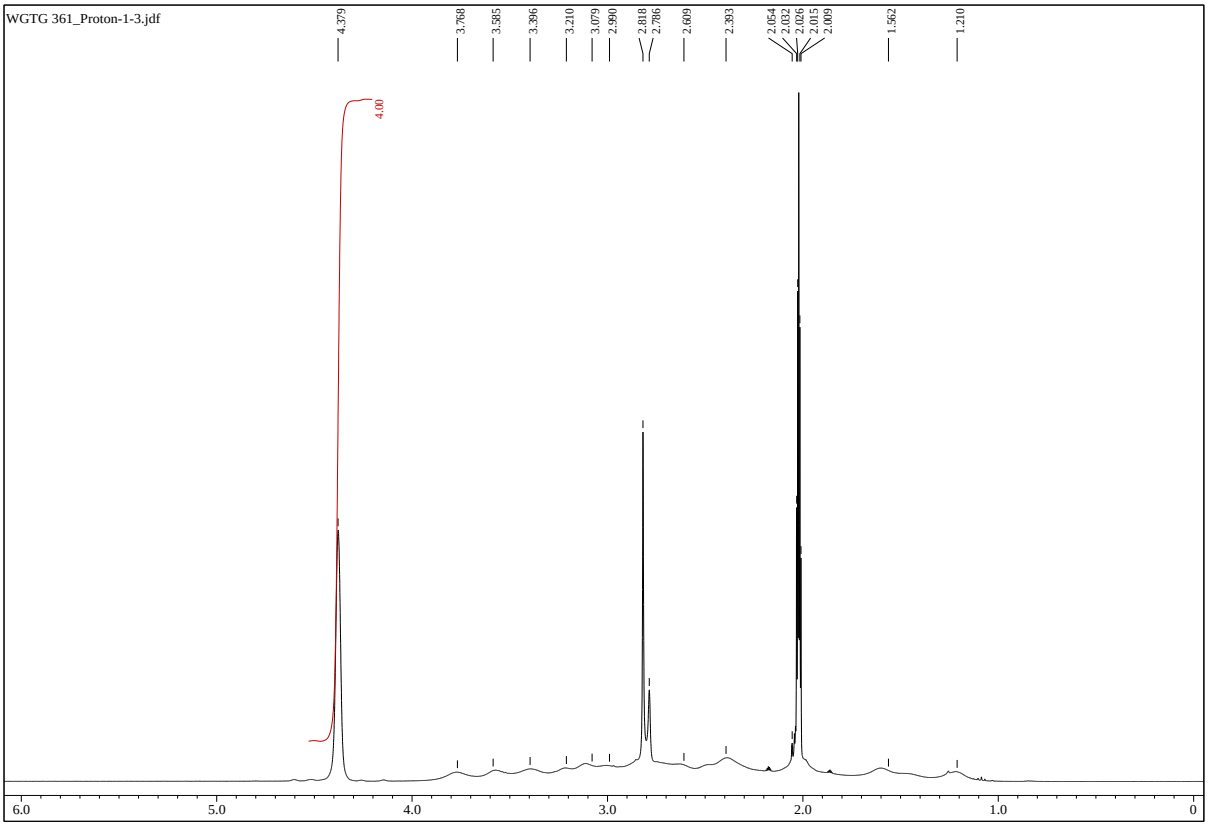

Fig. S62. ^{1}H NMR spectrum of Cs[CoSAN-Cl,Br] in acetone-d_6 (400 MHz).

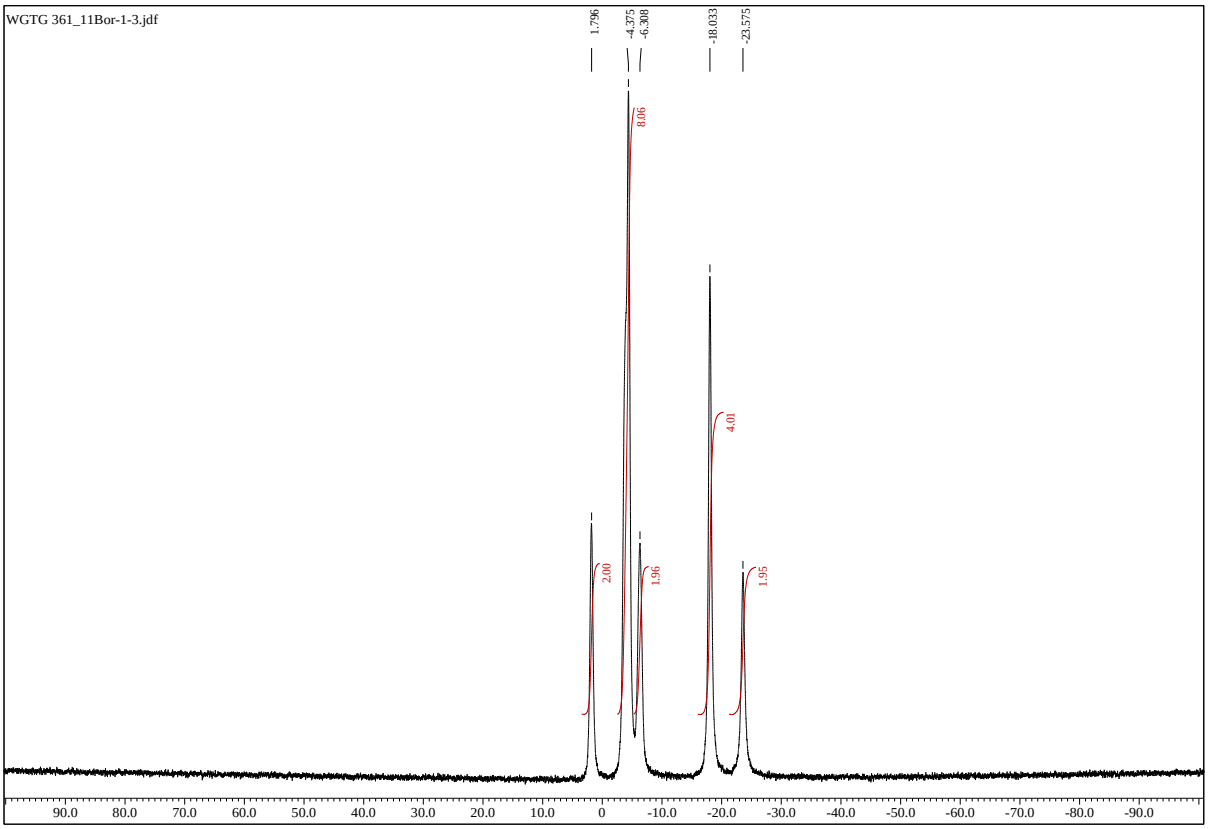

Fig. S63. $^{11}B\{^{1}H\}$ NMR spectrum of Cs[CoSAN-Cl,Br] in acetone-d_6 (128 MHz).

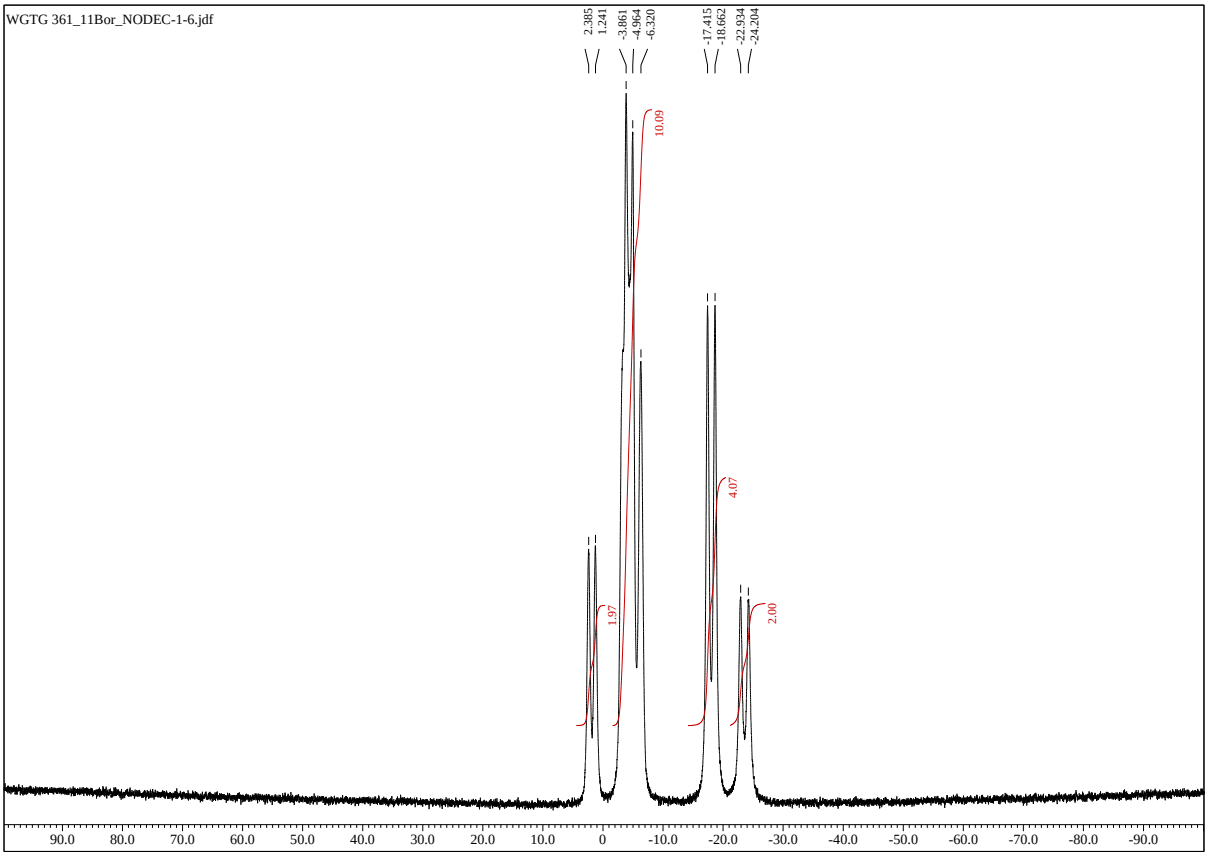

Fig. S64. ^{11}B NMR spectrum of Cs[CoSAN-Cl,Br] in acetone-d_6 (128 MHz).

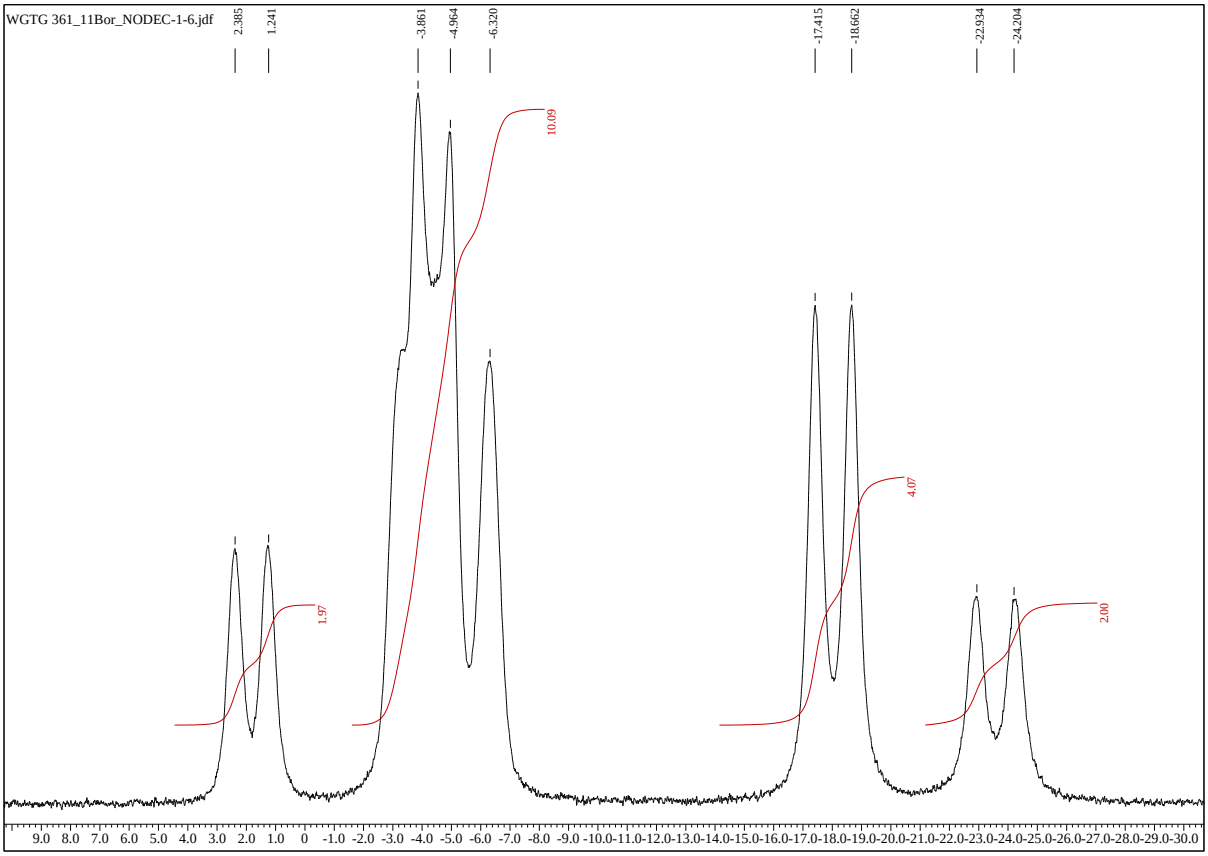

Fig. S65. Expanded ^{11}B NMR spectrum of Cs[CoSAN-Cl,Br] in acetone-d_6 (128 MHz).

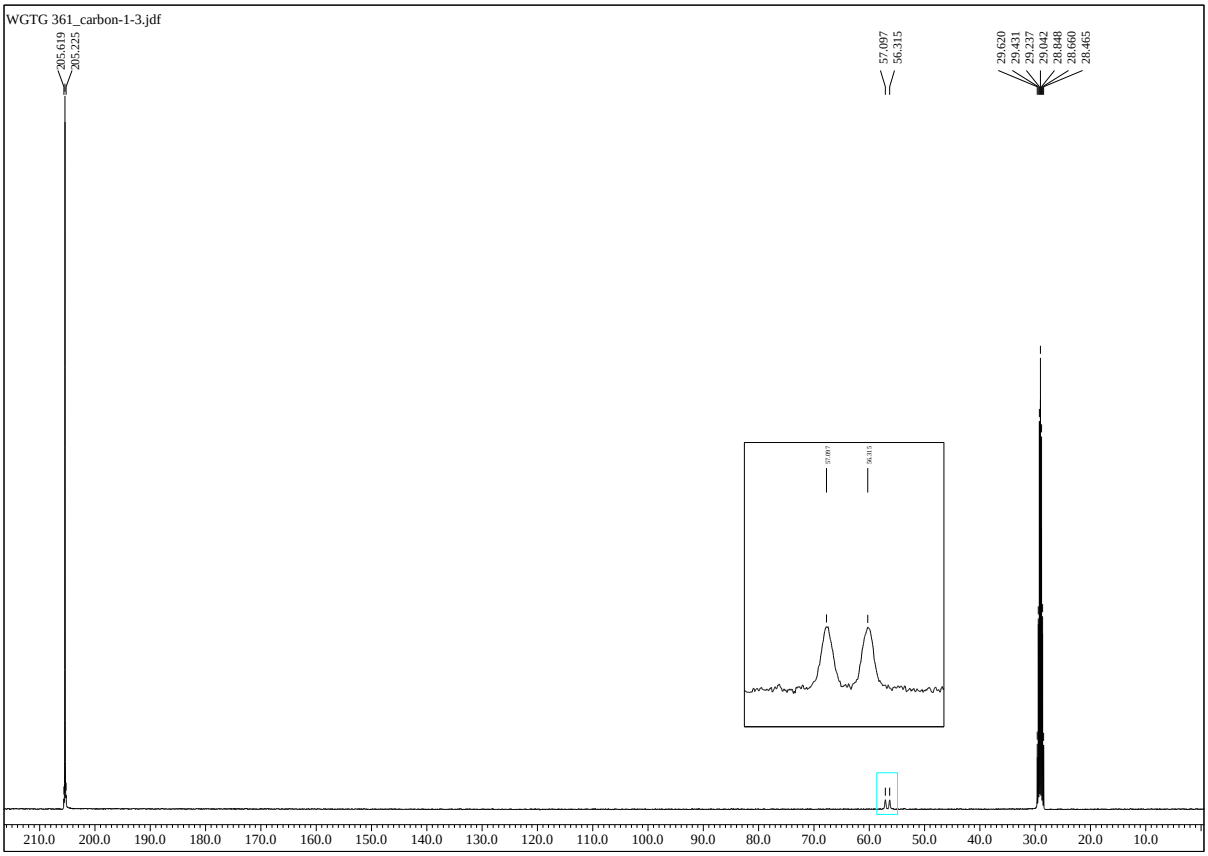

Fig. S66. $^{13}C\{^{1}H\}$ NMR spectrum of Cs[CoSAN-Cl,Br] in acetone-d_6 (100 MHz).

1.10 Characterization of **[CoSAN-I,Br]$^-$**

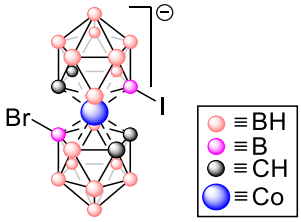

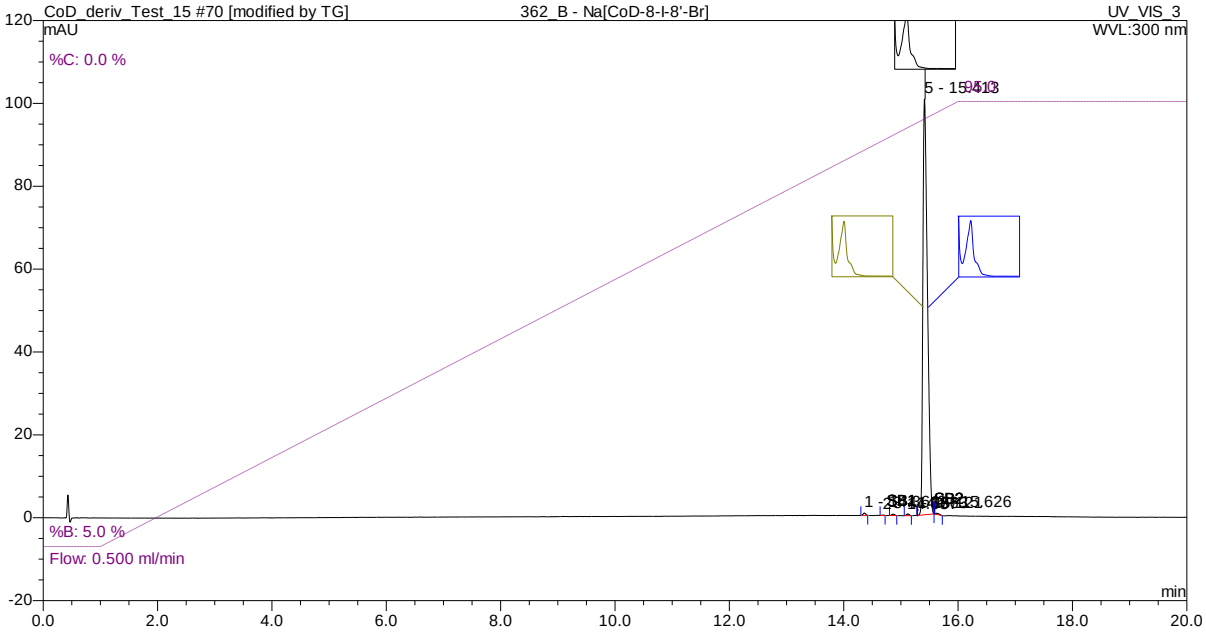

Fig. S67. HPLC chromatogram of [CoSAN-I,Br]$^-$. Purity – 98.96%

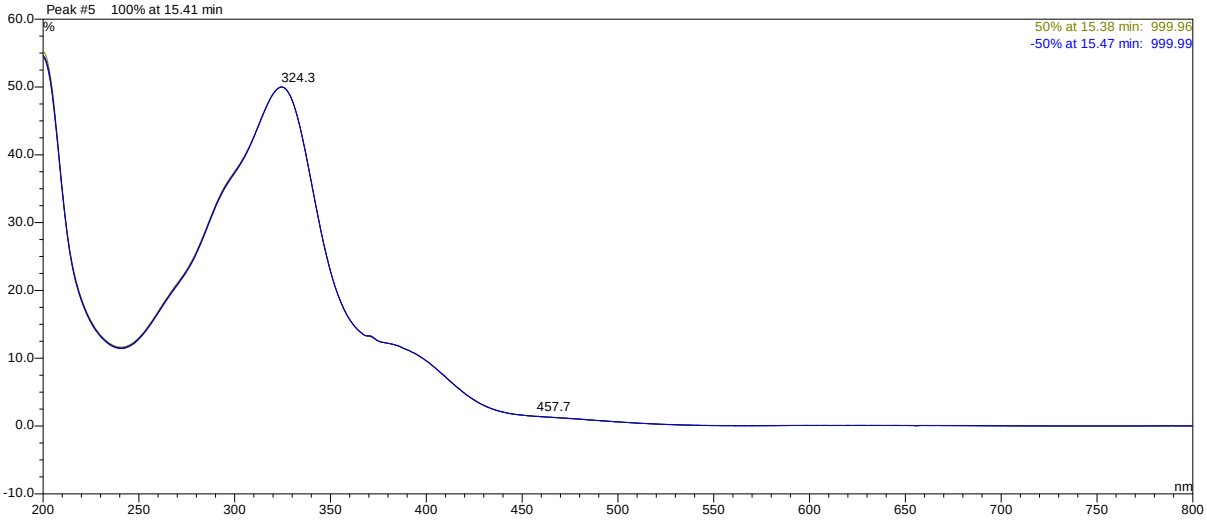

Fig. S68. UV-VIS spectrum of [CoSAN-I,Br]$^-$ (peak purity analysis).

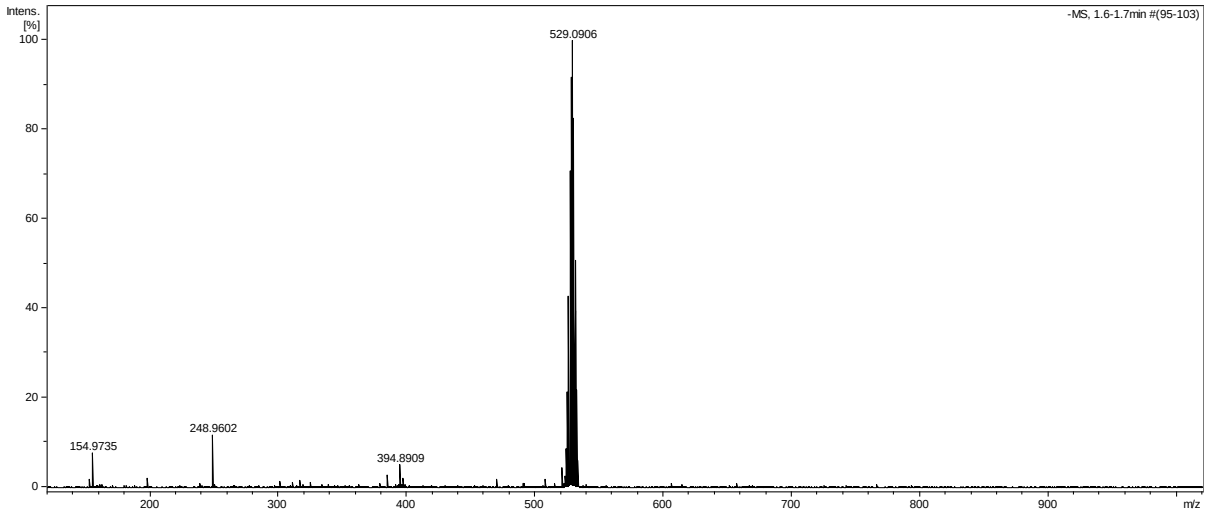

Fig. S69. ESI-MS spectrum of [CoSAN-I,Br]$^-$.

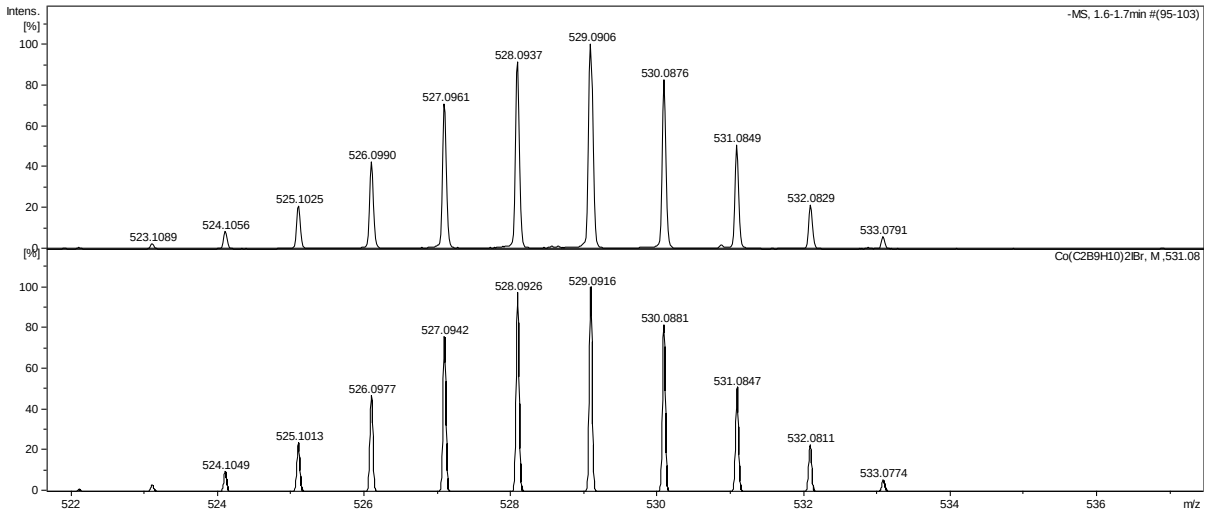

Fig. S70. Measured (top) and simulated (bottom) ESI-MS spectrum of [CoSAN-I,Br]$^-$ – isotope pattern.

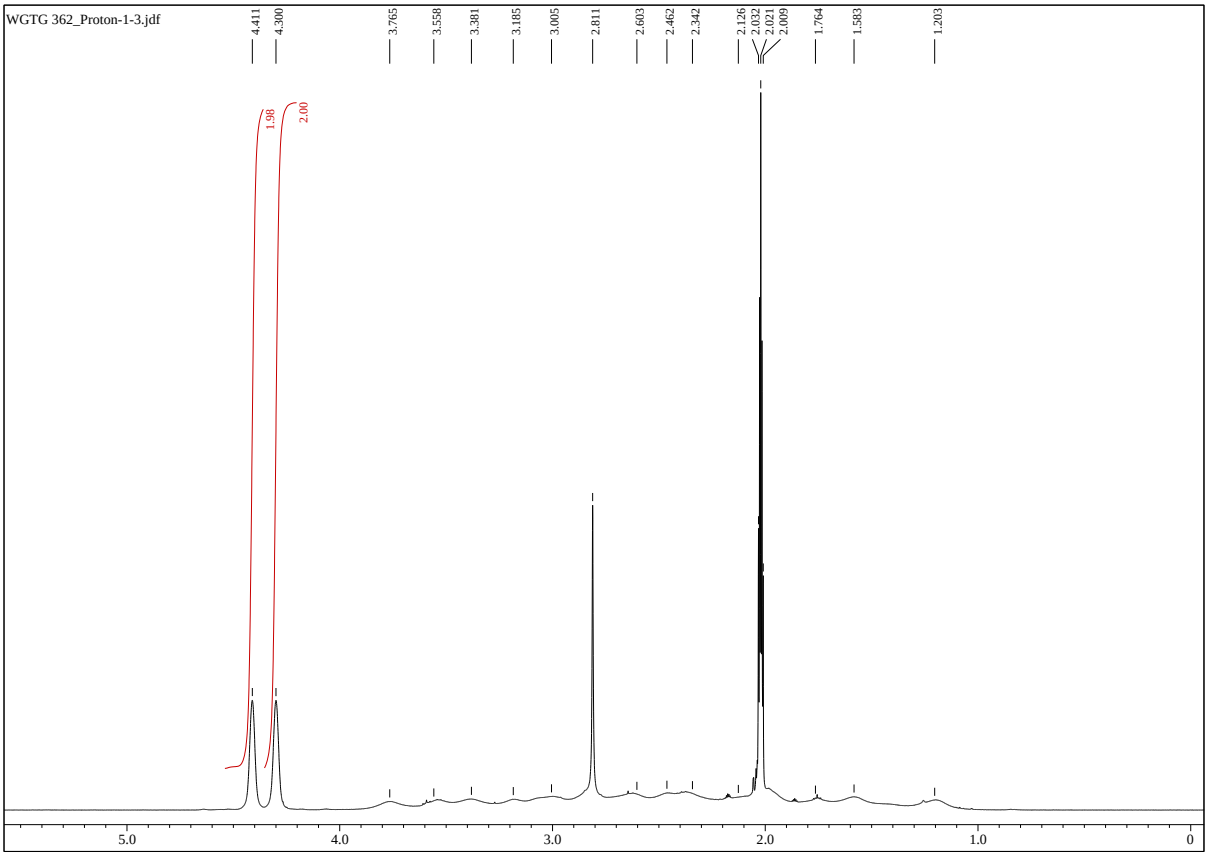

Fig. S71. ^{1}H NMR spectrum of Cs[CoSAN-I,Br] in acetone-d_6 (400 MHz).

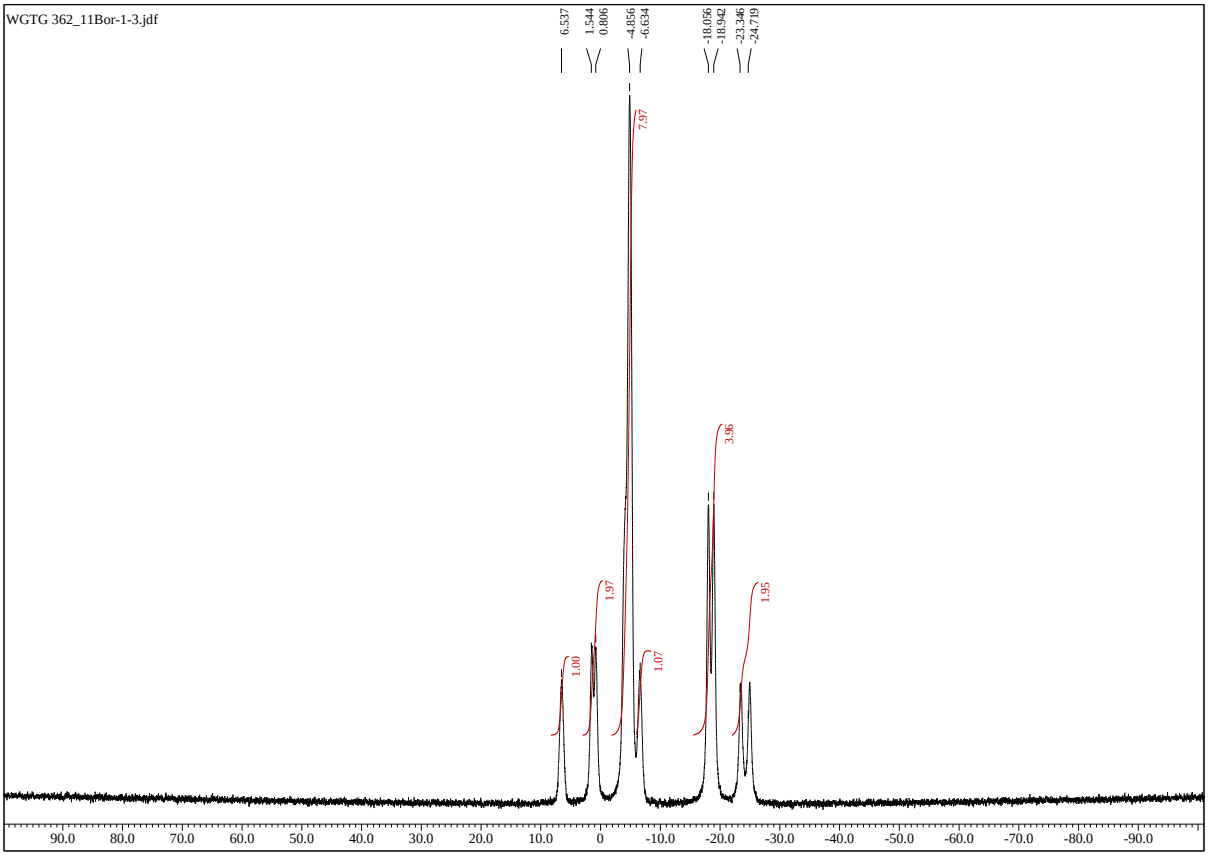

Fig. S72. $^{11}B\{^{1}H\}$ NMR spectrum of Cs[CoSAN-I,Br] in acetone-d_6 (128 MHz).

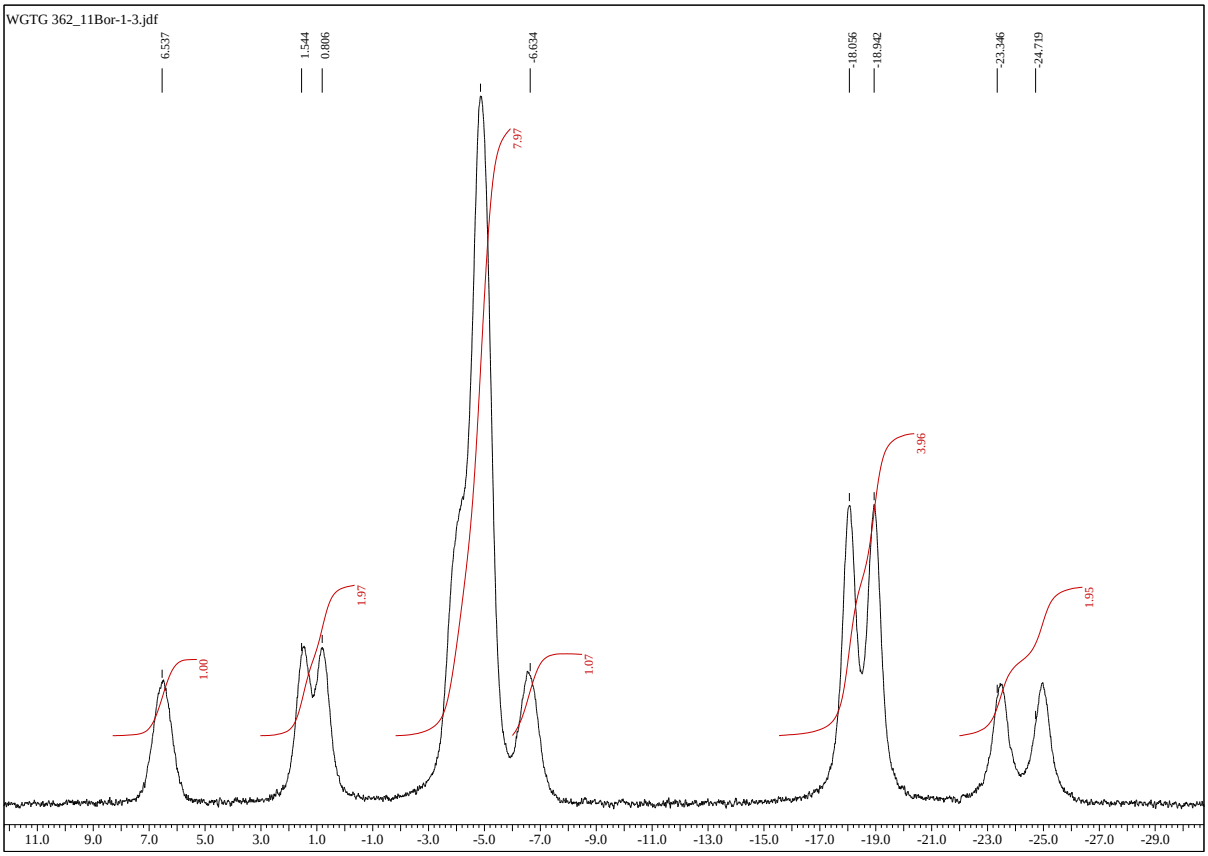

Fig. S73. Expanded $^{11}B\{^{1}H\}$ NMR spectrum of Cs[CoSAN-I,Br] in acetone-d_6 (128 MHz).

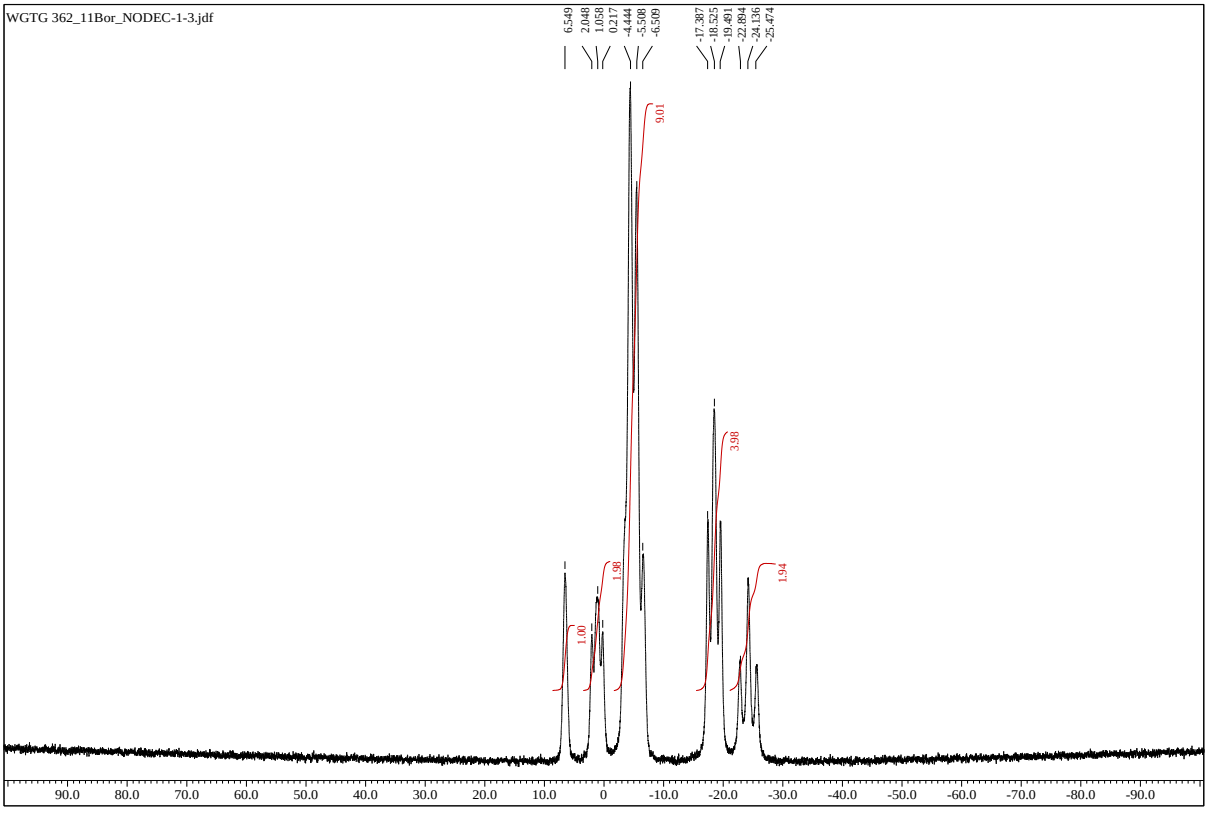

Fig. S74. ^{11}B NMR spectrum of Cs[CoSAN-I,Br] in acetone-d_6 (128 MHz).

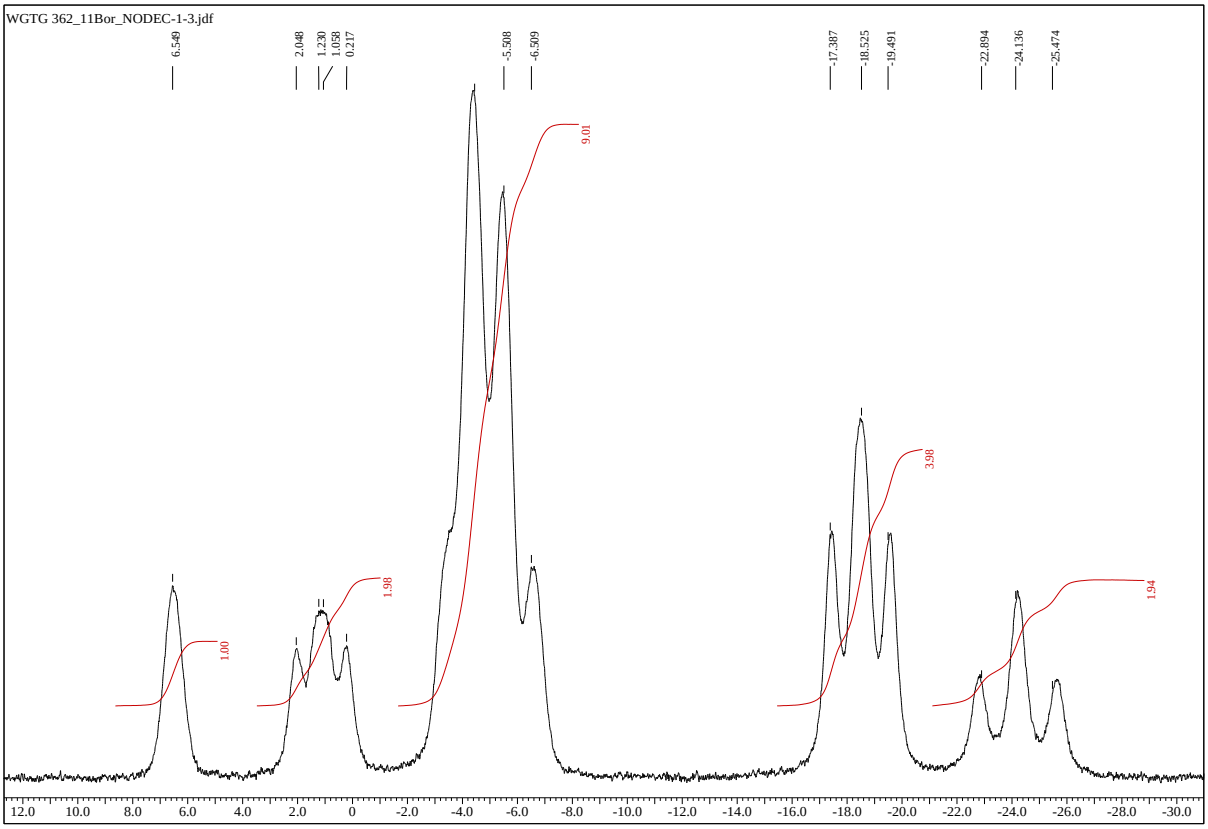

Fig. S75. Expanded ^{11}B NMR spectrum of Cs[CoSAN-I,Br] in acetone-d_6 (128 MHz).

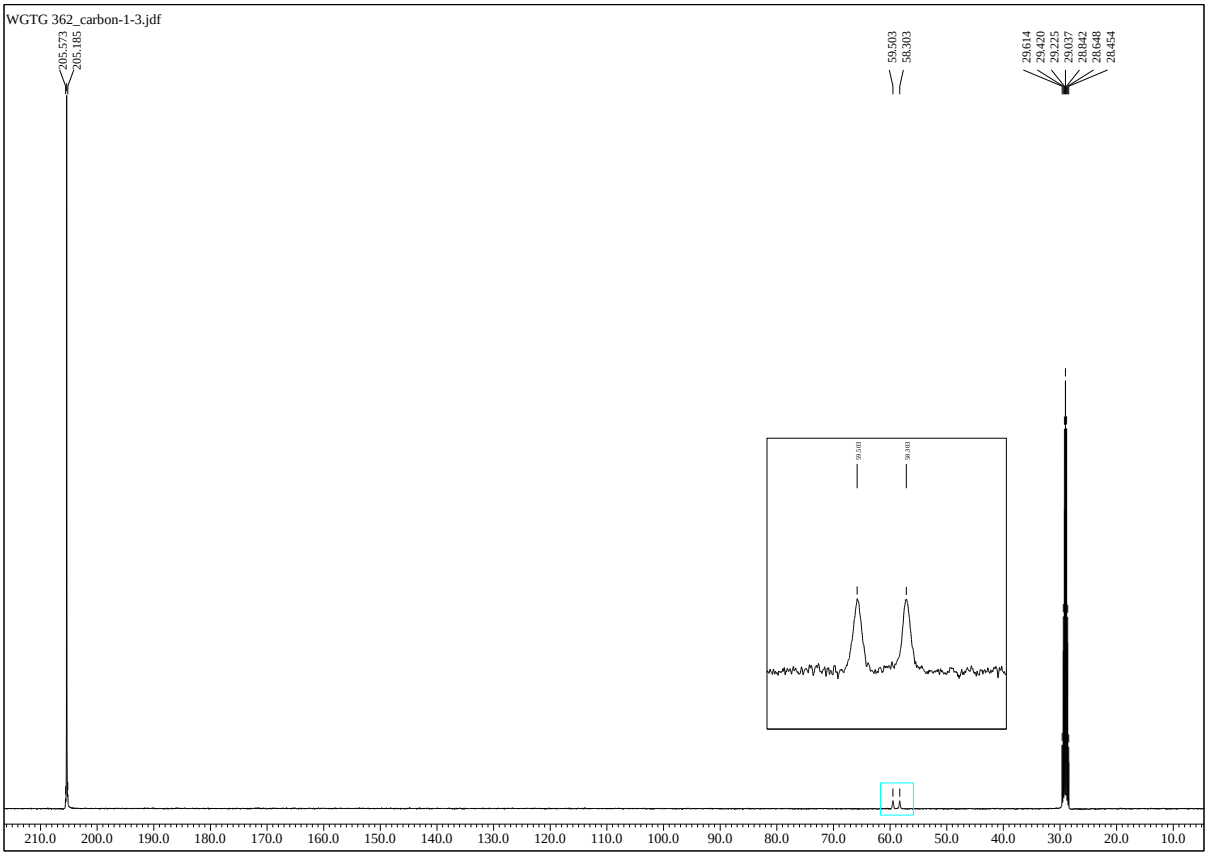

Fig. S76. $^{13}C\{^1H\}$ NMR spectrum of Cs[CoSAN-I,Br] in acetone-d_6 (100 MHz).

1.11 Characterization of **[CoSAN-I,Cl]$^-$**

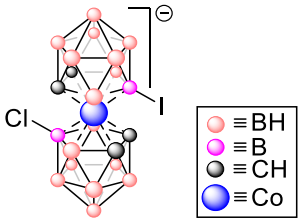

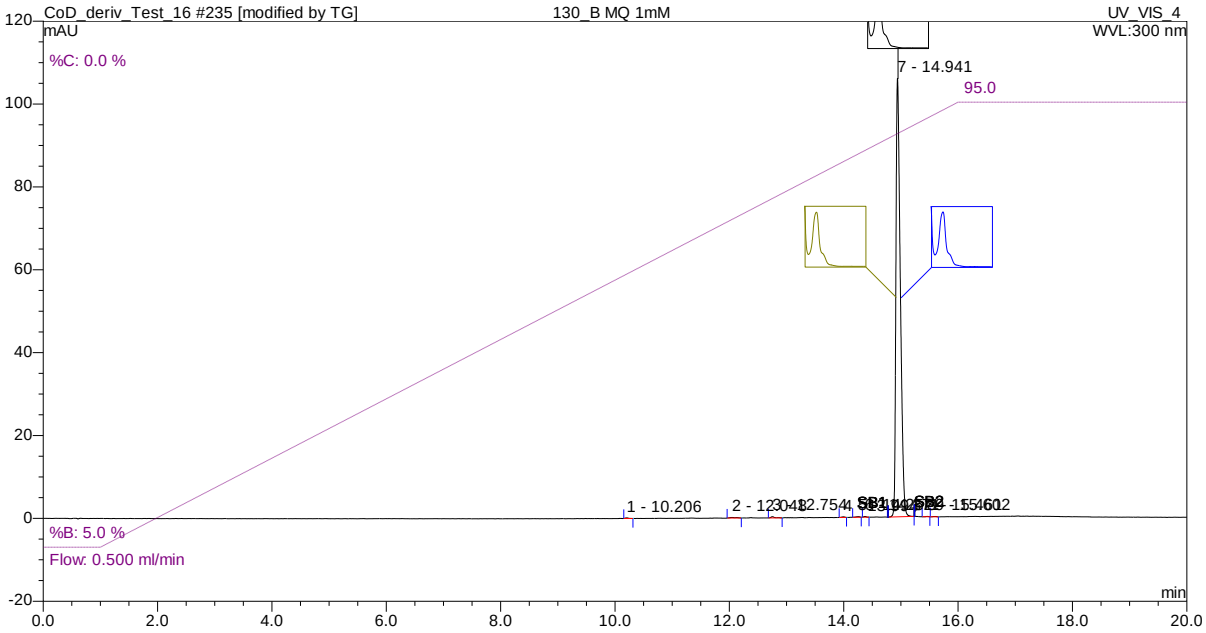

Fig. S77. HPLC chromatogram of [CoSAN-I,Cl]$^-$. Purity – 99.07%

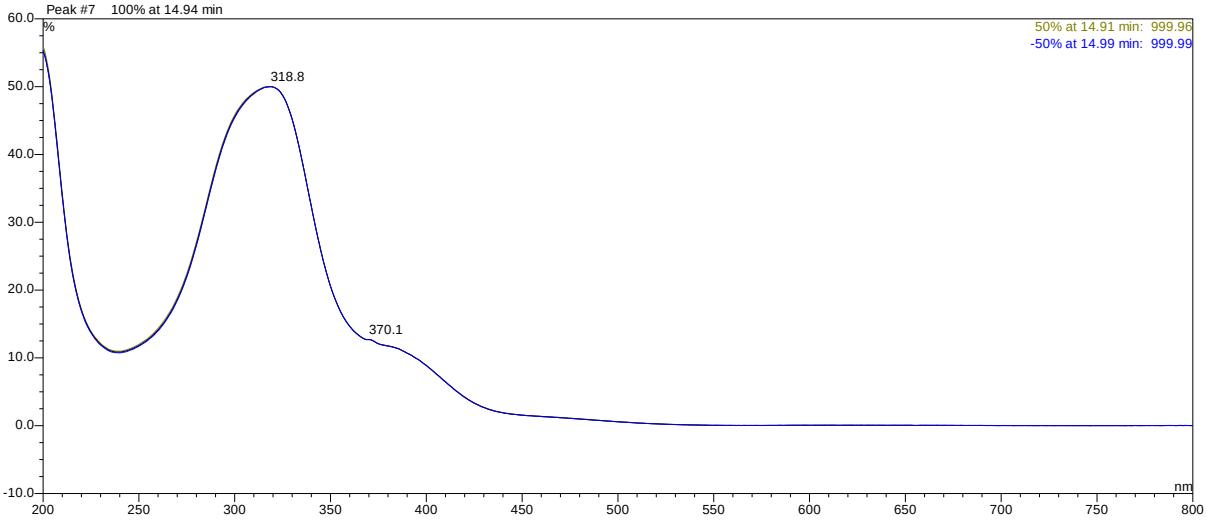

Fig. S78. UV-VIS spectrum of [CoSAN-I,Cl]$^-$ (peak purity analysis).

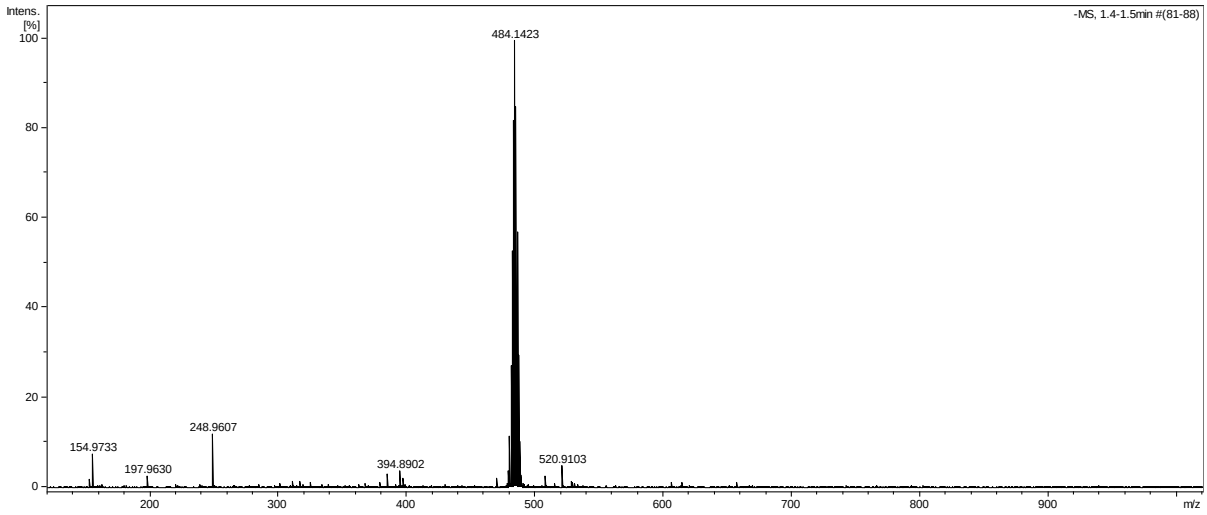

Fig. S79. ESI-MS spectrum of [CoSAN-I,Cl]$^-$.

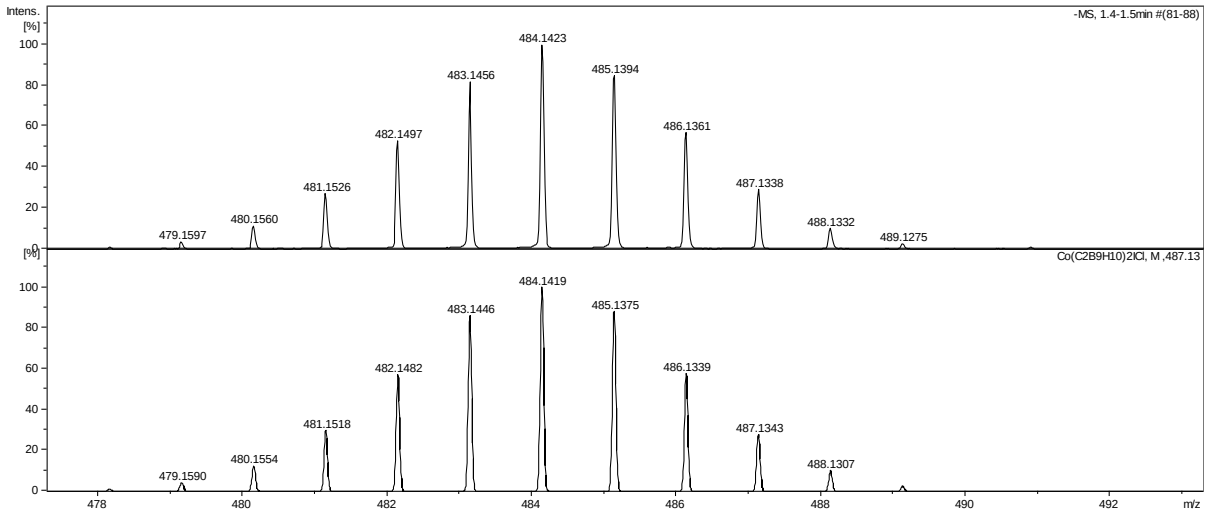

Fig. S80. Measured (top) and simulated (bottom) ESI-MS spectrum of [CoSAN-I,Cl]$^-$ – isotope pattern.

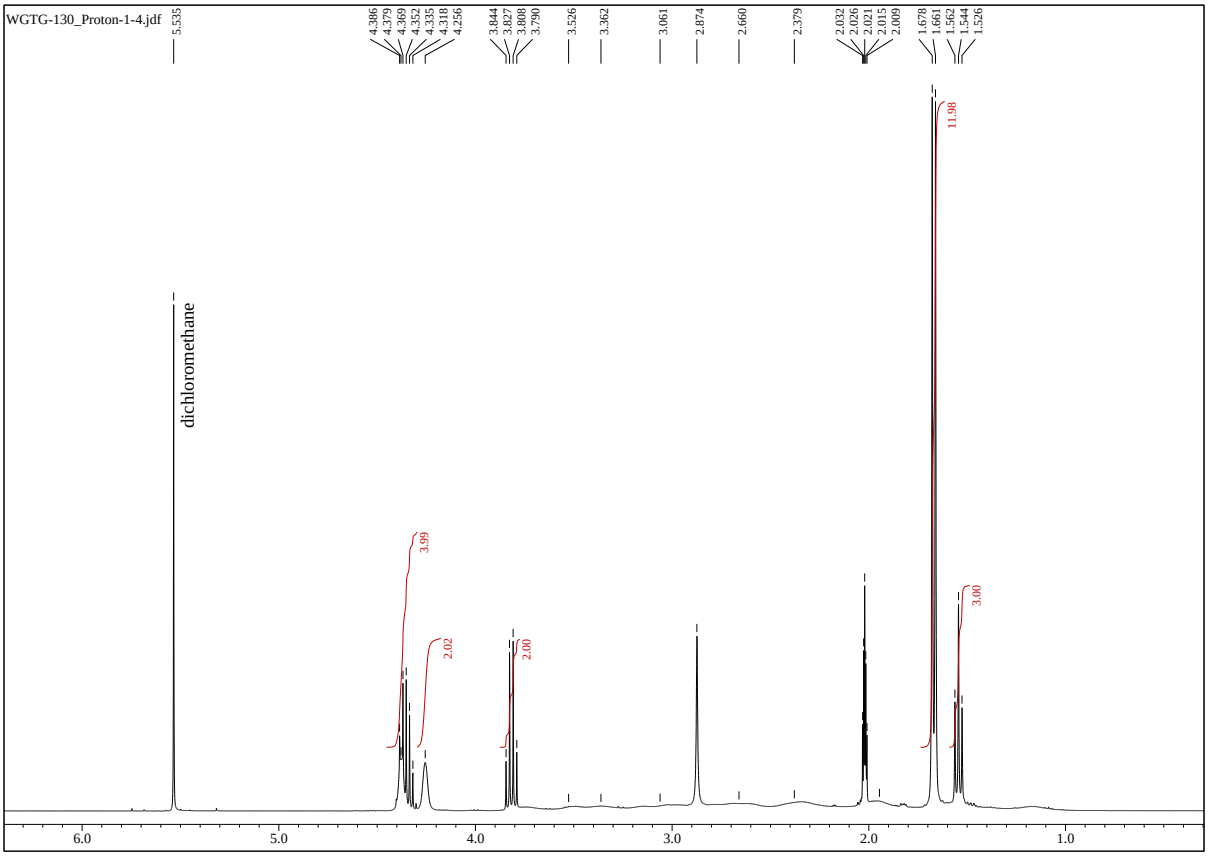

Fig. S81. ^{1}H NMR spectrum of [CoSAN-I,Cl] × [H(DIPEA)] in acetone-d_6 (400 MHz).

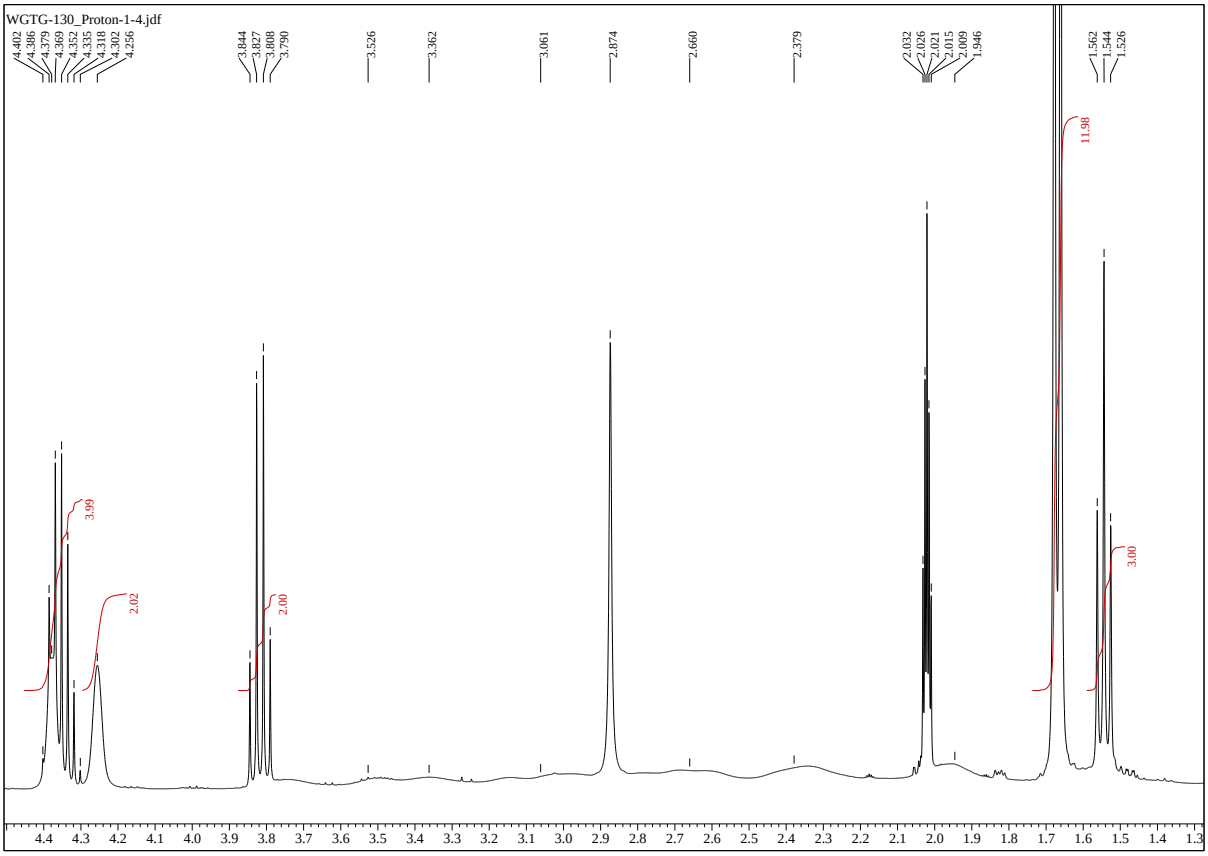

Fig. S82. Expanded ^{1}H NMR spectrum of [CoSAN-I,Cl] × [H(DIPEA)] in acetone-d_6 (400 MHz).

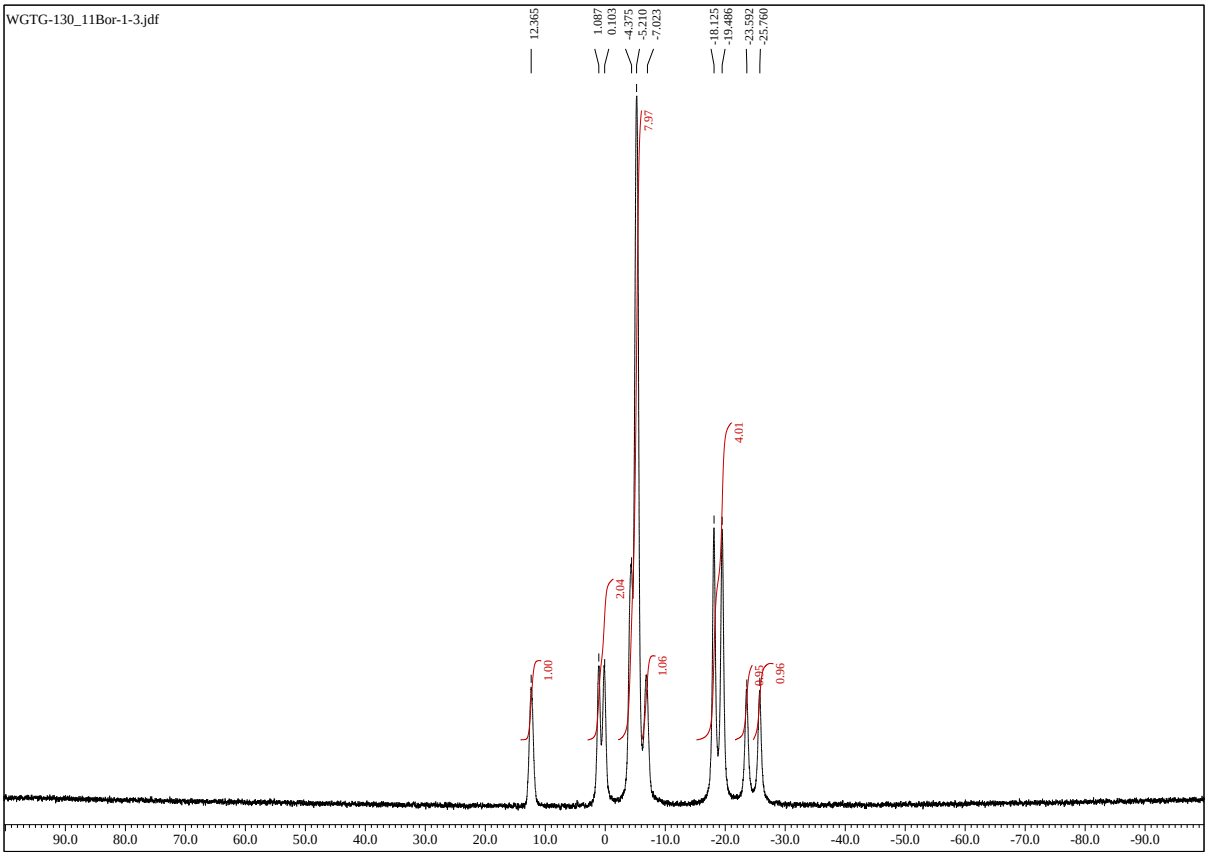

Fig. S83. $^{11}B\{^1H\}$ NMR spectrum of [CoSAN-I,Cl] × [H(DIPEA)] in acetone-d_6 (128 MHz).

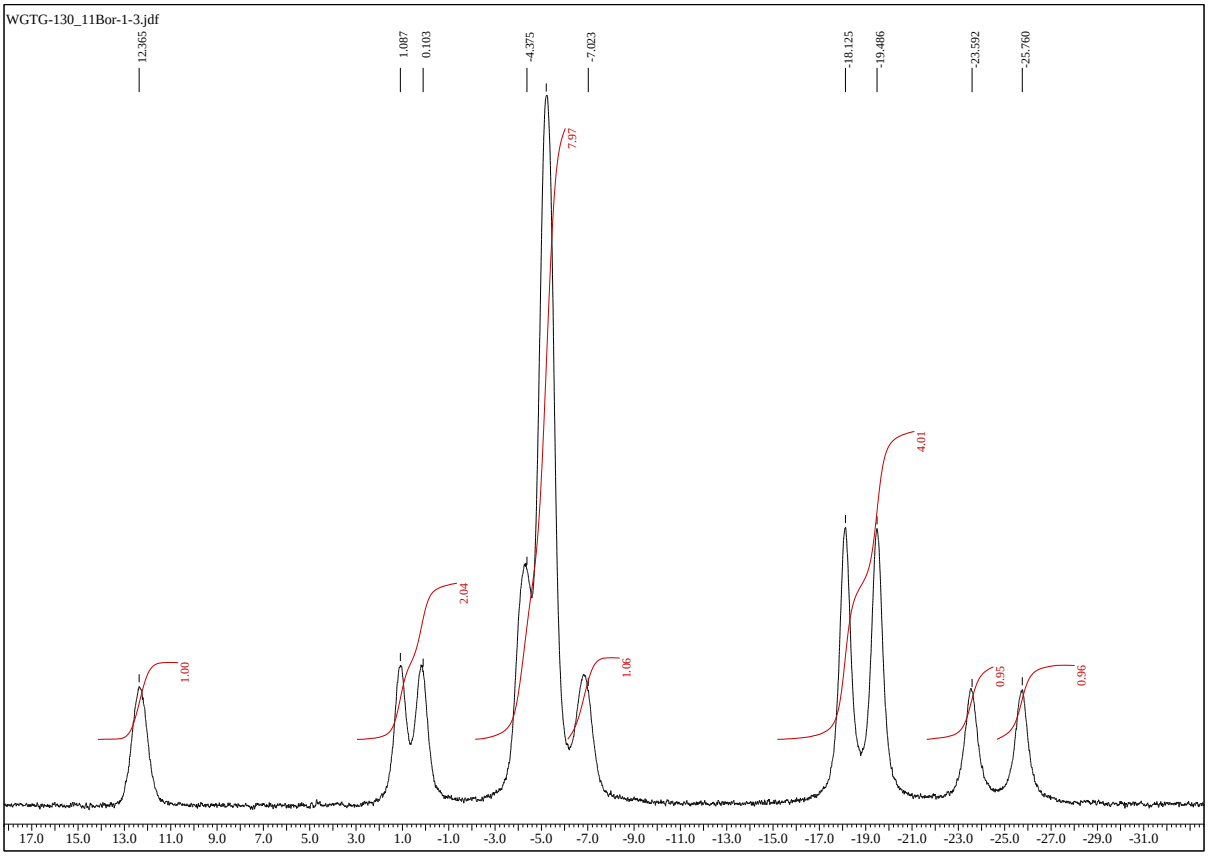

Fig. S84. Expanded $^{11}B\{^1H\}$ NMR spectrum of [CoSAN-I,Cl] × [H(DIPEA)] in acetone-d_6 (128 MHz).

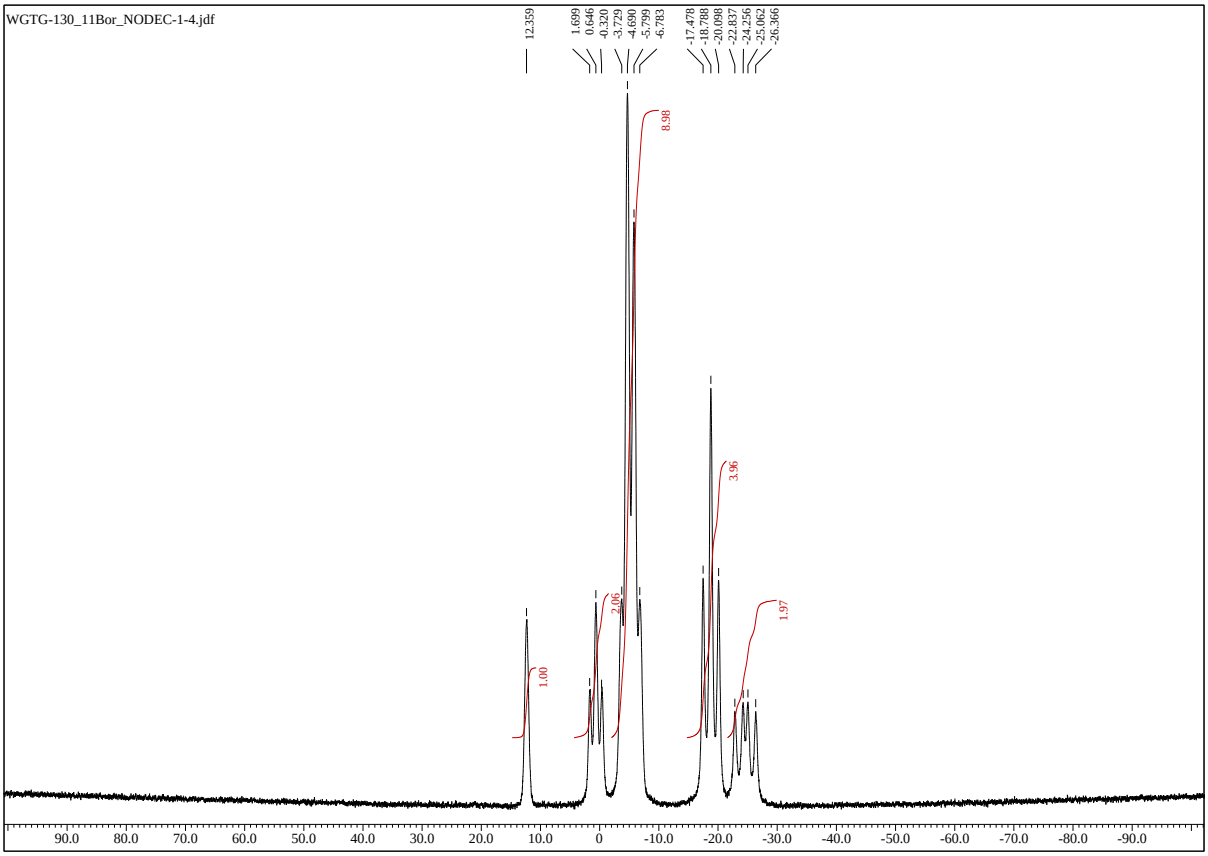

Fig. S85. ^{11}B NMR spectrum of [CoSAN-I,Cl] × [H(DIPEA)] in acetone-d_6 (128 MHz).

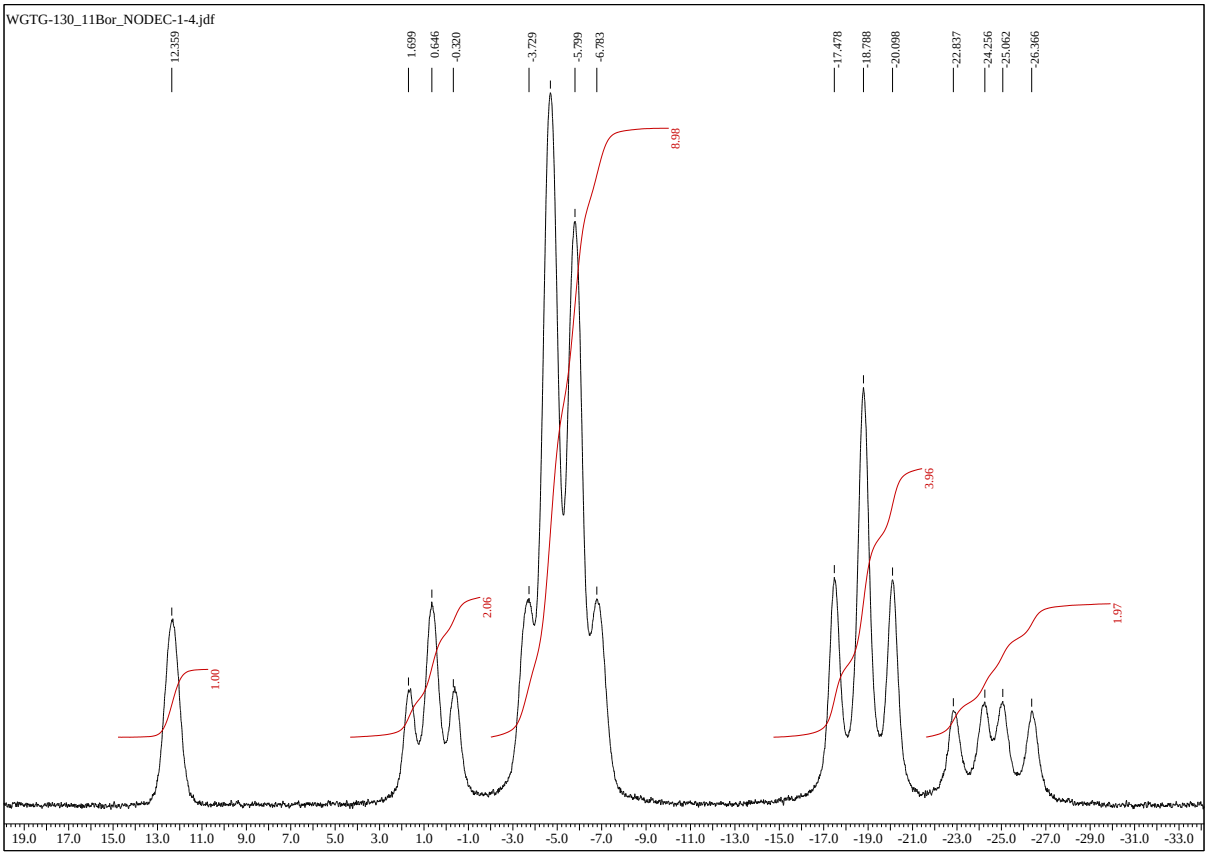

Fig. S86. Expanded ^{11}B NMR spectrum of [CoSAN-I,Cl] × [H(DIPEA)] in acetone-d_6 (128 MHz).

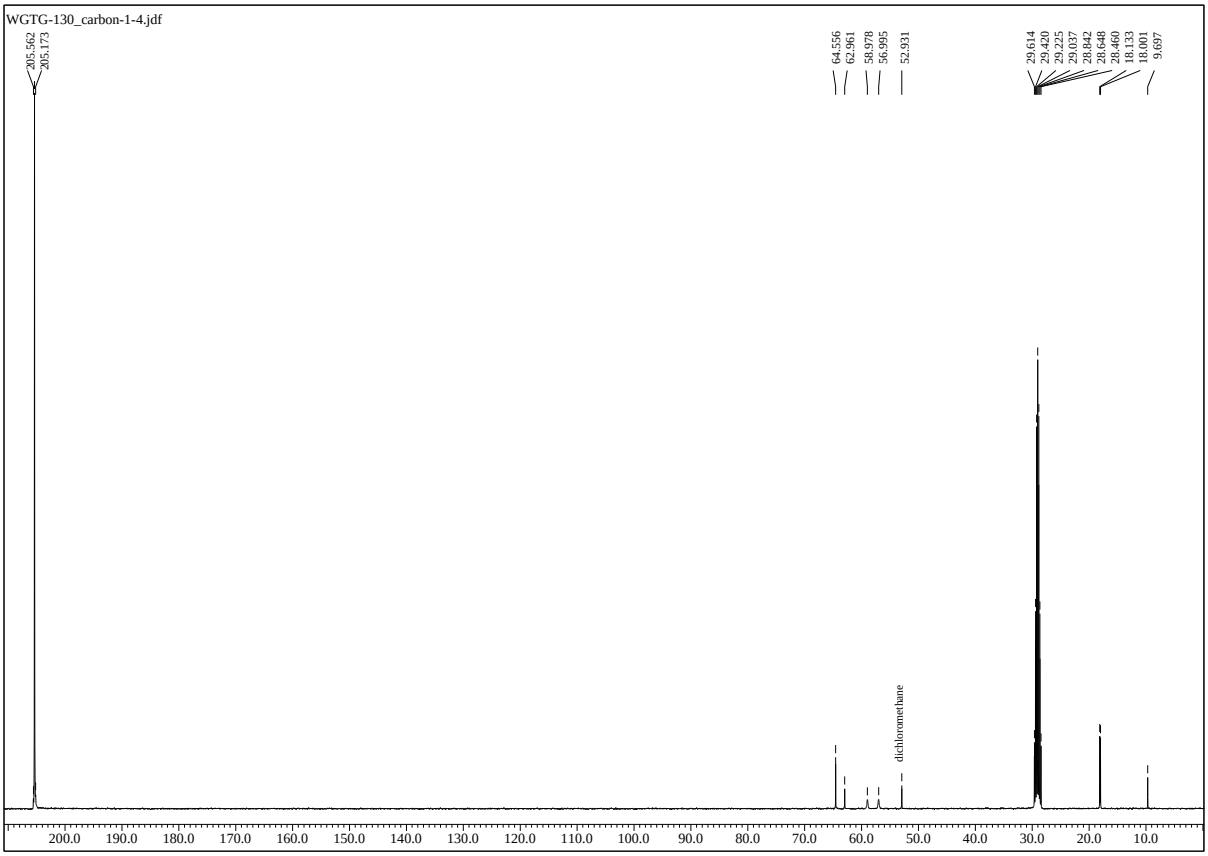

Fig. S87. $^{13}C\{^{1}H\}$ NMR spectrum of [CoSAN-I,Cl] × [H(DIPEA)] in acetone-d_6 (100 MHz).

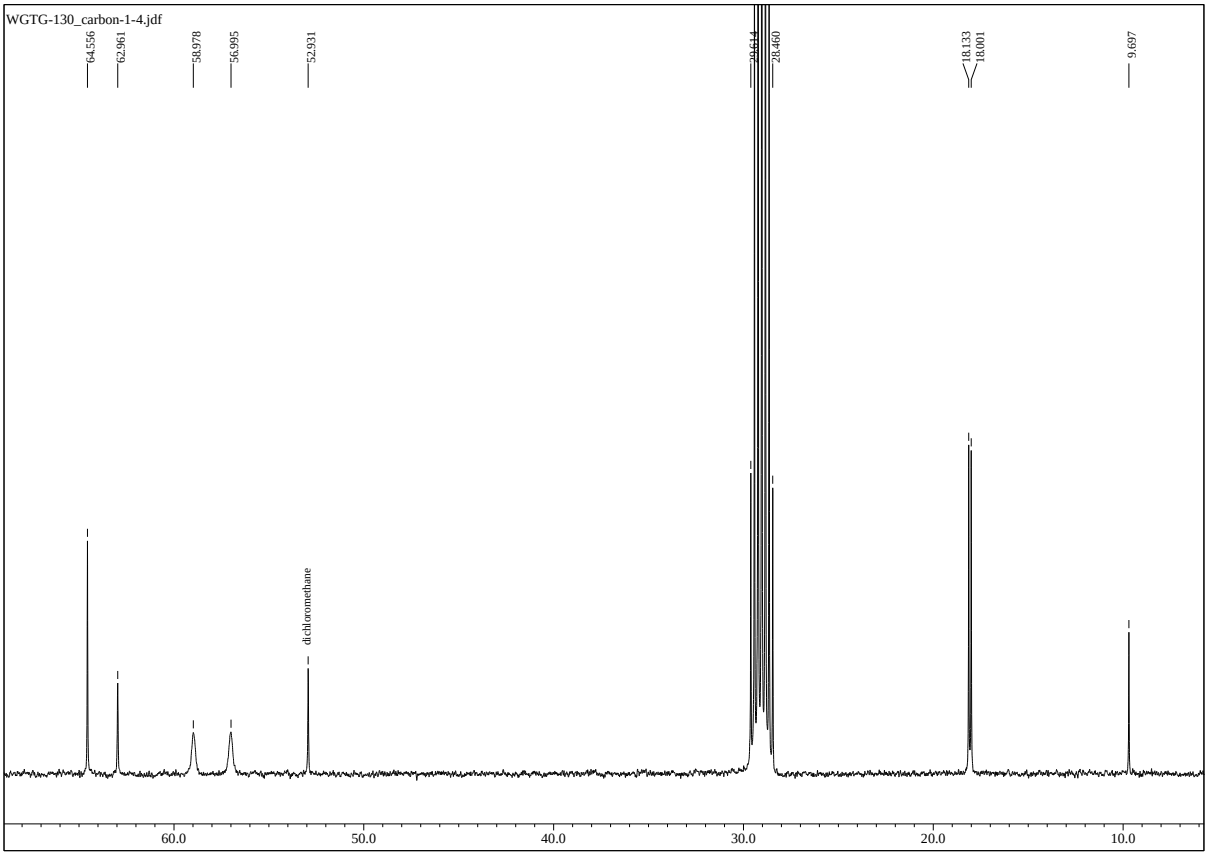

Fig. S88. Expanded $^{13}C\{^{1}H\}$ NMR spectrum of [CoSAN-I,Cl] × [H(DIPEA)] in acetone-d_6 (100 MHz).

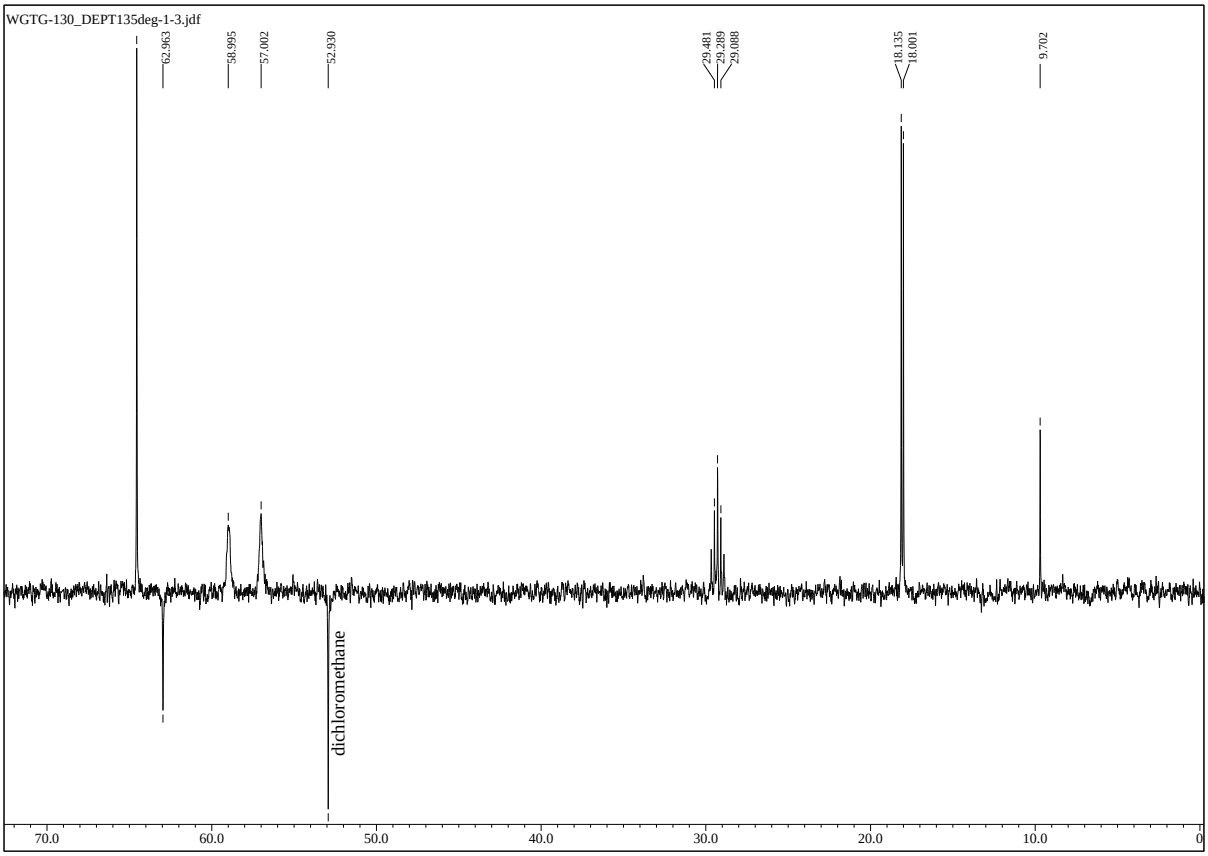

Fig. S89. DEPT 135 spectrum of [CoSAN-I,Cl] × [H(DIPEA)] in acetone-d_6 (100 MHz).

2. Single Crystal X-Ray Diffraction Data

Tab. S1. SCXRD selected experimental and refinement details of examined compounds at 295 K.

Compound	**Cs[CoSAN]**	**Cs[CoSAN-I_2]**	**Cs[CoSAN-I]**	**Cs[CoSAN-Br,Cl]**	**Cs[CoSAN-I,Br]**	**Cs[CoSAN-I,Cl]**
Crystal data						
Crystal system, space group	Monoclinic, $P2_1/c$	Monoclinic, $C2/c$	Monoclinic, $P2_1/n$	Orthorhombic, $Pna2_1$	Monoclinic, $P2_1/n$	Monoclinic, $P2_1/n$
M_r	456.63	708.42	582.53	569.98	661.43	616.97
a, b, c (Å)	6.963 (3), 12.215 (4), 21.505 (6)	18.987 (5), 8.871 (3), 12.529 (4)	7.469 (3), 13.177 (4), 20.735 (6)	19.994 (5), 6.847 (3), 14.381 (4)	6.802 (3), 14.587 (4), 10.462 (4)	6.795 (3), 14.507 (4), 10.395 (4)
α, β, γ (°)	90, 98.49 (3), 90	90, 91.78 (3), 90	90, 95.05 (3), 90	90, 90, 90	90, 100.34 (3), 90	90, 99.64 (3), 90
V (Å^3)	1809.1 (11)	2109.2 (11)	2032.8 (12)	1968.7 (11)	1021.2 (7)	1010.2 (7)
Z	4	4	4	4	2	2
μ (mm^{-1})	2.91	5.43	4.11	4.85	6.05	4.27
Crystal size (mm)	0.23 × 0.15 × 0.06	0.22 × 0.16 × 0.1	0.15 × 0.14 × 0.07	0.25 × 0.16 × 0.04	0.24 × 0.16 × 0.03	0.21 × 0.09 × 0.07
Data collection						
T_{min}, T_{max}	0.791, 1.000	0.813, 1.000	0.933, 1.000	0.621, 1.000	0.568, 1.000	0.845, 1.000
No. of measured, independent and observed [$I > 2\sigma(I)$] reflections	50568, 3695, 3274	41858, 2154, 2057	9242, 4144, 3234	76187, 4021, 3810	40896, 2096, 1896	20251, 2059, 1876
R_{int}	0.031	0.022	0.042	0.038	0.038	0.030
$(\sin \vartheta/\lambda)_{max}$ (Å^{-1})	0.625	0.625	0.625	0.625	0.625	0.625
Refinement						
$R[F^2 > 2\sigma(F^2)]$, $wR(F^2)$, S	0.022, 0.052, 1.03	0.016, 0.038, 1.11	0.035, 0.077, 1.05	0.023, 0.056, 1.03	0.025, 0.054, 1.16	0.059, 0.124, 1.35
No. of reflections	3695	2154	4144	4021	2096	2059
No. of parameters	217	120	226	236	121	121
No. of restraints	0	0	0	1	0	0
$\Delta\rho_{max}$, $\Delta\rho_{min}$ (e Å^{-3})	0.93, -0.52	0.71, -0.75	0.69, -0.79	0.48, -0.48	0.83, -0.76	0.92, -1.06
Absolute structure parameter	–	–	–	0.56 (2)	–	–

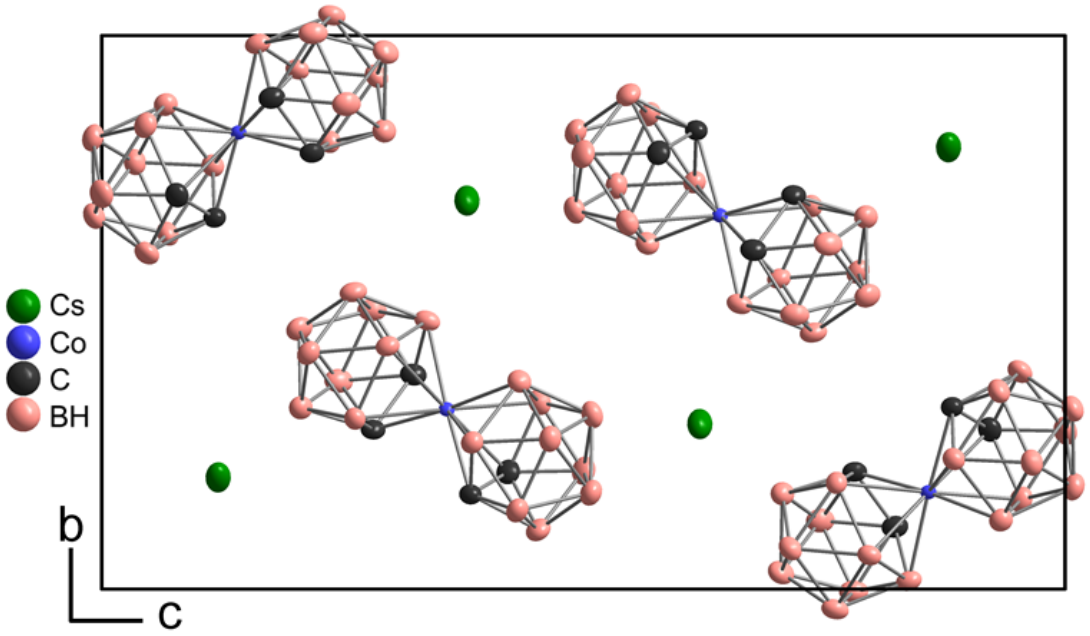

Fig. S90. Unit cell representation of Cs[CoSAN] in $P2_1/c$.

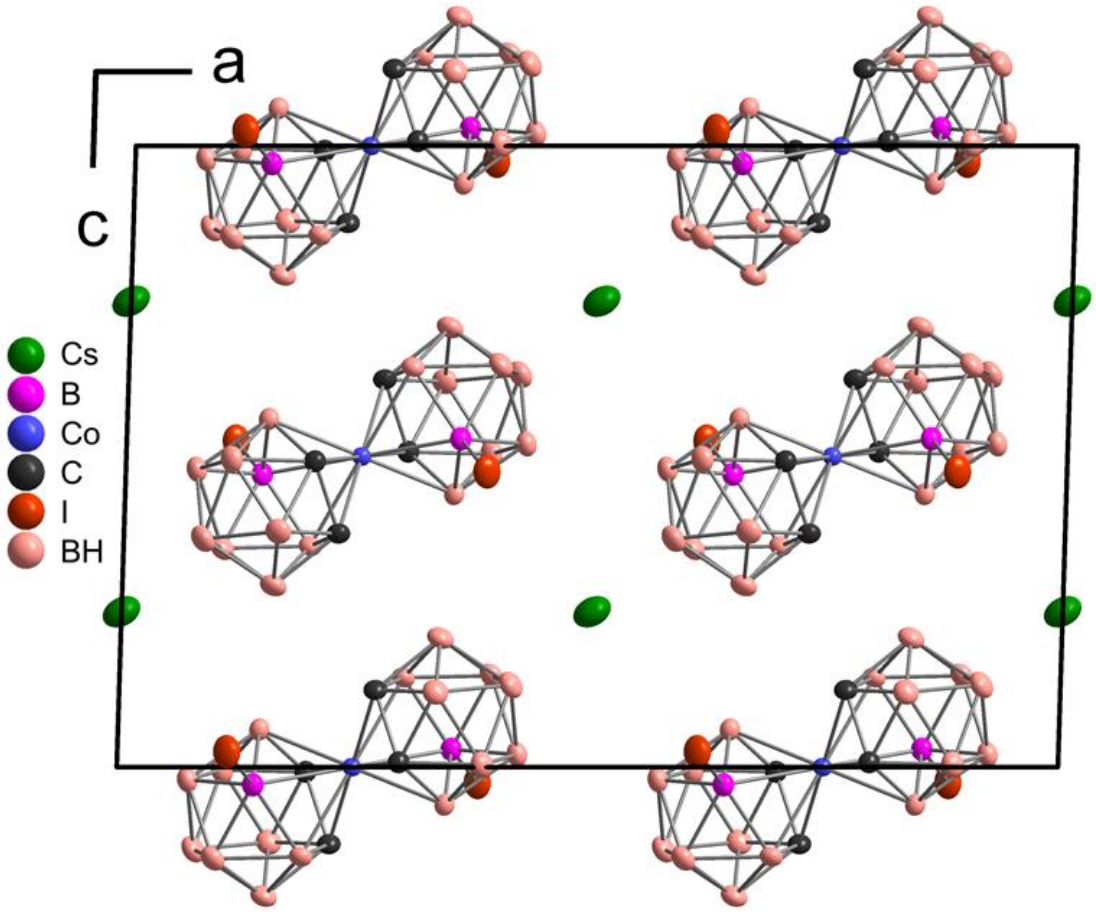

Fig. S91. Unit cell representation of Cs[CoSAN-I_2] in C2/c.

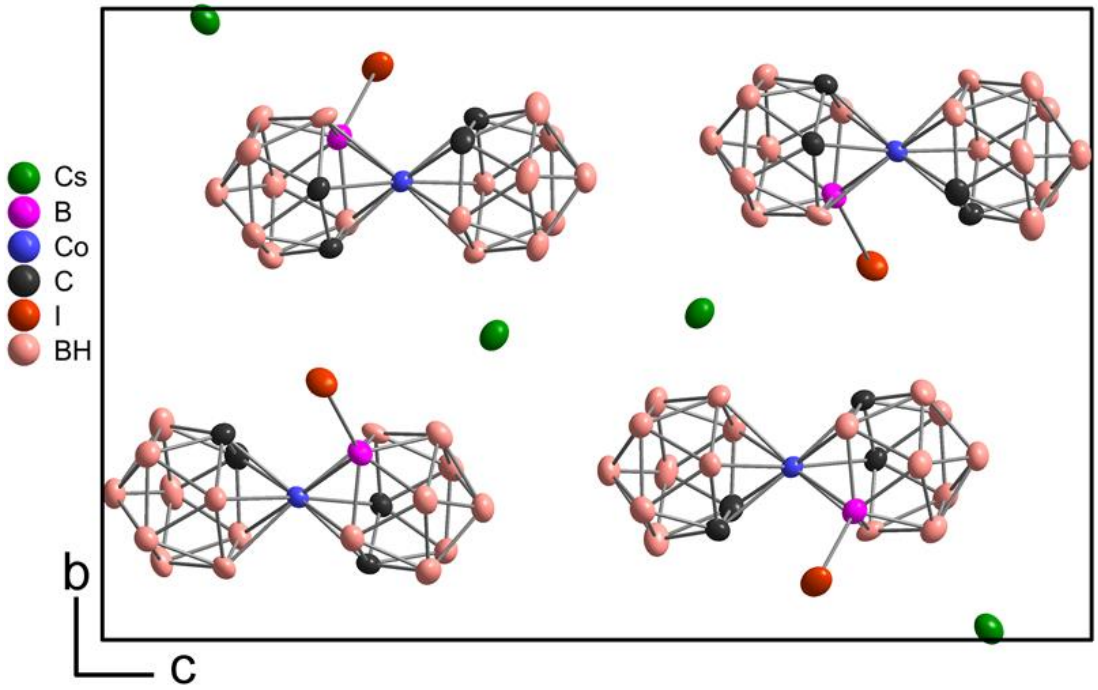

Fig. S92. Unit cell representation of Cs[CoSAN-I] in $P2_1/n$.

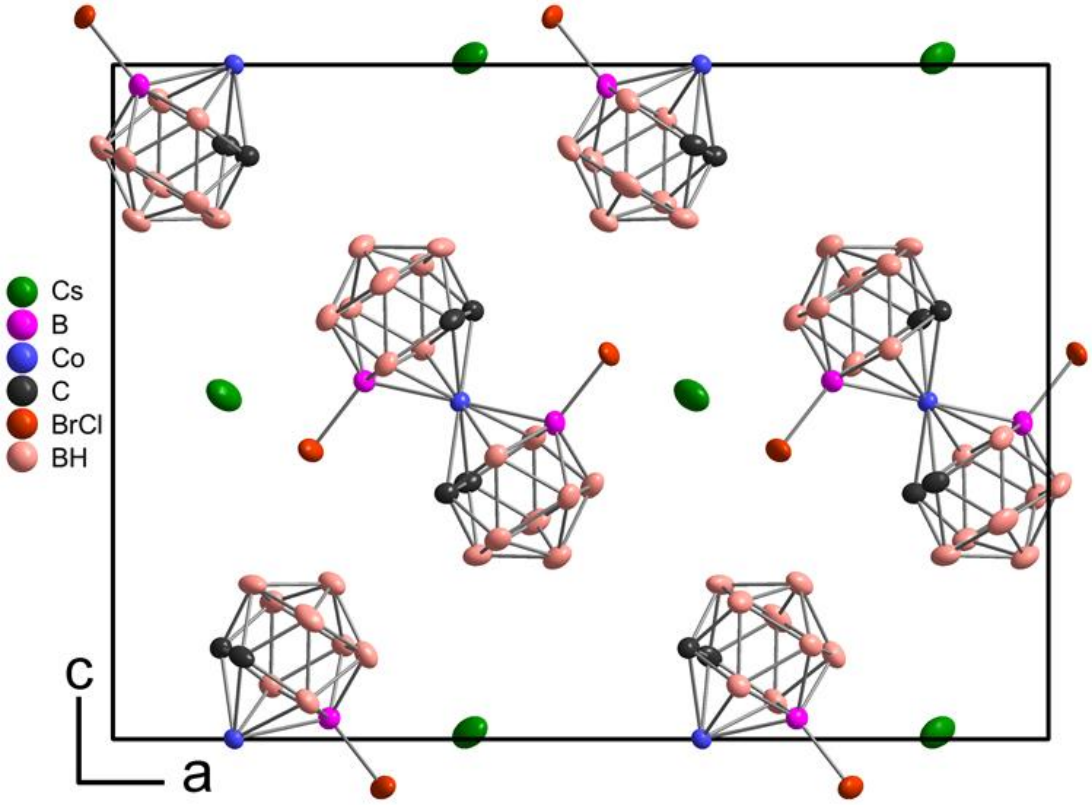

Fig. S93. Unit cell representation of Cs[CoSAN-Cl,Br] in $Pna2_1$.

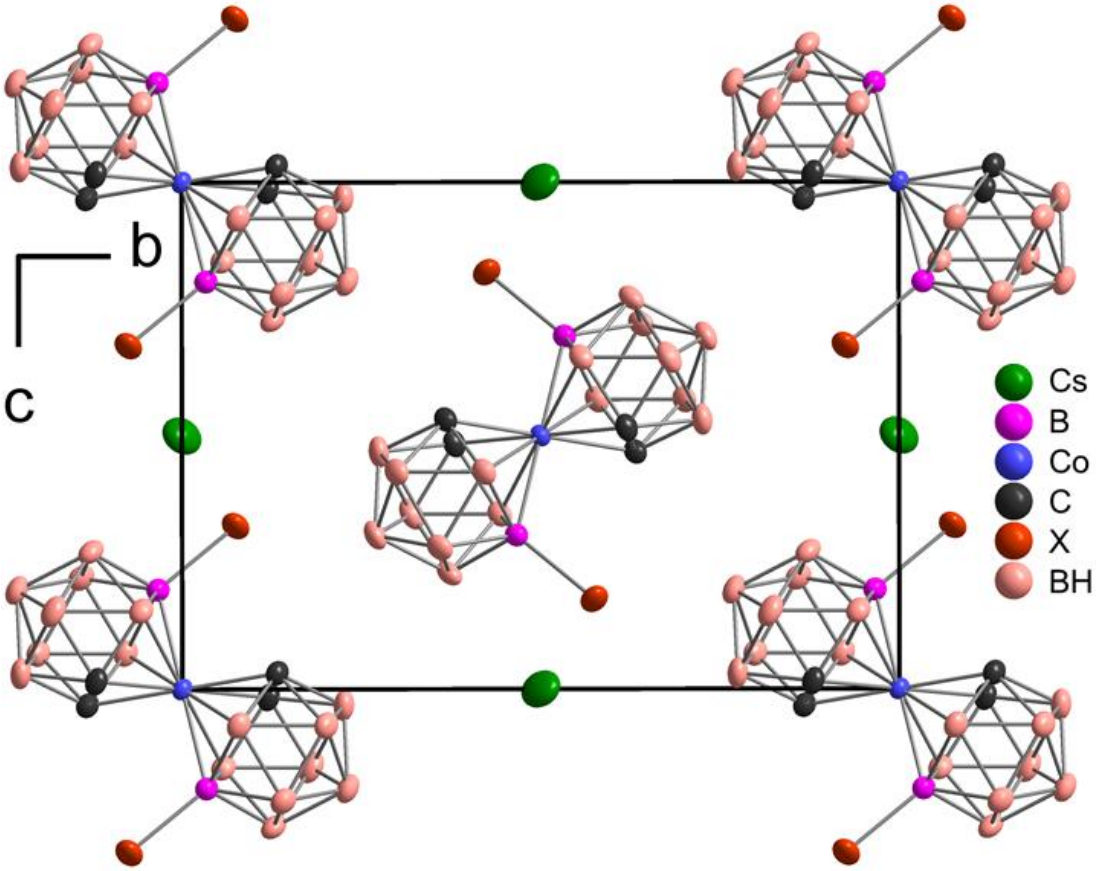

Fig. S94. Unit cell representation of Cs[CoSAN-I,Br] and Cs[CoSAN-I,Cl], both in $P2_1/n$.

3. Summary of biological and physicochemical data

Tab. S2. Biological and physicochemical properties of synthesized compounds. MIC - minimum inhibitory concentration, MBC - minimum bactericidal concentration, Van – vancomycin, Pol - polymyxin B, IC_{50} – half maximal inhibitory concentration of proliferation, MCF 10A – human mammary gland cells, HEK293 – human embryonic kidney cells, A549 – human lung cancer cells, MCF-7 – human breast cancer, SI *S. a.* – selectivity index calculated as $IC_{50\ MCF\ 10A}/MIC_{S.\ aureus}$, SI *E. f.* – selectivity index calculated as $IC_{50\ MCF\ 10A}/MIC_{E.\ faecium}$, Log P – decimal logarithm of partition coefficient, Log k_w – decimal logarithm of chromatographic lipophilicity index, SE – standard error, "-" not determined.

	S. aureus **ATCC 6538**		***E. faecium*** **PCM 2910**		***E. coli*** **PCM 2720**		***P. aeruginosa*** **PCM 1630**		**IC_{50} (95% CI)** [μM]				**SI *S. a.*** [-]	**SI *E. f.*** [-]	**Log P** (SE) [-]	**Log k_w** (SE) [-]
Compound	**MIC** [μM]	**MBC** [μM]	**MIC** [μM]	**MBC** [μM]	**MIC** [μM]	**MBC** [μM]	**MIC** [μM]	**MBC** [μM]	**MCF 10A**	**HEK293**	**A549**	**MCF-7**				
Na[CoSAN]	50	100	25	50	>100	>100	>100	>100	34.94 (-)	20.84 (33.43-50.87)	24.61 (20.21-29.67)	75.53 (56.18-189.6)	0.70	1.40	1.59 (0.01)	3.26 (0.01)
Na[CoSAN-F_2]	25	50	50	100	>100	>100	>100	>100	33.91 (-)	28.94 (24.49-34.28)	16.57 (14.44-19.00)	44.52 (37.54-53.74)	1.36	0.68	1.30 (0.01)	3.06 (0.02)
Na[CoSAN-Cl_2]	12.5	25	12.5	25	>100	>100	>100	>100	25.44 (20.99-29.93)	22.25 (19.34-25.53)	13.58 (11.84-15.56)	35.03 (27.26-45.60)	2.04	2.04	3.17 (0.02)	4.11 (0.02)
Na[CoSAN-Br_2]	3.1	6.2	6.2	12.5	>100	>100	>100	>100	23.93 (19.59-28.42)	22.56 (18.15-28.06)	12.86 (11.60-14.37)	33.78 (28.27-39.71)	7.72	3.86	3.65 (0.03)	4.33 (0.02)
Na[CoSAN-I_2]	1.6	3.1	1.6	12.5	>100	>100	>100	>100	17.47 (14.64-20.86)	17.78 (15.67-20.16)	11.29 (10.13-12.72)	24.64 (20.17-29.60)	10.92	10.92	4.23 (0.04)	4.68 (0.03)
Na[CoSAN-Cl]	12.5	25	12.5	25	>100	>100	>100	>100	32.67 (-)	29.43 (24.12-37.02)	16.17 (13.68-19.07)	51.39 (43.28-62.42)	2.61	2.61	2.15 (0.01)	3.60 (0.02)
Na[CoSAN-Br]	3.1	6.2	6.2	25	>100	>100	>100	>100	31.66 (-)	26.59 (22.16-32.28)	15.91 (13.96-18.12)	41.69 (35.64-49.61)	10.21	5.11	2.40 (0.02)	3.75 (0.03)
Na[CoSAN-I]	0.8	1.6	1.6	12.5	>100	>100	>100	>100	31.28 (25.92-35.19)	20.84 (16.63-26.31)	12.82 (11.20-14.68)	36.57 (32.57-41.52)	39.10	19.55	2.79 (0.01)	3.96 (0.02)
Na[CoSAN-Br,Cl]	6.2	12.5	12.5	25	>100	>100	>100	>100	29.41 (24.27-32.85)	23.74 (20.48-27.45)	12.36 (10.91-13.99)	36.49 (30.12-43.57)	4.74	2.35	3.33 (0.02)	4.23 (0.02)
Na[CoSAN-I,Br]	1.6	3.1	6.2	12.5	>100	>100	>100	>100	20.65 (16.82-25.06)	25.67 (21.10-30.60)	11.87 (-)	34.92 (27.58-42.39)	12.91	3.33	4.12 (0.03)	4.53 (0.03)
Na[CoSAN-I,Cl]	1.6	3.1	6.2	12.5	100	>100	>100	>100	11.15 (-)	11.66 (10.22-13.26)	8.45 (7.28-9.60)	16.89 (13.77-20.56)	6.97	1.80	3.78 (0.03)	4.42 (0.03)
Van	<0.4	0.4	<0.4	50/ 100	-	-	-	-	-	-	-	-	-	-	-	-
Pol	-	-	-	-	0.8	1.6	1.6	1.6	-	-	-	-	-	-	-	-

Table S3. HPLC quantitative analysis of synthesized compounds.

Compound	Mw (g/mol)	c (mg/ml)	c (mM)	HPLC - R_t (min)	HPLC - λ_{max} (nm)	HPLC Peak area (mAU×min)	Precision (%)
Na[CoSAN]×4H_2O	418.80	41.88	100	12.526	283	22.3298	101
Cs[CoSAN]	465.65	45.67		12.530		22.1530	
Na[CoSAN-F_2]	382.72	38.27	100	12.088	298	14.4292	103
H[CoSAN-F_2]	360.74	36.07		12.086		14.8004	
Na[CoSAN-Cl_2]	415.63	41.56	100	14.531	316	21.2860	102
Cs[CoSAN-Cl_2]	525.54	52.55		14.524		20.8399	
Na[CoSAN-Br_2]	504.53	50.45	100	15.043	321	19.9212	96.1
Cs[CoSAN-Br_2]	614.44	61.44		15.035		20.7320	
Na[CoSAN-I_2]	598.53	59.85	100	15.766	290	10.7511	95.4
Cs[CoSAN-I_2]	708.45	70.85		15.768		11.2657	
Na[CoSAN-Cl]	381.18	38.12	100	13.405	306	21.7939	94.6
Cs[CoSAN-Cl]	491.10	49.11		13.403		23.0441	
Na[CoSAN-Br]	425.63	42.56	100	13.742	311	19.6381	94.6
Cs[CoSAN-Br]	535.55	53.56		13.738		20.7516	
Na[CoSAN-I]	472.63	47.26	100	14.127	290	12.1121	101
Cs[CoSAN-I]	582.55	58.26		14.126		12.0087	
Na[CoSAN-Br,Cl]	460.08	46.01	100	14.779	319	20.6934	95.5
Cs[CoSAN-Br,Cl]	569.99	57.00		14.775		21.6588	
Na[CoSAN-I,Br]	551.53	55.15	100	15.413	324	12.4771	95.8
Cs[CoSAN-I,Br]	661.45	66.15		15.411		13.0222	
Na[CoSAN-I,Cl]	507.08	50.71	100	14.941	319	10.3553	101
Cs[CoSAN-I,Cl]	617.00	61.70		14.943		10.2554	

4. Antiproliferative activity

4.1 IC_{50} comparison for tested cell lines

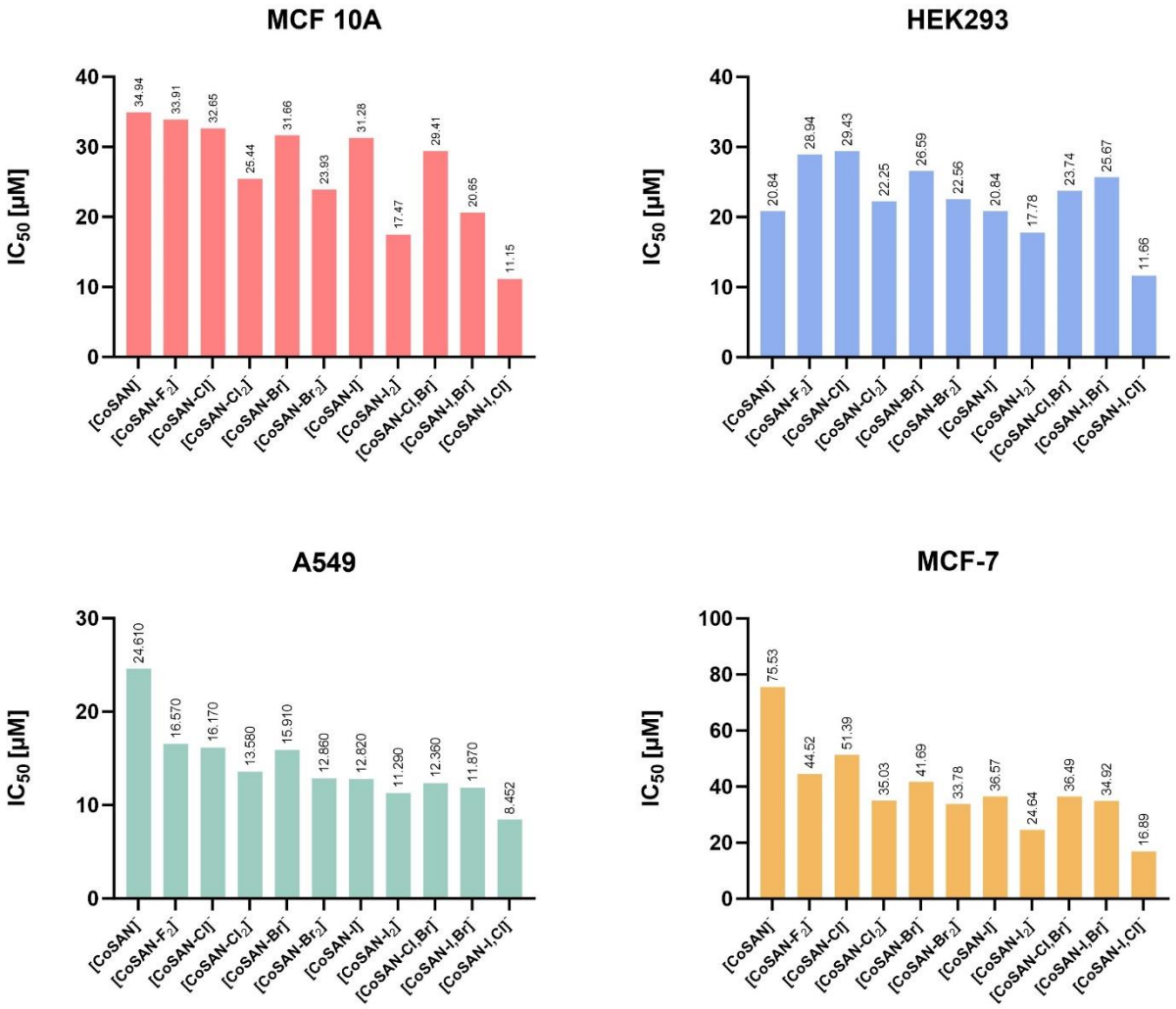

Fig. S95. IC_{50} comparison graphs across MCF 10A (epithelial human mammary gland cell line), HEK293 (epithelial human embryonic kidney cell line), A549 (epithelial human lung adenocarcinoma) and MCF-7 (epithelial human breast adenocarcinoma).

4.2 Dose-response curve for **Na[CoSAN]**

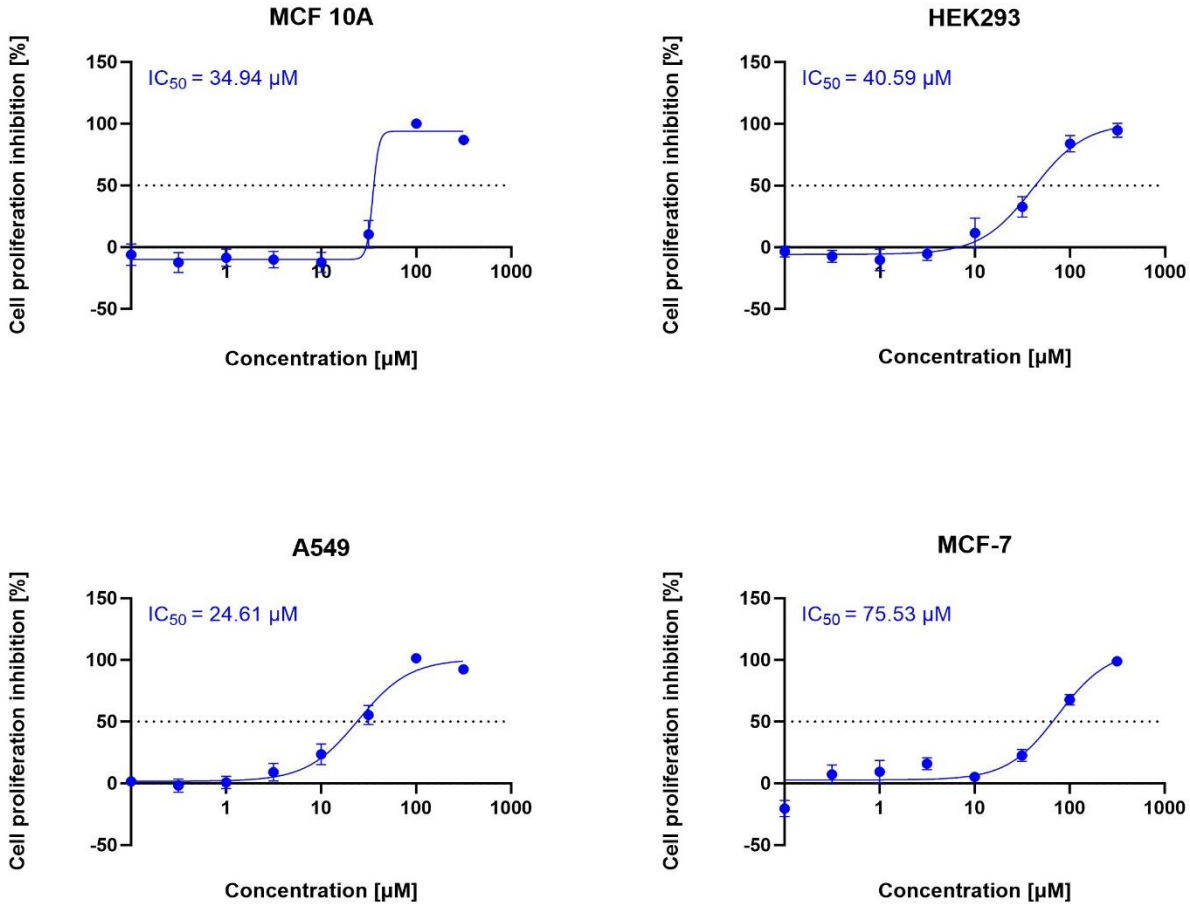

	95% CI [µM]
MCF 10A	-
HEK293	33.43 to 50.87
A549	20.21 to 29.67
MCF-7	56.18 to 189.6

Fig. S96. Antiproliferative activity of Na[CoSAN] against MCF 10A (epithelial human mammary gland cell line), HEK293 (epithelial human embryonic kidney cell line), A549 (epithelial human lung adenocarcinoma) and MCF-7 (epithelial human breast adenocarcinoma) - 72-hour dose-response curve. The table contains 95% confidence intervals.

4.3 Dose-response curve for **Na[CoSAN-F_2]**

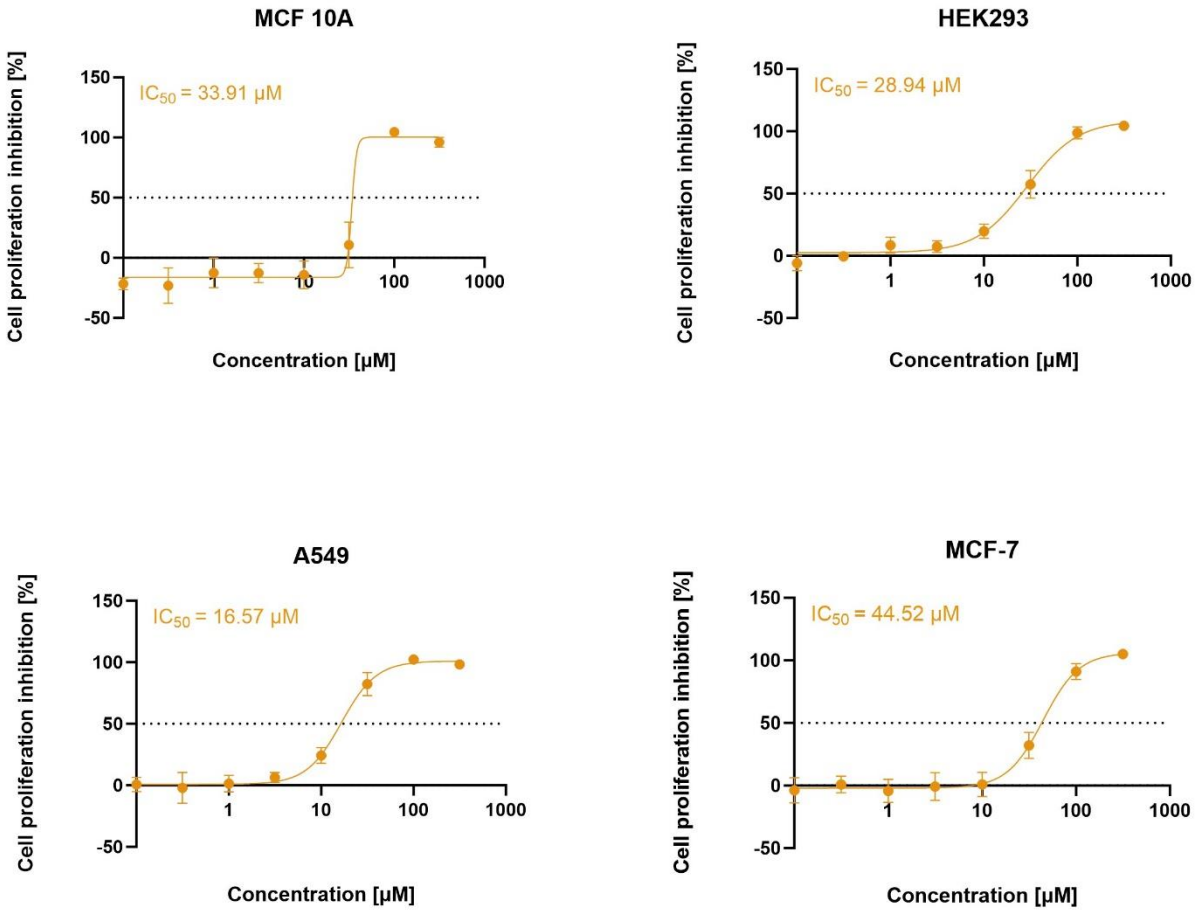

	95% CI [µM]
MCF 10A	-
HEK293	24.49 to 34.28
A549	14.44 to 19.00
MCF-7	37.54 to 53.74

Fig. S97. Antiproliferative activity of Na[CoSAN-F_2] against MCF 10A (epithelial human mammary gland cell line), HEK293 (epithelial human embryonic kidney cell line), A549 (epithelial human lung adenocarcinoma) and MCF-7 (epithelial human breast adenocarcinoma) - 72-hour dose-response curve. The table contains 95% confidence intervals.

4.4 Dose-response curve for **Na[CoSAN-Cl$_2$]**

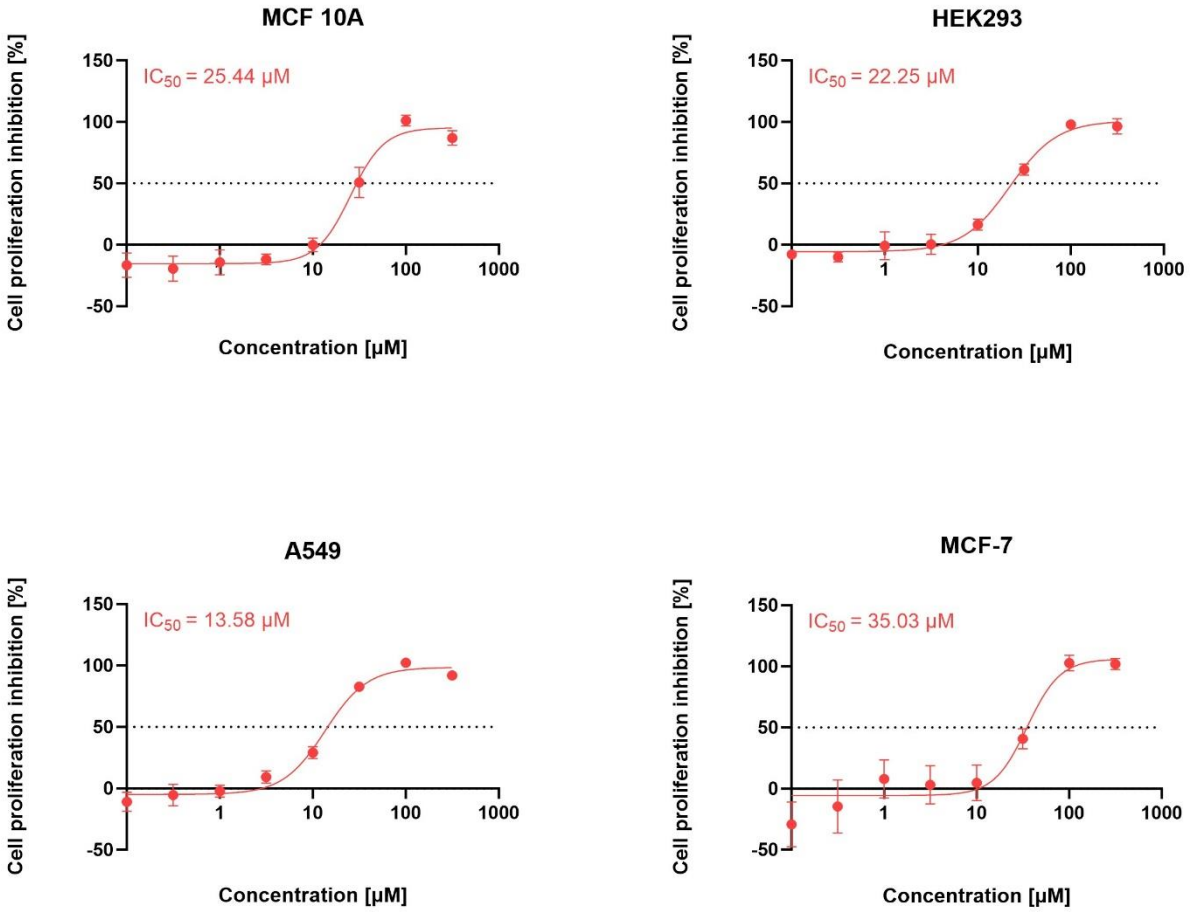

	95% CI [µM]
MCF 10A	20.99 to 29.93
HEK293	19.34 to 25.53
A549	11.84 to 15.56
MCF-7	27.26 to 45.60

Fig. S98. Antiproliferative activity of Na[CoSAN-Cl$_2$] against MCF 10A (epithelial human mammary gland cell line), HEK293 (epithelial human embryonic kidney cell line), A549 (epithelial human lung adenocarcinoma) and MCF-7 (epithelial human breast adenocarcinoma) - 72-hour dose-response curve. The table contains 95% confidence intervals.

4.5 Dose-response curve for **Na[CoSAN-Br$_2$]**

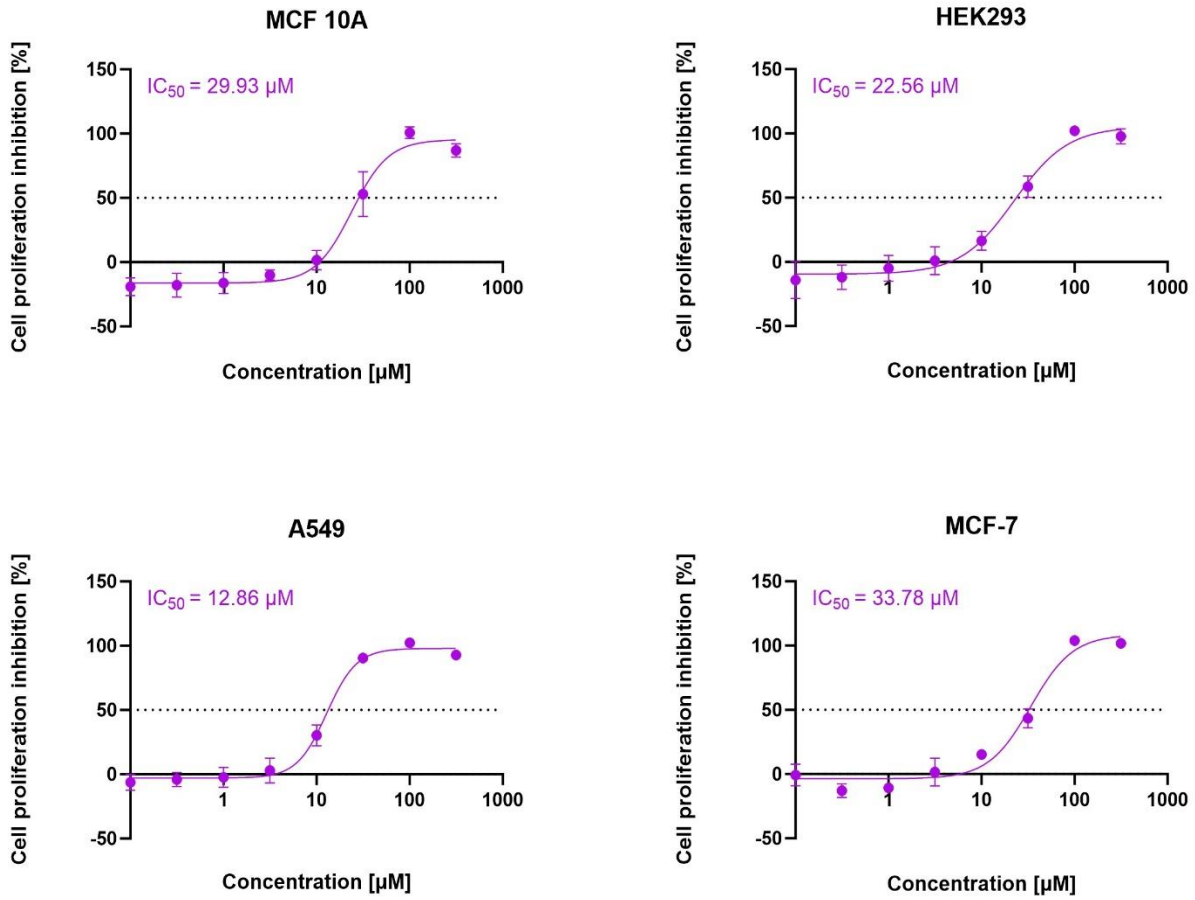

	95% CI [µM]
MCF 10A	19.59 to 28.42
HEK293	18.15 to 28.06
A549	11.60 to 14.37
MCF-7	28.27 to 39.71

Fig. S99. Antiproliferative activity of Na[CoSAN-Br$_2$] against MCF 10A (epithelial human mammary gland cell line), HEK293 (epithelial human embryonic kidney cell line), A549 (epithelial human lung adenocarcinoma) and MCF-7 (epithelial human breast adenocarcinoma) - 72-hour dose-response curve. The table contains 95% confidence intervals.

4.6 Dose-response curve for **Na[CoSAN-I_2]**

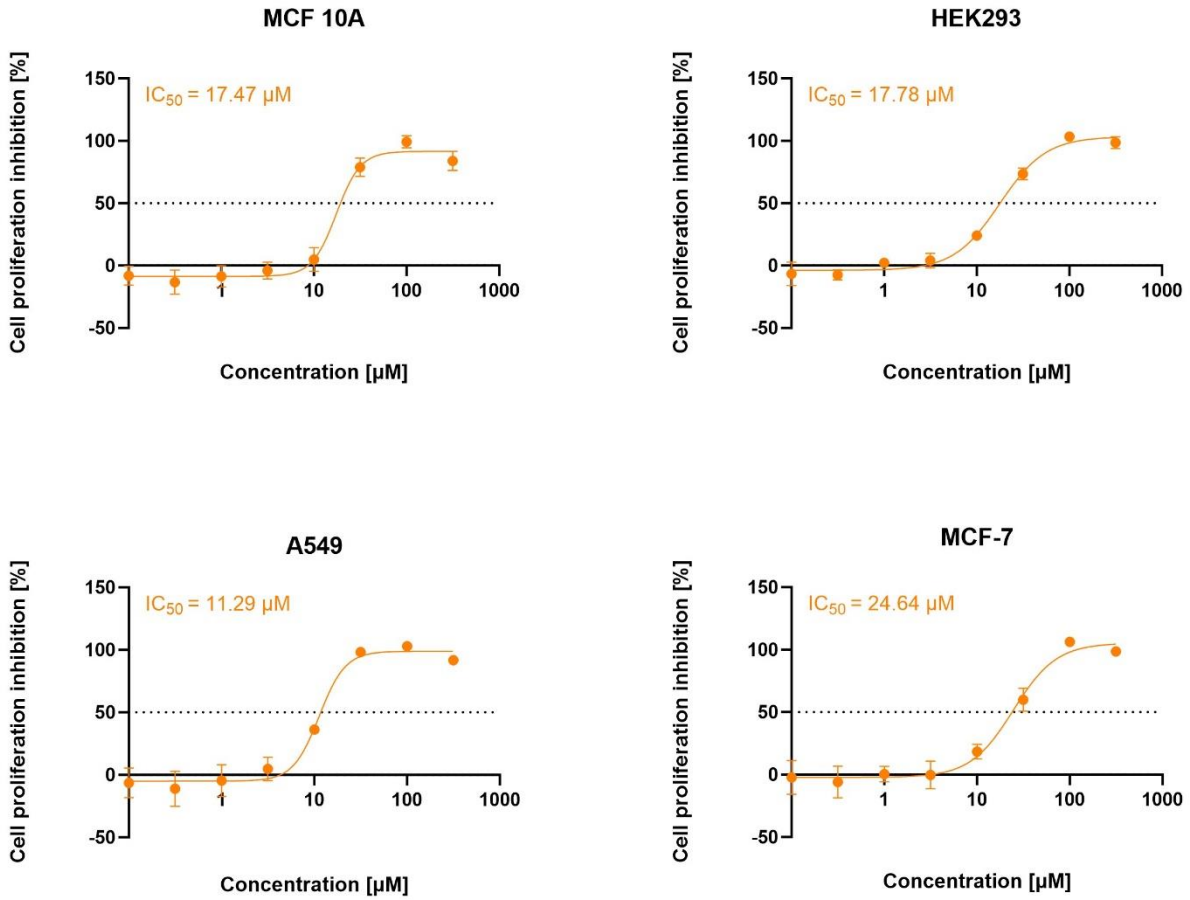

	95% CI [µM]
MCF 10A	14.64 to 20.86
HEK293	15.67 to 20.16
A549	10.13 to 12.72
MCF-7	20.17 to 29.60

Fig. S100. Antiproliferative activity of Na[CoSAN-I_2] against MCF 10A (epithelial human mammary gland cell line), HEK293 (epithelial human embryonic kidney cell line), A549 (epithelial human lung adenocarcinoma) and MCF-7 (epithelial human breast adenocarcinoma) - 72-hour dose-response curve. The table contains 95% confidence intervals.

4.7 Dose-response curve for **Na[CoSAN-Cl]**

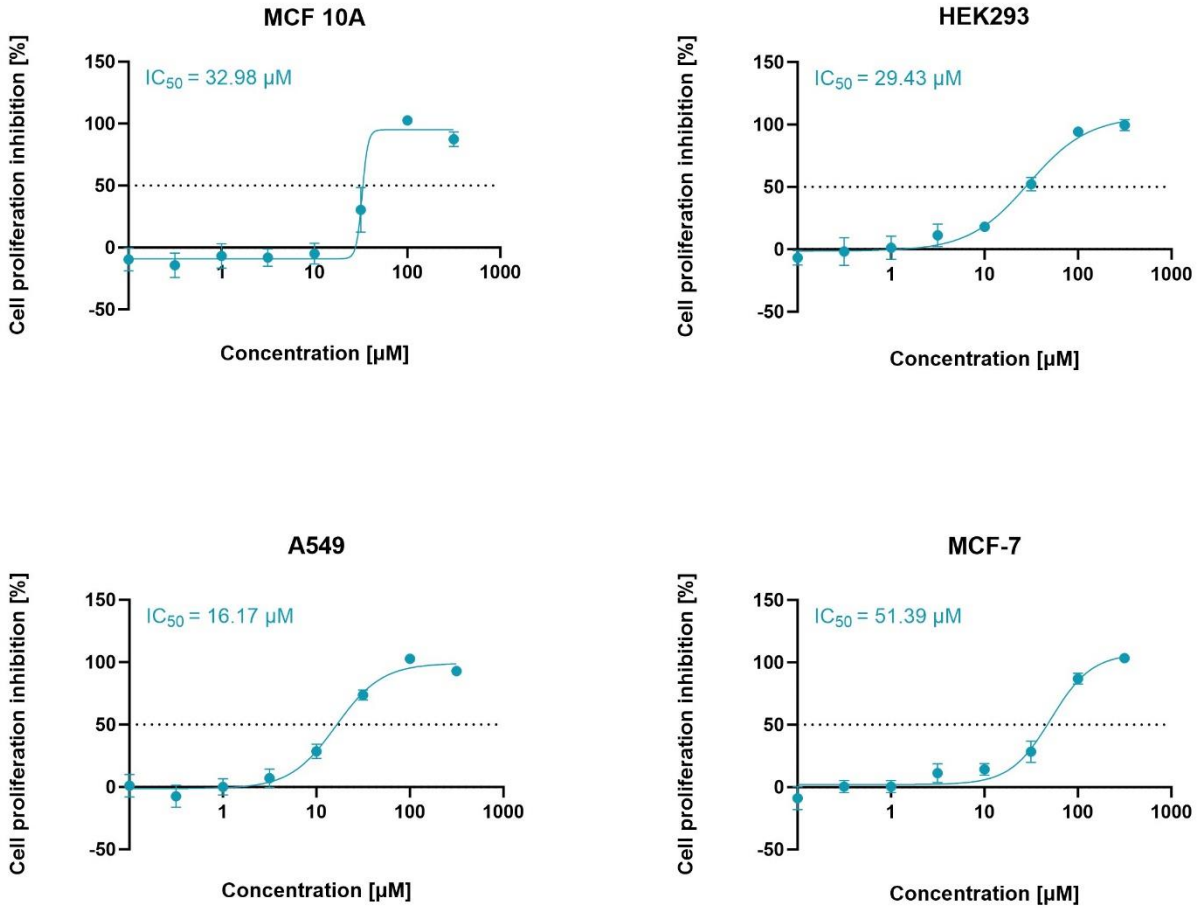

	95% CI [µM]
MCF 10A	-
HEK293	24.12 to 37.02
A549	13.68 to 19.07
MCF-7	43.28 to 62.42

Fig. S101. Antiproliferative activity of Na[CoSAN-Cl] against MCF 10A (epithelial human mammary gland cell line), HEK293 (epithelial human embryonic kidney cell line), A549 (epithelial human lung adenocarcinoma) and MCF-7 (epithelial human breast adenocarcinoma) - 72-hour dose-response curve. The table contains 95% confidence intervals.

4.8 Dose-response curve for **Na[CoSAN-Br]**

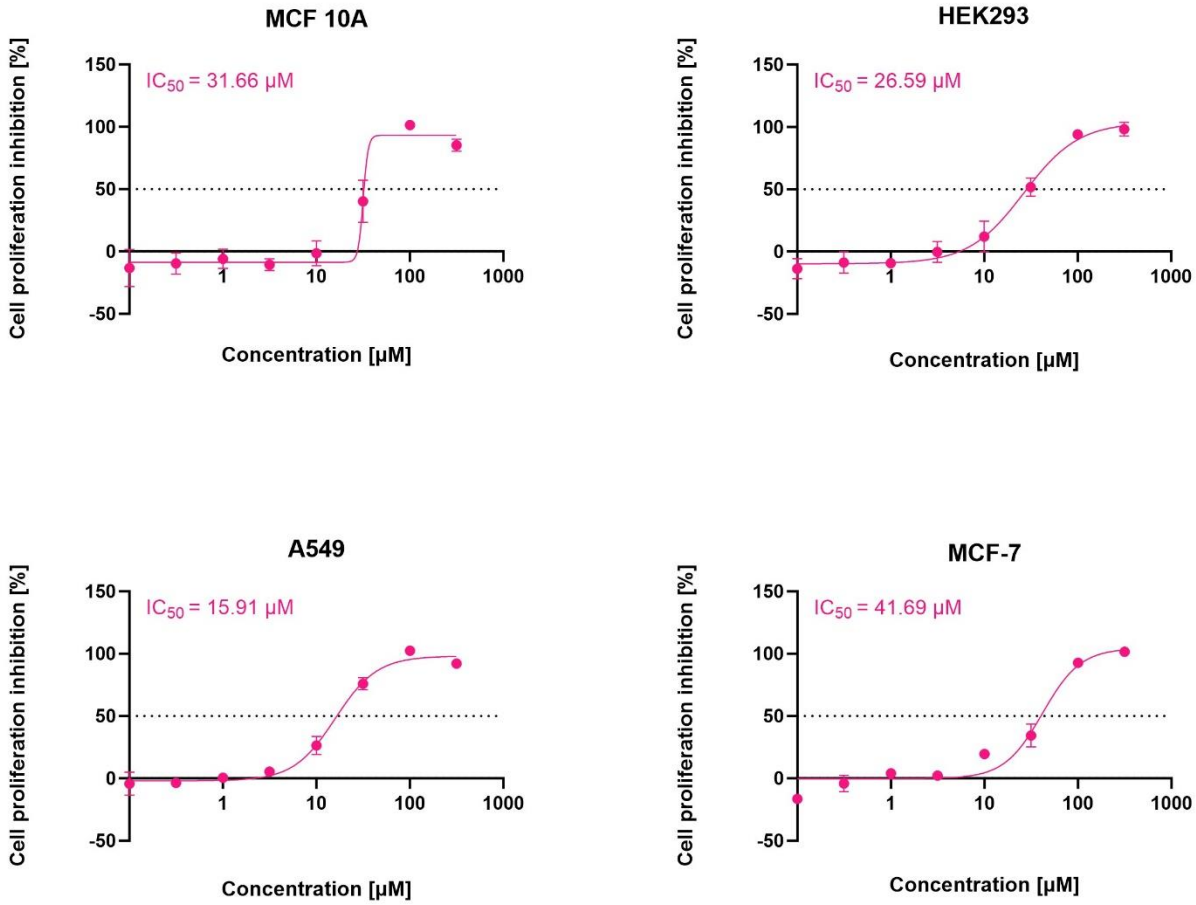

	95% CI [µM]
MCF 10A	-
HEK293	22.16 to 32.28
A549	13.96 to 18.12
MCF-7	35.64 to 49.61

Fig. S102. Antiproliferative activity of Na[CoSAN-Br] against MCF 10A (epithelial human mammary gland cell line), HEK293 (epithelial human embryonic kidney cell line), A549 (epithelial human lung adenocarcinoma) and MCF-7 (epithelial human breast adenocarcinoma) - 72-hour dose-response curve. The table contains 95% confidence intervals.

4.9 Dose-response curve for **Na[CoSAN-I]**

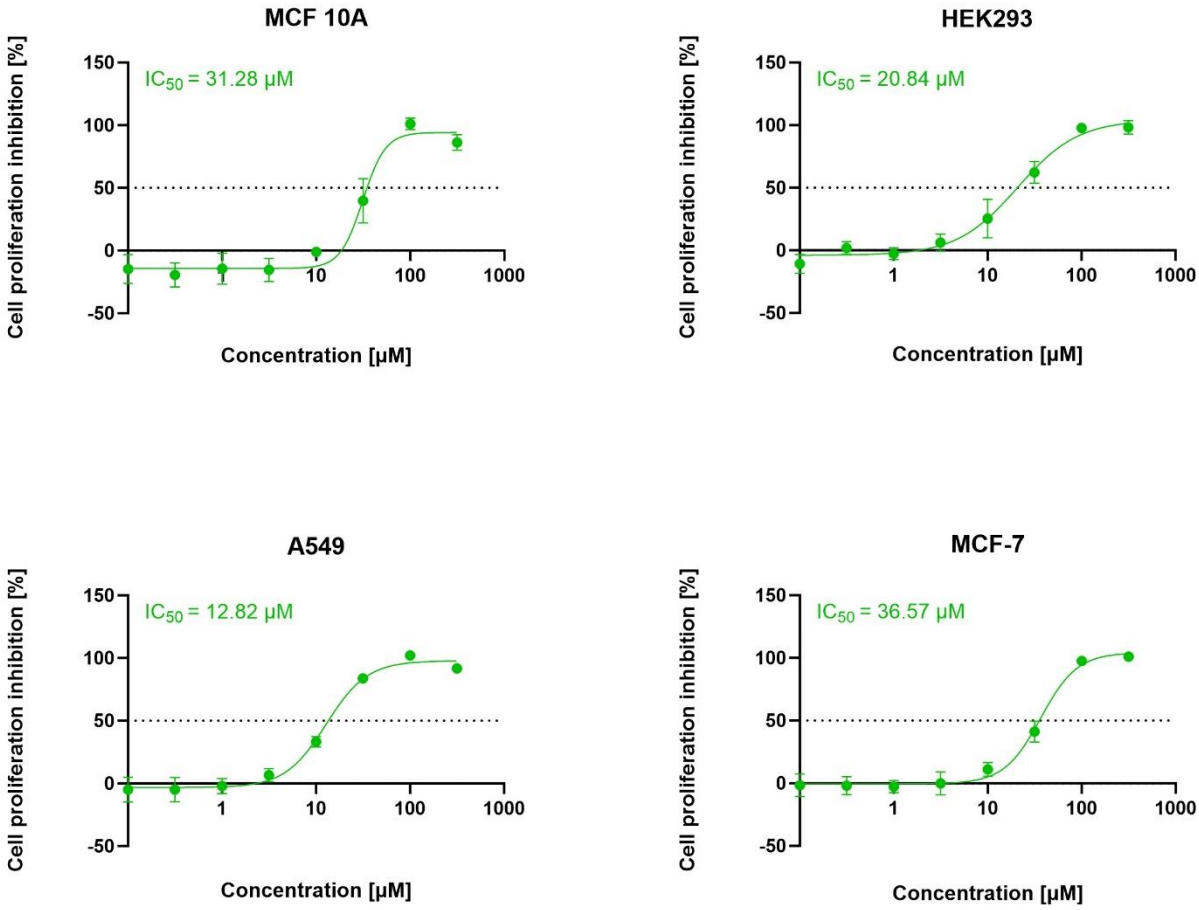

	95% CI [µM]
MCF 10A	25.92 to 35.19
HEK293	16.63 to 26.31
A549	11.20 to 14.68
MCF-7	32.57 to 41.52

Fig. S103. Antiproliferative activity of Na[CoSAN-I] against MCF 10A (epithelial human mammary gland cell line), HEK293 (epithelial human embryonic kidney cell line), A549 (epithelial human lung adenocarcinoma) and MCF-7 (epithelial human breast adenocarcinoma) - 72-hour dose-response curve. The table contains 95% confidence intervals.

4.10 Dose-response curve for **Na[CoSAN-Cl,Br]**

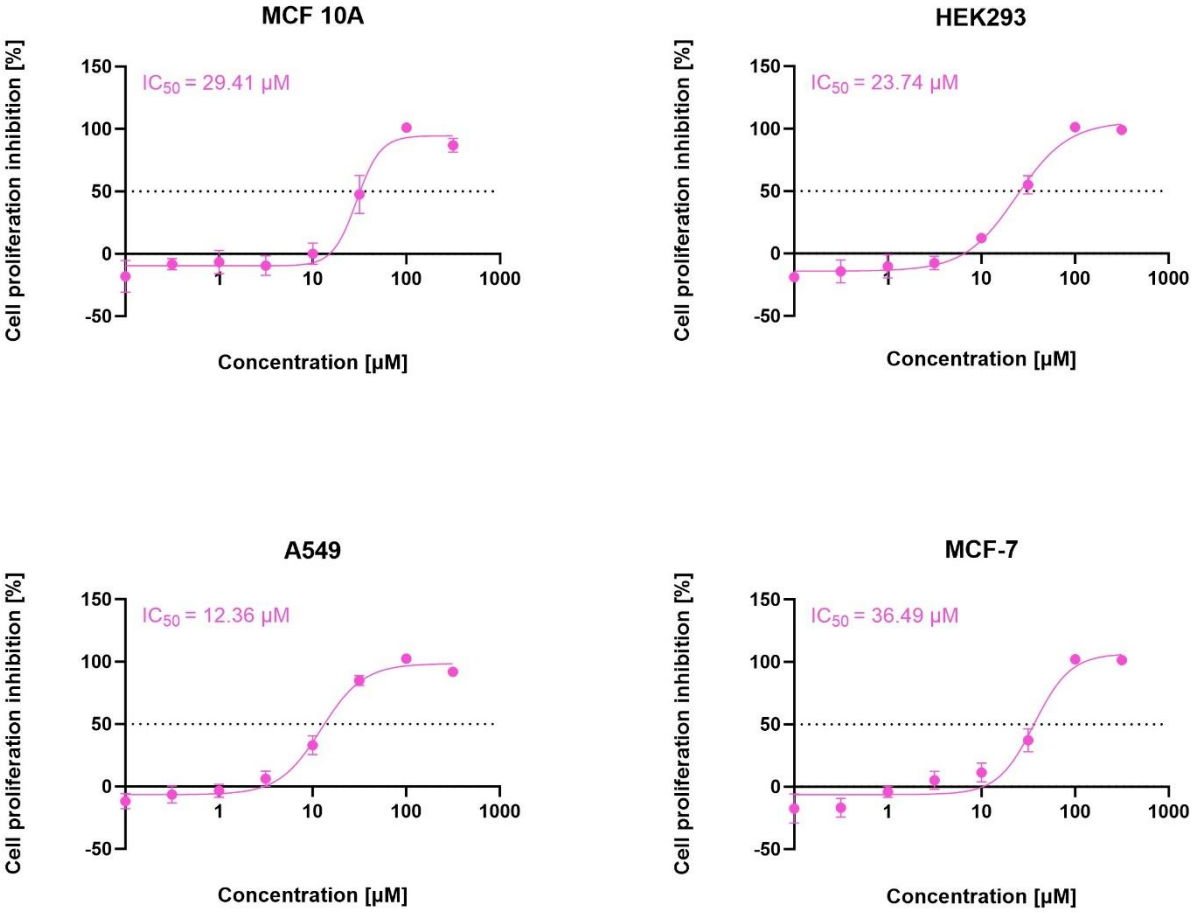

	95% CI [μM]
MCF 10A	24.27 to 32.85
HEK293	20.48 to 27.45
A549	10.91 to 13.99
MCF-7	30.12 to 43.57

Fig. S104. Antiproliferative activity of Na[CoSAN-Cl,Br] against MCF 10A (epithelial human mammary gland cell line), HEK293 (epithelial human embryonic kidney cell line), A549 (epithelial human lung adenocarcinoma) and MCF-7 (epithelial human breast adenocarcinoma) - 72-hour dose-response curve. The table contains 95% confidence intervals.

4.11 Dose-response curve for **Na[CoSAN-I,Br]**

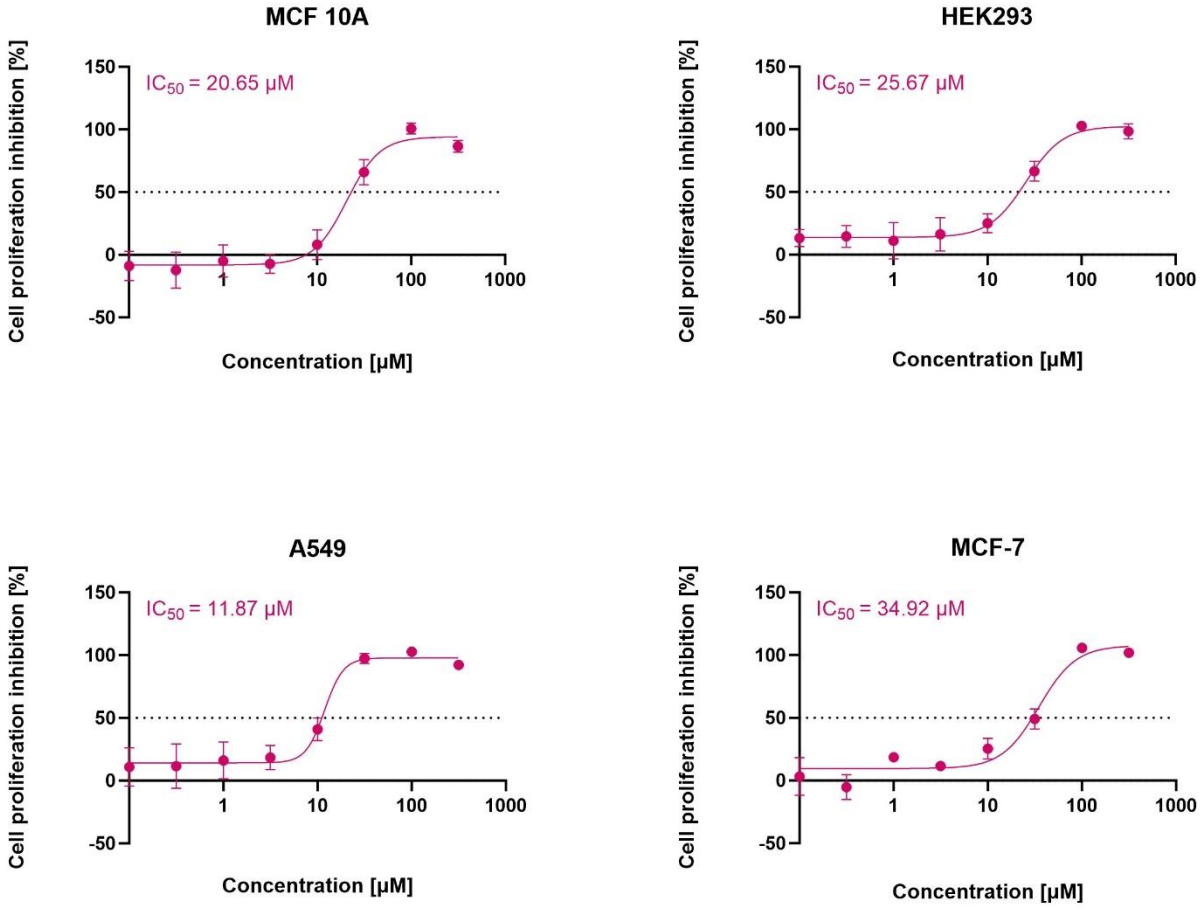

	95% CI [µM]
MCF 10A	16.82 to 25.06
HEK293	21.10 to 30.60
A549	-
MCF-7	27.58 to 42.39

Fig. S105. Antiproliferative activity of Na[CoSAN-I,Br] against MCF 10A (epithelial human mammary gland cell line), HEK293 (epithelial human embryonic kidney cell line), A549 (epithelial human lung adenocarcinoma) and MCF-7 (epithelial human breast adenocarcinoma) - 72-hour dose-response curve. The table contains 95% confidence intervals.

4.12 Dose-response curve for **Na[CoSAN-I,Cl]**

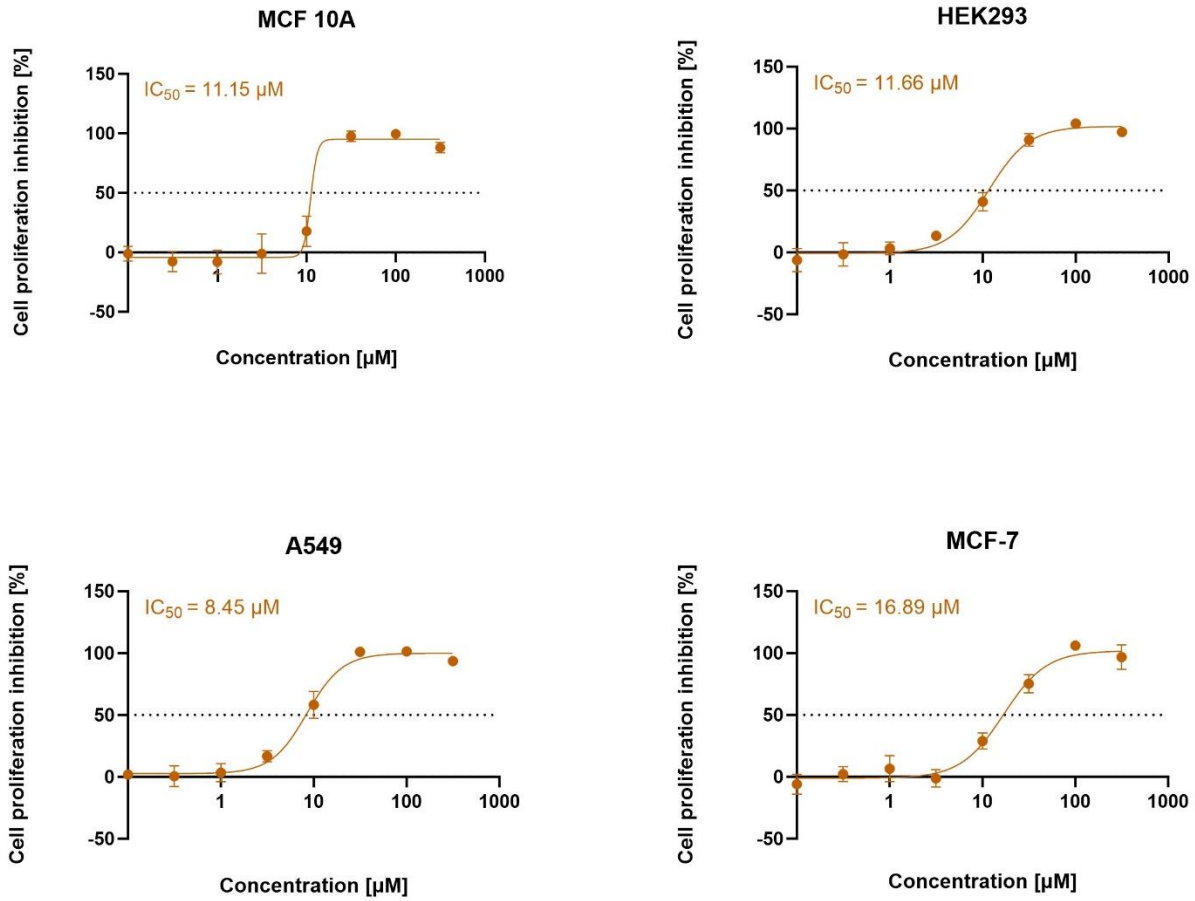

	95% CI [µM]
MCF 10A	-
HEK293	10.22 to 13.26
A549	7.28 to 9.60
MCF-7	13.77 to 20.56

Fig. S106. Antiproliferative activity of Na[CoSAN-I,Cl] against MCF 10A (epithelial human mammary gland cell line), HEK293 (epithelial human embryonic kidney cell line), A549 (epithelial human lung adenocarcinoma) and MCF-7 (epithelial human breast adenocarcinoma) - 72-hour dose-response curve. The table contains 95% confidence intervals.